

CLONING AND EXPRESSION OF THE OVINE CARDIAC  
SODIUM-CALCIUM EXCHANGER

by

Michael A. Burson

A DISSERTATION

Presented to the Department of Physiology and Pharmacology  
and the Oregon Health Sciences University  
School of Medicine  
in partial fulfillment of  
the requirements for the degree of

Doctor of Philosophy

May 1996

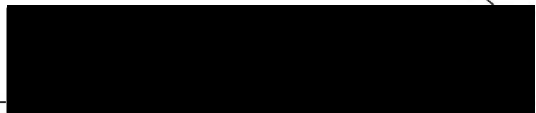
School of Medicine  
Oregon Health Sciences University

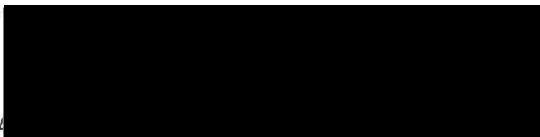
CERTIFICATE OF APPROVAL

This is to certify that the Ph.D. thesis of

Michael A. Burson

has been approved

  
-----  
Professor in charge of thesis

  
-----  
Associate Dean for Graduate Studies

## Table of Contents

Acknowledgments.....	v
Abstract.....	vi
Chapter One: Introduction.....	1-69
Section I: Cardiac Development; An Overview.....	1-10
Section II: Calcium and Excitation-Contraction Coupling.....	11-41
II.a: General Calcium Homeostasis.....	11
II.b: Calcium Pools and Calcium Transport Proteins.....	15
II.c: Calcium and Myocardial Contraction.....	16
Section III: Calcium Transport Proteins and Myocardial Relaxation.....	42-69
III.a: Sarcoplasmic Reticulum Ca <sup>2+</sup> -ATPase.....	42
III.b: Sarcolemmal Sodium-Calcium Exchanger.....	50
III.c: Development of the SERCA and NCX.....	63
Chapter Two: Calcium Transport Proteins in the Developing Sheep Heart.....	70-132
Purpose of Study.....	70
Section IV: General Techniques.....	72
Section V: Polymerase Chain Reaction Amplification and Cloning of the Sheep Sodium-Calcium Exchanger.....	84

Solutions.....	101
Section VI: Results and Conclusions.....	104
Section VII: Discussion.....	127
References.....	133-146

## ACKNOWLEDGMENTS

I wish to thank everyone in the who has helped me through these difficult and rewarding years at OHSU. First and foremost my parents, who stood by me through the years of my development both emotionally and intellectually. With out the constant support and love of my parents I am certain that I would not have reached this point in my life.

I have also made a great deal of wonderful friends during the past six years at OHSU, each of which deserves a personal thank you. I am indebted to the members of the Thornburg lab who helped in the development and completion of this project. Bob Webber and Robin Shaughnessy provided hours of social support. Although I may have completed this project without their influence it certainly would not have been as much fun or rewarding.

In addition to Bob and Robin I must pay a special thanks to Cathy Mace. Without her assistance and year long continuous support I would not have been able to complete this project. I am forever indebted to her for the many months of waiting for me to have a spare minute to do something not work related and also for the sleepless nights she spent editing this work. Thank you Cathy! In addition, I must thank Dafe Uwanogho for providing me with the training I needed to complete this project. Dafe taught me to think and work like a molecular biologist. Without Dafe's expertise I don't believe this project would have been quite as complete. I must also add Cathy and Dafe to the list of social support. They made doing science a fun, although not necessarily healthy, experience.

Finally I owe much of my development as a scientist to my mentor and friend Kent Thornburg. If I had to list the most important thing I have learned from Kent it would be the ability to work independently without being afraid to say "I don't know". Kent has also provided me with the training needed to approach interesting questions and design experiments to answer them. Thank you Kent for all you guidance and help.

## ABSTRACT

Studies have shown that the fetal cardiac myocyte contains less sarcoplasmic reticulum (SR) relative to the adult myocyte. Studies of mammals born in an immature state (altricial), show that the SR  $\text{Ca}^{2+}$ -ATPase (SERCA) is primarily responsible for sequestering  $\text{Ca}^{2+}$  in the mature myocyte, while the sarcolemmal  $\text{Na}^{+}$ - $\text{Ca}^{2+}$  exchanger (NCX) is relatively more important in the immature myocyte. I hypothesized that in sheep, a precocial mammal, there is a gradual decrease in the myocyte's use of the NCX during development with concomitant increase in the myocyte's use of the SERCA. To test this hypothesis I used Northern blot analysis to compare the expression levels of the genes which code for the SERCA and the NCX. The cDNA probe specific for the rabbit SERCA2a was a generous gift from Dr. David MacLennan. Preliminary studies tested the cross-reactivity of this probe between rabbit and sheep and the results were positive. No modifications of the SERCA2a cDNA probe were made. The cDNA probe specific for the guinea pig cardiac NCX was a generous gift from Dr. Ken Philipson. Unfortunately the cDNA probe did not cross-hybridize well with the sheep gene. A fetal sheep heart cDNA library was constructed, and with subsequent screening using a sheep specific cDNA probe, I cloned the sheep NCX gene.

Utilizing PCR-based cloning methods, I generated a fetal sheep heart cDNA library. Clones were analyzed for sequence homology with known NCX sequences. Sequence analysis revealed all clones were truncated near nucleotide +1330. Using PCR based cloning with genomic DNA as the template, the 5'-end of the ovine cardiac NCX gene was obtained. The ovine

cardiac NCX is 96% homologous to the bovine NCX at the nucleotide level and 97% identical at the amino acid level. Northern blots of total RNA from hearts of fetal (80 days gestation; 150 day term) and adult animals were sequentially probed with the NCX and SERCA specific cDNA probes. The SERCA mRNA levels were lower in the fetal sheep heart compared to the adult. This was similar to the expression observed in the altricial rabbit heart. This finding correlated with western blot data. In support of these findings I also probed the blots with a cDNA probe specific for the rabbit ryanodine receptor gene (also a gift from Dr. MacLennan). The mRNA levels of the ryanodine receptor were lower in the 80 day fetal heart compared to the adult heart. To our surprise, the NCX mRNA levels were comparable across the ages. This finding correlated with western blot analysis. I conclude that in precocial mammals the maturational expression pattern of the NCX is different from that observed in the altricial mammal.

## Chapter I: Introduction



Section I: The Development of the Heart:  
An Overview

## SECTION I: CARDIAC DEVELOPMENT: AN OVERVIEW

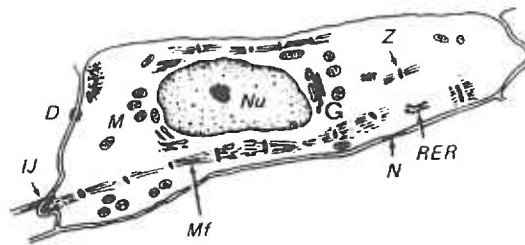
The sole responsibility of the heart is to serve as the muscular pump which drives the circulation. Although this function may seem simple, the mechanisms that underlie heart function throughout the lifetime of a mammal are complicated. While cardiac function was studied as far back as 200 B.C. (10), developmental cardiac physiology has only recently become a subject of investigation. Both fetal and adult hearts use the same muscle events which lead to appropriate tissue perfusion: contraction and relaxation. Although the fetal heart is capable of performing these tasks throughout gestation, many functional and cellular differences distinguish it from the adult heart. Adult myocardium develops greater tension per cross-sectional area than does immature myocardium (1,2,3,4,5), and immature myocardium relaxes more slowly than adult myocardium (6). Thus it is apparent that the heart undergoes changes which affect both systolic and diastolic function as it develops. Although several functional studies have characterized these changes (1,7,8,9), the cellular and molecular bases that underlie these changes have not been thoroughly investigated.

### Altricial vs. Precocial mammals:

Most studies of heart development have been performed using small altricial mammals such as rats and rabbits. These species undergo much of their cardiac development postnatally whereas the sheep, a large precocial mammal, is more mature at birth. The fetal sheep heart has been shown to be an important model of the immature human heart (11,12, 13). The fetal

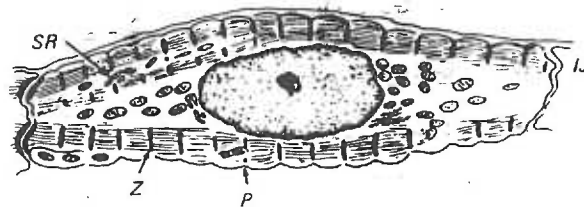
Figure 1: (From Brooks et al.)

(a) 29 days gestation



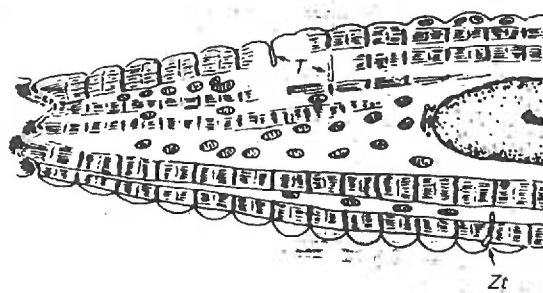
Schematic representation of 29 day fetal sheep cardiac myocyte. A few myofibrils (Mf) are present although not organized. No sarcoplasmic reticulum is visible. Mitochondria are scattered throughout the cytoplasm.

(b) 51 days gestation



Schematic representation of 51 day fetal sheep cardiac myocyte. Myofibrils are localized to the periphery, just beneath the sarcolemma. Evidence of forming sarcoplasmic reticulum (SR) is observed near the myofibrils. Mitochondria are more abundant yet still observed throughout the cytoplasm

(c) 145 days gestation (term)



Schematic of 145 day fetal sheep cardiac myocyte (term is 150 days). The myofibrillar content has increased as well as the organization. The myofibrils are seen extending more internally compared to less mature myocytes. Mitochondria are becoming organized between the myofilaments.

sheep heart is large enough to allow for chronic preparations which are not physically possible in rats and rabbits. Such preparations allow for perturbations to be induced while hemodynamics and other features of heart function can be monitored in the intact unanesthetized animal.

### Ultrastructure & Development:

All mammalian species follow a standard pattern of cardiac development. Whether myocyte ultrastructure develops postnatally (altricial) or prenatally (precocial) a similar sequence of events occurs. In general, the major change in myocyte ultrastructure is a progressive increase in the amount and organization of contractile protein and the development of an elaborate internal membrane system. In this discussion, cardiac myocytes will be considered to be immature regardless of species until the adult organization is present. Figure 1 is a schematic of the major cellular changes at various ages in the developing sheep myocyte. The key features will be discussed individually below. Of particular interest however, is the increase in sarcoplasmic reticulum content and formation of transverse tubules with development (figure 2). These adaptations are necessary to ensure that the excitation contraction coupling system operates throughout the enlarging cell.

### Myofibrils:

The bundles of myofilaments in striated muscle are collectively called "myofibrils"; each muscle fiber contains thousands of these myofibrils, as seen in the cross section of figure 2. The myofibril itself is made up of both myosin and actin filaments which are the contractile proteins of the muscle. With electron microscopy a clear alternating pattern of light and dark bands

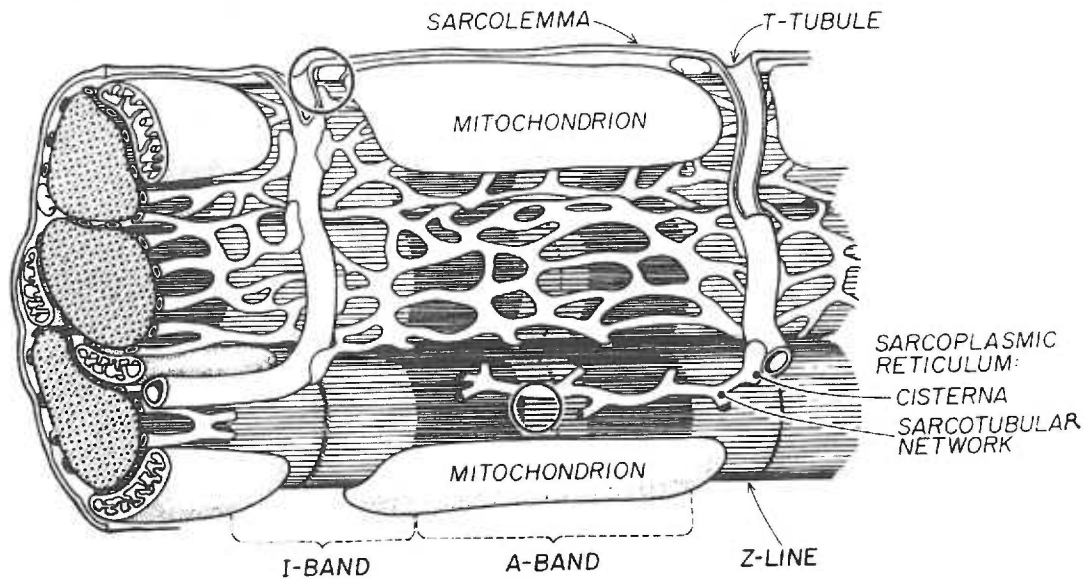


Figure 2: Schematic representation of a cross-section through a mature cardiac myocyte. This figure shows a good representation of the T-tubular and sarcoplasmic reticulum (SR) network. The T-tubules are seen invading the myocyte and running parallel to the myofilaments. In the mature cardiac myocyte an intimate relationship between the mitochondrion, sarcoplasmic reticulum and myofilaments exists. This is depicted here. The sarcoplasmic reticulum network is seen surrounding and in close approximation to the myofilaments. The mitochondria are organized around the myofilaments as well. The longitudinal SR extends from one end of the saromere to the other. The SR terminal cisternae is seen abutting the T-tubule membrane. (From Katz, 1992).

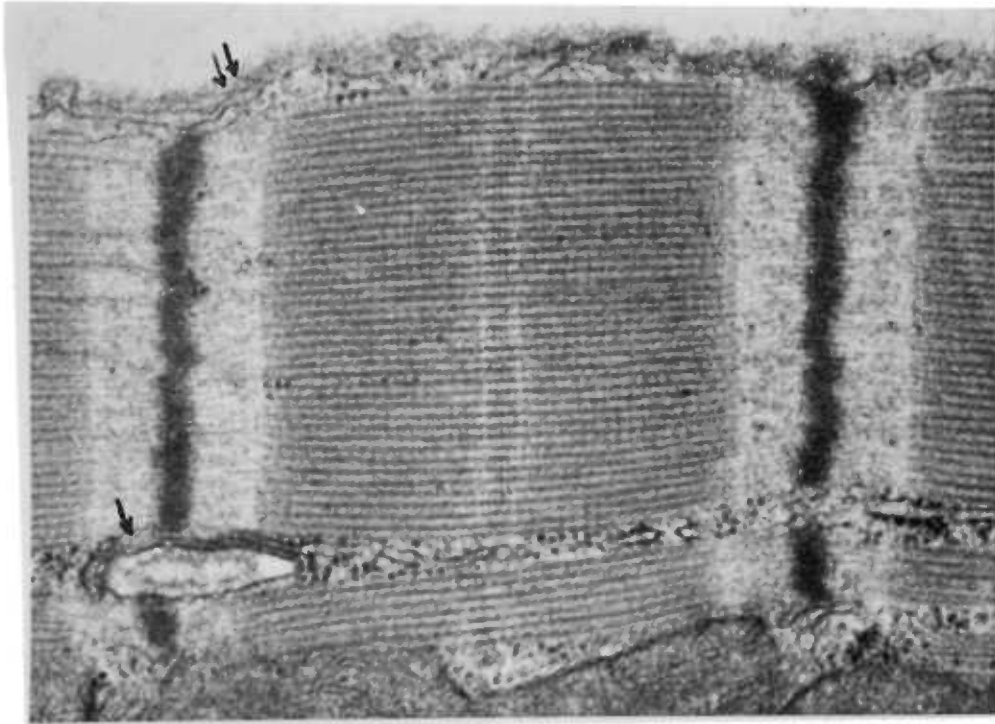


Figure 3: Electronmicrograph of a 130 day fetal sheep cardiac myocyte. A single sarcomere unit is shown here. Although this is a rather mature myocyte i.e. T-tubules are present (arrow) the myofilaments are still observed near the sarcolemmal (double arrow). The T-tubule is localized to the Z-disk as it is in the adult myocyte. Also visible are glycogen granules which are localized between the two visible myofilaments. (From K. Thornburg with permission)

are seen (Fig 3). The light bands (isotropic, I-bands) are composed of primarily actin filaments, while the dark bands (anisotropic, A-bands) contain myosin filaments as well as the ends of the actin filaments. The dark band traversing the midregion of the I-band is the Z band (Z-line, Z-disk, Z-body). The region between two consecutive Z-lines demarcates an individual sarcomere, the contractile unit of the muscle.

The immature myocyte is characterized by randomly scattered myofibrils which are localized to the periphery (14-18) (fig 1). As development continues the myofibrils become more organized and extend to the cell interior. The newborn lamb myocyte has an appearance very much like the adult myocyte, with myofibrils aligned in long parallel rows from one end of the cell to the other (11). Recent studies have identified a very large (3 megadalton) structural protein, titin (157). It is at least 1 $\mu$ m in length and extends from Z-disk to M-line. Titin has been shown to interact with actin and myosin (158) and has thus been hypothesized to serve as the template for sarcomere formation. Future studies on the development of this protein will be interesting because it is likely that the expression and localization of titin will show significant maturational patterns similar to the contractile proteins.

#### Sarcoplasmic Reticulum:

The myofibrils are surrounded by the intracellular membranous network known as the sarcoplasmic reticulum system (fig. 2). The sarcoplasmic reticulum is composed of two major parts: a) long longitudinal tubules that terminate in b) large chambers called terminal cisternae that abut the transverse tubules. The sarcoplasmic reticulum (SR) is the main storage site for activator  $Ca^{2+}$  in the mature myocyte.

Although SR has been observed at birth in all mammalian species studied, many studies have shown that the immature myocyte lacks a well developed and probably functional SR (18-24). During the course of development, the SR content increases and becomes greatly organized. The maturational increase in cell size has been linked with the development and localization of the SR close to the myofibrils. A close relationship between the contractile units and the source of activator calcium is required to ensure an efficient contractile system in the adult myocyte. The adult myocyte, (figure 2a), is organized such that the SR extends from one end of the cell to the other in close proximity to the myofibrils and mitochondria.

Transverse (T) tubules:

Extending deep into the cell interior of each myocyte are invaginations of the sarcolemma, the transverse tubules (T-tubules). These T-tubules penetrate deeply into the myocyte providing a connection between the extracellular space and the interior of the myocyte (figure 2). The T-tubules also interlace among the myofibrils; in cardiac muscle, there is a single T tubule at each Z-disk.

The T-tubules are one of the last organelles to form in the developing myocyte. As the myocytes grow in size the distance between sarcolemma and the myofibrils increases. Without the T-tubule a diffusional limitation would eventually prevent growing cells from contracting normally. It has been suggested that as the myocyte grows in diameter, the T system penetrates so that the cell becomes divided into manageable "units" of similar size (19). This sub-division arrangement results in an adequate surface-volume ratio for each unit such that myofibril activation is not limited by diffusional



constraints. Indeed the T-tubules have been shown to increase in number and surface area as the cell volume increases (16,17, 18,19,20,27).

#### Mitochondria:

The immature myocyte has abundant glycogen granules with few and scattered mitochondria (18-22). These findings indicate that prenatal myocytes have potential for a high rate of anaerobic metabolism. The functional glycogen content is reduced and mitochondria numbers increased as development proceeds. With the concomitant increase in the density of myofibrils, mitochondria aggregate around the myofibrils. This arrangement of mitochondria and myofibrils in the mature myocyte ensures an adequate energy supply for the contractile apparatus.

Together, these studies suggest that all mammalian species follow a similar pattern of ultrastructural development regardless of their particular developmental schedule (altricial vs. precocial). The cues for each event during development are not understood but it is likely that alterations in the hemodynamic and humoral environment are both important.

#### Functional Maturation:

The immature heart behaves much the same as the adult heart. At all stages of development, the heart beats in a rhythmic fashion thus forcing blood through the vascular network. Studies in cats, rats, rabbits and sheep indicate that the immature heart is significantly different from that of the adult (4,27). While many studies have shown that the immature heart develops less tension when compared to the adult (1,5), Friedman demonstrated that the fetal sheep myocyte is "intrinsically" the same as the mature myocyte. This was determined by normalizing the tension generated

by the amount of contractile protein per myocyte. The immature myocardium of the sheep fetus generated a normalized tension similar to the adult myocardium. Thus, it is evident that the immature heart is weaker than the adult, but that individual sarcomeres are similar in strength.

Friedman elegantly showed, using the force-velocity relationship, that the fetal sheep myocardium has an equal unloaded velocity of shortening of contraction ( $V_{\max}$ ) to adult myocardium (1). The  $V_{\max}$  is an index of myosin ATPase activity which determines that rate of cross-bridge recycling (see Section II.c). Thus, at least in sheep, developmental changes in the intrinsic properties of the individual myofibrils do not occur. Other species, however, undergo developmental changes in the type of myosin heavy chain (MHC) expressed. Each type has a unique ATPase activity. The developing rat heart has been shown to switch from the fast MHC isoform (V1) to the slow MHC isoform (V3) postnatally (28-30). This has functional and energetic significance because the V3 isoform is more efficient.

The immature heart is also different than the mature heart with respect to diastolic relaxation. The half-time to relaxation is greater in immature hearts than mature hearts (6). In the adult, myocardial relaxation is dependent upon the SR-dependent sequestration of cytoplasmic  $\text{Ca}^{2+}$  following systole. Differences between mature and immature hearts have been hypothesized to be due to the poorly developed SR in immature myocardium. To address this question, investigators have studied the response of fetal hearts to isoproterenol, a  $\beta$ -adrenergic agonist (4,31). Isoproterenol stimulates the SR  $\text{Ca}^{2+}$ -ATPase thus increasing the rate at which  $\text{Ca}^{2+}$  is taken up from the cytoplasm, thereby enhancing myocardial relaxation. The response to isoproterenol is significantly less in newborn rabbits and puppies (4,31). From these studies it is apparent that the lack of

abundant SR could be responsible for the slower rate of relaxation in the immature heart.

Studies from this lab have also shown significant developmental changes in the sheep heart function. By measuring the diastolic properties of the intact near term fetal heart in vivo, Hirsch et al showed that the time constant  $\tau$  (msec) , an index of the rate of relaxation, was not significantly different compared to the adult (32). Two explanations may explain these results: a) the fetal lamb heart has functional SR similar to the adult, or b) the fetal lamb heart has an additional powerful calcium extrusion mechanism. These two issues will be discussed further below.

## Section II: Calcium and Excitation-Contraction Coupling

## SECTION II.A: GENERAL CALCIUM HOMEOSTASIS

The calcium ion ( $\text{Ca}^{2+}$ ) is important for maintaining normal cell function in all mammalian species. Because  $\text{Ca}^{2+}$  homeostasis has been the subject of many textbook level reviews, this section will serve simply as an overview of the current principles.  $\text{Ca}^{2+}$  has been shown to play many intracellular signaling roles and thus regulatory mechanisms have evolved to maintain plasma and intracellular  $\text{Ca}^{2+}$  concentration within strict limits ( $10^{-3}$ - $10^{-7}$  M). The concentration of calcium in the extracellular compartment, including blood plasma, is controlled by the movement of calcium in to and out of bone deposits in response to parathyroid hormone (PTH) and calcitonin (CTN) (1). Together, PTH and CTN act to increase or decrease  $\text{Ca}^{2+}$  absorption from the bone matrix as needed to maintain  $\text{Ca}^{2+}$  concentration in the extracellular fluids within the normal physiological range.

Total plasma  $\text{Ca}^{2+}$  concentration is maintained at approximately 3.0 mM yet only 50% of this total is ionized (33). Circulating calcium is found in one of three states: (a) 40% is bound to plasma protein, (b) 10% is complexed with anions such as citrate or phosphate, and (c) 50% is in free ionized form. It is ionic calcium which is important for most signalling functions of calcium, including regulation of bone formation, neuronal communication, and muscular contraction.

Intracellular  $\text{Ca}^{2+}$  is maintained at micromolar levels by the cooperative action of specialized proteins (36). Unlike the free  $\text{Ca}^{2+}$  in the circulation which represents about 50% of the total  $[\text{Ca}^{2+}]_o$ , cytoplasmic free  $\text{Ca}^{2+}$  is maintained at 0.1% or less of the total  $[\text{Ca}^{2+}]_i$  in the resting cell (37).

Active transport mechanisms are responsible for maintaining the micromolar resting  $\text{Ca}^{2+}$  levels (see below).

The inward movement of  $\text{Ca}^{2+}$  across the cell membrane is primarily governed by voltage-dependent  $\text{Ca}^{2+}$  channels. The voltage-dependent  $\text{Ca}^{2+}$  channel is a uni-directional transporter thus only contributing a net gain in cytoplasmic  $\text{Ca}^{2+}$ . These channels open in response to membrane depolarization which allows  $\text{Ca}^{2+}$  to flow down its concentration gradient into the cell. The electrochemical gradient for  $\text{Ca}^{2+}$  across the cell membrane is the driving force for the  $\text{Ca}^{2+}$  flux through the channel. This situation is particularly suited for  $\text{Ca}^{2+}$  to serve as an intracellular signaling molecule since even minor changes in the permeability of the plasma membrane for calcium will produce significant increases in the cytoplasmic  $\text{Ca}^{2+}$  concentration.

#### Intracellular Calcium Homeostasis:

Calcium can be classified as a second messenger because it controls cellular events via reversible complexation to specialized  $\text{Ca}^{2+}$  binding proteins (38). In excitable cells such as neurons and myocytes,  $\text{Ca}^{2+}$  serves to induce intracellular events in response to a propagating action potential by interacting with target proteins. Synaptic communication is, for example, controlled by the  $[\text{Ca}^{2+}]$  within the nerve ending. The nerve impulse increases the permeability of the ending to  $\text{Ca}^{2+}$ , and the  $\text{Ca}^{2+}$  is responsible for the release of neurotransmitter. Muscular contraction, as will be discussed below, is mediated by  $\text{Ca}^{2+}$  interacting with the  $\text{Ca}^{2+}$  binding protein troponin in response to membrane depolarization (section II.c) (35).

Two classes of intracellular  $\text{Ca}^{2+}$  binding proteins have been characterized; soluble and intrinsic membrane proteins. The soluble proteins

Ligand	$K_d$ ( $\mu\text{M}$ )	[Ligand] <sub>i</sub> ( $\mu\text{M}$ )
Camodulin	0.38	24
Troponin C	0.50	70
Phosphocreatine	$71 \times 10^3$	$12 \times 10^3$
SR binding sites	1.0	47
SL binding sites	100	1124

Table 1. Properties of  $\text{Ca}^{2+}$  ligands, based on data from Fabiato (1983). (Data is as represented in original report)

are relatively small (Mw 10-20kD) and are responsible for reversibly binding  $\text{Ca}^{2+}$  in the cytoplasm and translating the stimulus. Table 1 lists the important  $\text{Ca}^{2+}$  binding proteins and membrane binding sites which are known to participate in  $\text{Ca}^{2+}$  buffering. Calmodulin and troponin-C are perhaps the most widely known examples of this class of protein. Both of these proteins have multiple  $\text{Ca}^{2+}$  binding sites and undergo conformational changes to induce subsequent intracellular events. Calmodulin, for example, has been shown to mediate the activity of many cellular enzymes, including; a) adenylate cyclase, b) cyclic nucleotide phosphodiesterase, c) phospholamban, and the endo(sarco)plasmic reticulum  $\text{Ca}^{2+}$ -ATPase (40). Thus it is apparent that  $\text{Ca}^{2+}$  can induce cellular events either directly (e.g. muscular contraction via troponin-C), or indirectly (e.g. SR  $\text{Ca}^{2+}$  uptake via phospholamban) (53).

The intrinsic membrane  $\text{Ca}^{2+}$  binding proteins are responsible for translocating  $\text{Ca}^{2+}$  across cellular membranes. The cardiac myocyte is considered to have a large buffering capacity for  $\text{Ca}^{2+}$  considering that total cell  $\text{Ca}^{2+}$  content can increase by several mM/L cell water while free  $\text{Ca}^{2+}$  increases only by  $\mu\text{M}/\text{L}$  cell water (41). Calcium transport proteins serve as high capacity  $\text{Ca}^{2+}$  buffers. Eukaryotic cells contain  $\text{Ca}^{2+}$  transport systems in the plasma membrane (sarcolemma), in mitochondria, and in endo(sarco)plasmic reticulum.



## SECTION II.B: CALCIUM POOLS AND CALCIUM TRANSPORT PROTEINS

Studies by Langer have defined five kinetic phases associated with the  $\text{Ca}^{2+}$  exchange in the ventricular muscle (Table 2) (62). This early study looked at isotopic  $\text{Ca}^{2+}$  exchange in perfused papillary muscle. In this preparation, papillary muscle is perfused with isotonic Ringer solution containing  $^{45}\text{Ca}^{2+}$  until steady state uptake is reached (approximately 60 min). At this point, the perfusion solution is changed to isotonic Ringer containing "cold"  $\text{Ca}^{2+}$  and the effluent is collected at regular time points. Although switching between perfusates (5-10 sec) and sampling rate (2-6 drops/min) was not very fast, distinct kinetic phases were observed (fig. 4).

Quantitative analysis of the  $^{45}\text{Ca}^{2+}$  in effluent indicated four exponential phases; each is thought to represent a distinct  $\text{Ca}^{2+}$  compartment. The plot in figure 4 represents the rate at which  $^{45}\text{Ca}^{2+}$  is "released" or exchanged from within the papillary muscle into the perfusion solution. The most rapidly exchanged ( $t_{1/2}=0.3$  min)  $^{45}\text{Ca}^{2+}$  comes from the vascular space, termed Phase 0. Because the movement of  $\text{Ca}^{2+}$  within the vasculature is not hindered by membrane barriers, this fraction exchanges very rapidly. Phase 1 ( $t_{1/2}=1.2$  min) represents the  $\text{Ca}^{2+}$  which is localized to the interstitial space. This fraction exchanges more slowly since the  $\text{Ca}^{2+}$  must pass from the interstitial space into the vasculature.

The more slowly exchangeable  $\text{Ca}^{2+}$  pools were then hypothesized to reside within the cell although precise localization could not be made using the papillary muscle preparation. In order to further localize the intracellular  $\text{Ca}^{2+}$  compartments a better perfusion system had to be developed. Langer and colleagues successfully developed a non-perfusion-limited  $\text{Ca}^{2+}$  exchange system which helped define subcellular  $\text{Ca}^{2+}$

Table 2: Summary exchangeable  $\text{Ca}^{2+}$  pools, From Langer (1968).

Phase	Rate Constant (min <sup>-1</sup> )	T1/2 of Exchange	Probable Origin
0	3.5	0.2	Vascular
1	0.59	1.2	Interstitial
2	0.116	6.0	Membrane bound
3	0.021	33	Intracellular

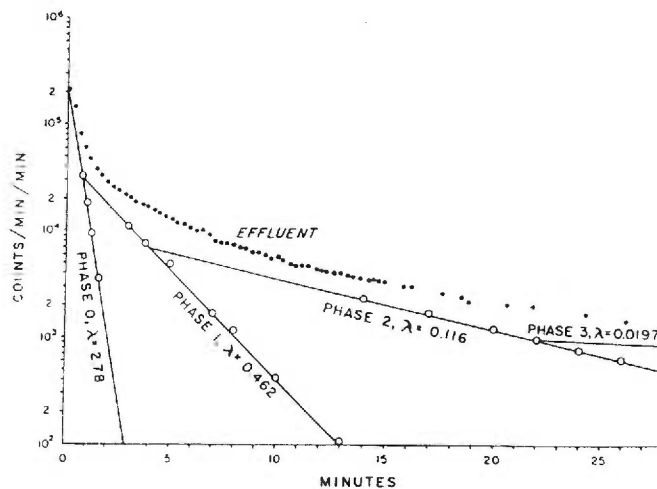


Figure 4: Semilogarithmic plot of  $^{45}\text{Ca}^{2+}$  activity in the venous effluent from an arterially perfused papillary muscle. The papillary muscle was preloaded with  $^{45}\text{Ca}^{2+}$  containing solution for approximately 60 min until steady state was reached. Venous effluent was collected and  $^{45}\text{Ca}^{2+}$  was measured. The solid dots ( $\bullet$ ) represent the actual washout curve, whereas the ( $\circ$ ) represents the resolved kinetic phases. Four phases are shown, each of which represents the efflux of  $\text{Ca}^{2+}$  from a specific  $\text{Ca}^{2+}$  pool (see table 2 above).

compartments (63). In this preparation isolated rat ventricular myocytes are studied under conditions which allow perfusion rates up to 40 ml/min without being washed away. Rapid effluent collection and on-line scintillation counting provide a means of observing rapidly exchangeable  $\text{Ca}^{2+}$  compartments. Furthermore, because of the ease with which solutions can be changed, chemical probes are used to define subcellular sites of particular  $\text{Ca}^{2+}$  pools.

Using the non-perfusion-limited flow system described above, Langer reported four  $\text{Ca}^{2+}$  compartments associated with the isolated cell. Using Lanthanum ( $\text{La}^{3+}$ ), an ion which binds to the sarcolemma and effectively displaces ions non-specifically Langer et al had previously determined that a large  $\text{La}^{3+}$  displaceable pool exists (139). However, the resolution was limited in these studies as indicated above. Figure 5.a shows the effect of adding  $\text{La}^{3+}$  to the cells. It is apparent that a significant amount of  $\text{Ca}^{2+}$  is localized to cellular sites which are accessible to  $\text{La}^{3+}$ . With the non-perfusion limited system a very rapidly exchanged ( $t_{1/2} < 1\text{sec}$ )  $\text{La}^{3+}$  displaceable  $\text{Ca}^{2+}$  compartment was observed. Figure 5.b is a  $^{45}\text{Ca}^{2+}$  washout curve which shows that the  $\text{La}^{3+}$  displaceable pool has already exchanged by 2 seconds after washout is initiated. Based on these findings the rapidly exchangeable Ca compartment has been localized to the sarcolemma.

In addition to the rapid compartment, an "intermediate" compartment with biphasic kinetics ( $t_{1/2} = 3$  and  $19$  sec) was observed. Caffeine and ryanodine were added to the perfusion solution to test if the intermediate  $\text{Ca}^{2+}$  pool was localized to the SR. The results of this test are shown in figure 6. Upon the addition of caffeine (arrow),  $^{45}\text{Ca}^{2+}$  was released into the effluent suggesting that it may have been derived from the SR. Furthermore, ryanodine, which depletes the SR  $\text{Ca}^{2+}$  stores, was used to

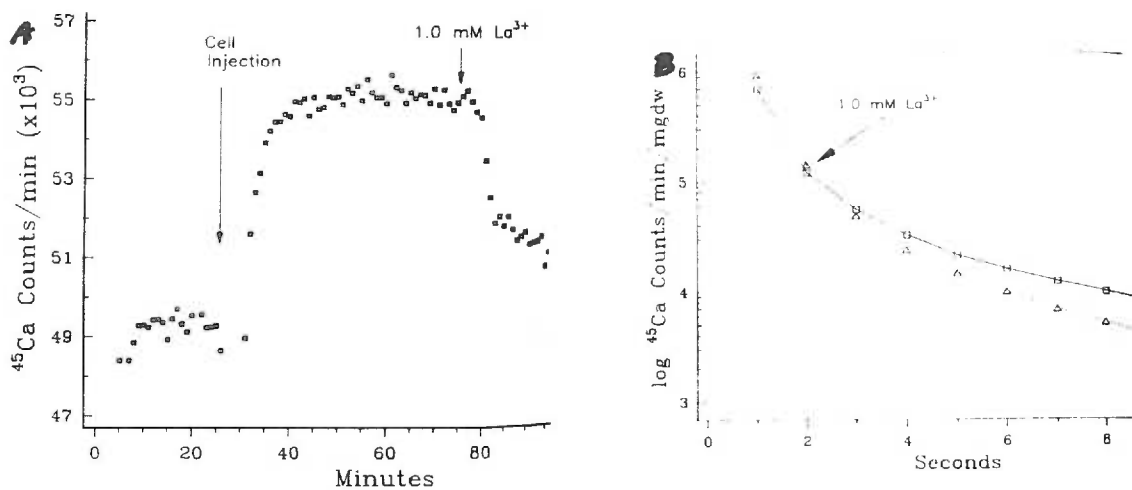


Figure 5: (A) Typical  $^{45}\text{Ca}^{2+}$  washout curve using the non-perfusion system of Langer. During the first 30 minutes of the trace cells are absent from the flow chamber, thus the counts/min (CPM) at this point represent the background. With addition of cells the CPM increases significantly and reaches a plateau by 60 minutes. This indicates that the cells have taken up  $^{45}\text{Ca}^{2+}$  and a steady state has been reached. At about 75 minutes  $\text{La}^{3+}$  is added to the flow chamber and CPM drop rapidly. The magnitude of the displaced Ca indicates that nearly 50% of the Ca is localized to a site which is  $\text{La}^{3+}$  accessible. (B) This plot shows the first 10 seconds of a typical  $^{45}\text{Ca}^{2+}$  washout curve. At the 2 second point 1.0mM  $\text{La}^{3+}$  was added to the perfusion solution. No additional  $^{45}\text{Ca}^{2+}$  release is observed. This finding indicates that the  $\text{La}^{3+}$  pool is depleted within 2 seconds of initiating the washout.

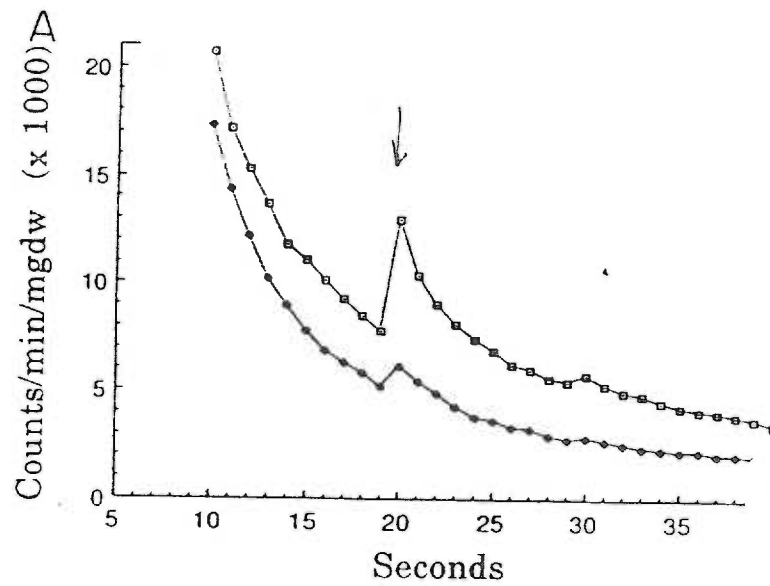


Figure 6: Effect of caffeine and ryanodine + caffeine on  $^{45}\text{Ca}^{2+}$  washout. The top curve is a standard washout curve except that 10 mM caffeine was added to the perfusion solution at 20 seconds. Caffeine induces the release of  $\text{Ca}^{2+}$  from the SR by opening the  $\text{Ca}^{2+}$  release channel. The increase of CPM at this point represents the release of  $\text{Ca}^{2+}$  from the SR. The lower trace represents the  $^{45}\text{Ca}^{2+}$  washout curve from cells which have been preincubated in the presence of  $1\mu\text{M}$  ryanodine for 60 minutes. This preincubation period was performed to "empty" the SR  $\text{Ca}$  stores. The addition of 10 mM caffeine was repeated in the ryanodine treated cells and the amount of  $\text{Ca}$  released from the SR was decreased significantly. The time constants of the post-caffeine washout curves were comparable to the time constant associated with the intermediate compartment. This supported the hypothesis that the intermediate compartment was associated with the SR.

further test this hypothesis. The lower trace in figure 6 is the  $^{45}\text{Ca}^{2+}$  washout curve in the presence of ryanodine. The magnitude of the  $^{45}\text{Ca}^{2+}$  release is reduced, thus supporting the hypothesis that the intermediate  $\text{Ca}^{2+}$  pool is localized to the SR.

Finally, a "slow" compartment ( $t_{1/2} = 3.6$  min) was observed and suggested to be localized to the mitochondria. The mitochondria have been shown to accumulate  $\text{Ca}^{2+}$  by a proton-augmented exchange mechanism (67). Using  $\text{NaH}_2\text{PO}_4$  as a proton donor and Warfarin as an inhibitor of mitochondrial respiration, it has been shown that the slow compartment is localized to mitochondria (results not shown). Due to the slow time constant of  $\text{Ca}^{2+}$  exchange associated with the mitochondrial  $\text{Ca}^{2+}$  pool, it is clear that this pool is not affected by beat-to-beat changes in cytoplasmic  $\text{Ca}^{2+}$ .

The  $\text{Ca}^{2+}$  compartments described in the preceding paragraphs are cellular compartments in addition to the two compartments previously described for the vascular and interstitial space. As expected, some  $\text{Ca}^{2+}$  is not exchanged at all during exchange studies. This could be due to the limitations of the methodology or, more likely, the irreversible binding of  $\text{Ca}^{2+}$  to intracellular and or extracellular matrix materials. Nonetheless, the  $\text{Ca}^{2+}$  compartments which are exchanged and the transport proteins which mediate them are important for further consideration. In every case, (excluding the rapid  $\text{La}^{3+}$ -displaceable  $\text{Ca}^{2+}$  compartment), the exchange of  $\text{Ca}^{2+}$  is mediated by a specific transport protein. A brief description of the  $\text{Ca}^{2+}$  transport proteins of the cardiac myocyte is given here to serve as an introduction to  $\text{Ca}^{2+}$  transport across cellular membranes.

### Calcium Transport in the Sarcolemma (SL):

Three mechanisms are responsible for transport  $\text{Ca}^{2+}$  across the SL; a) voltage-sensitive  $\text{Ca}^{2+}$  channels, b)  $\text{Ca}^{2+}$ -ATPases, c) sodium-calcium exchangers (NCX). Each of these transport systems has a different kinetic property and each is designed to satisfy the requirements of cells during the cardiac cycle.

Studies using the patch clamp technique have shown that the  $\text{Ca}^{2+}$  channels across species are very similar (45). Two unique  $\text{Ca}^{2+}$  channels have been identified in cardiac cells from several mammalian species including the rabbit, dog, sheep and guinea pig (44). A low threshold  $\text{Ca}^{2+}$  channel has been described in atrial tissue (46). This is the T-type channel which has a relatively small  $\text{Ca}^{2+}$  conductance of 8 pico siemens (pS) and is not believed to contribute significantly to  $\text{Ca}^{2+}$  influx in ventricular myocytes. However due to the low threshold of activation and relative abundance in sinoatrial nodal cells, this channel is thought to be important in pacemaking of some species (47).

The second well characterized voltage-dependent  $\text{Ca}^{2+}$  channel is the high threshold, large conductance L-type channel. This channel is abundant in ventricular myocytes of most species (44) and is known to provide most of the  $\text{Ca}^{2+}$  current for the plateau of the cardiac AP. The L-type channel has a  $\text{Ca}^{2+}$  conductance of 15-25 pS. Upon membrane depolarization the L-type channel opens and large quantities of  $\text{Ca}^{2+}$  enter the cell. The rate at which  $\text{Ca}^{2+}$  enters, or magnitude of the  $\text{Ca}^{2+}$  current is dependent on the number of channels open and the driving force. The probability that a given channel will be open increases as the membrane depolarizes.

The L-type  $\text{Ca}^{2+}$  channel is also regulated by  $\text{Ca}^{2+}$  and  $\beta$ -adrenergic stimulation. As cytoplasmic  $[\text{Ca}^{2+}]$  rise during the plateau phase, the  $\text{Ca}^{2+}$

channels begin to inactivate in response to the elevated  $[Ca^{2+}]$ . This limits the duration of the AP as well as the amount of  $Ca^{2+}$  which can enter during a single beat. During  $\beta$ -adrenergic stimulation the  $Ca^{2+}$  current is enhanced. This effect is mediated by  $G_S$  (stimulating G-protein), which stimulates a cyclic AMP-dependent protein kinase that phosphorylates the channel and directly increases the probability of opening (48). The net result of  $\beta$ -adrenergic stimulation on cardiac myocytes is an increase in the strength of contraction as more  $Ca^{2+}$  channels open.

The SL  $Ca^{2+}$ -ATPase probably does not contribute to the beat-to-beat regulation of intracellular  $Ca^{2+}$ . However, it does participate in the maintenance of basal sarcoplasmic  $Ca^{2+}$  levels (41). The SL  $Ca^{2+}$ -ATPase is a high affinity ( $K_m=0.5\mu\text{mol/l}$ ) low capacity ( $0.5\text{nmol/mg SL/sec}$ ) transport system (42). This ATPase functions to pump  $Ca^{2+}$  out of the cell into the extracellular space. Because of the high affinity it will continue extruding  $Ca^{2+}$  even during rest when small quantities of  $Ca^{2+}$  may leak across the SL. However, it does not have the capacity to be important when intracellular  $Ca^{2+}$  concentrations are high. Even though this  $Ca^{2+}$ -ATPase appears to play a minor role in controlling cytoplasmic  $Ca^{2+}$  it has been shown to be modulated by both calmodulin (37) and cAMP-dependent protein kinase (43).

The SL NCX is a large-capacity ( $20\text{nmol/mg SL/sec}$ ) low-affinity  $Ca^{2+}$  pump ( $1-20\text{ mmol/l}$ ). Unlike the two previously mentioned SL  $Ca^{2+}$  transport systems, the NCX is electrogenic and reverses pumping direction depending on  $Ca^{2+}$  and  $Na^+$  concentration gradients (49). This reversal is possible because the NCX is driven by the electrochemical gradient for  $Na^+$ . During the cardiac action potential when membrane is depolarized and cytoplasmic  $Na^+$  levels are increased the NCX may transport  $Ca^{2+}$  into the



cell. Such a reversal would result in accumulation of  $\text{Ca}^{2+}$  within the myocyte.

#### Calcium Transport Across Intracellular Membranes:

The  $\text{Ca}^{2+}$  crossing the sarcolemma triggers important intracellular events and thus is vital to myocyte function, but most of the calcium needed for cell activity is extracted from intracellular stores. Two organelles actively participate in  $\text{Ca}^{2+}$  buffering, the mitochondria and the sarcoplasmic reticulum. Mitochondria are thought to play a minor role in regulating cytoplasmic  $\text{Ca}^{2+}$  levels (5,35,38). However because the control of mitochondrial matrix  $\text{Ca}^{2+}$  levels is essential for cellular processes a brief mention of the  $\text{Ca}^{2+}$  buffering system will be made.

Although originally believed to be an important player in maintaining cytoplasmic  $\text{Ca}^{2+}$ , mitochondria are now known to contain very little  $\text{Ca}^{2+}$  (35). The mitochondrion is important however, in maintaining mitochondrial matrix  $\text{Ca}^{2+}$  for energy production.  $\text{Ca}^{2+}$  accumulates within mitochondria via a uniporter which is driven by the proton-motive force across the inner membrane (37). Matrix  $\text{Ca}^{2+}$  is removed via an electroneutral NCX which is different than the NCX found in the sarcolemma. The mitochondrial NCX is a low affinity slow transport mechanism (37). Together, the uniporter and NCX maintain matrix  $[\text{Ca}^{2+}]$  yet so little  $\text{Ca}^{2+}$  is exchanged that they do not contribute significantly to the changes in cytoplasmic  $\text{Ca}^{2+}$  pool.

The sarcoplasmic reticulum (SR) is the predominant intracellular storage organelle for  $\text{Ca}^{2+}$ . It is similar in structure to the endoplasmic reticulum of non-muscle cells. The SR is separated into discrete regions, each of which performs a specific function with respect to  $\text{Ca}^{2+}$  handling. Fig. 7 is a

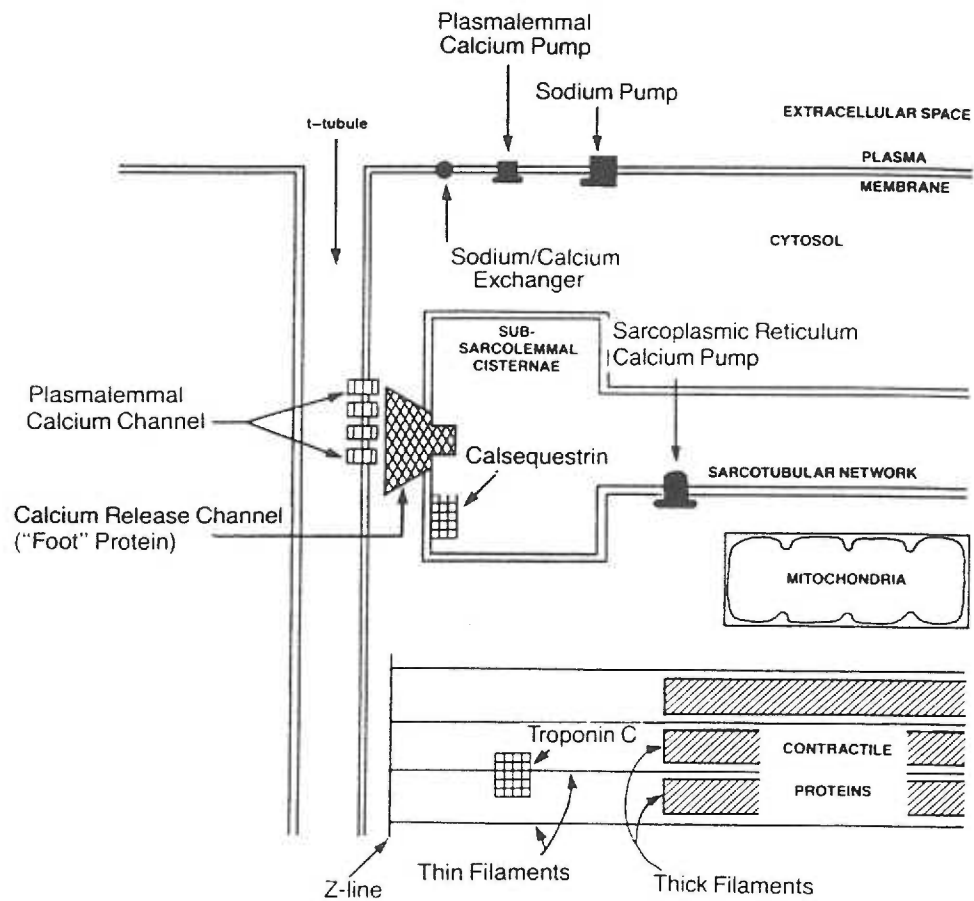


Figure 7: Schematic showing the key structures involved in controlling the movement of Ca. The relationship between the SR and the T-tubule is depicted. The terminal cisternae abuts the T-tubule forming the junctional complex. The L-type  $\text{Ca}^{2+}$  channels of the SL are in close approximation to the  $\text{Ca}^{2+}$  release channel of the SR. The longitudinal SR runs parallel to the myofilaments. The  $\text{Ca}^{2+}$  ATPase is located in the longitudinal SR.

simplified diagram of the key structures including the T-tubule, SR and sarcomere. The junctional SR which abuts the T-tubules is the site of  $\text{Ca}^{2+}$  release, whereas the longitudinal SR which is juxtaposed to the myofibrils is the site of  $\text{Ca}^{2+}$  sequestration. Together, these distinct sites control the movement of  $\text{Ca}^{2+}$  into and out of the cytoplasm to control myocardial contraction.

The movement of  $\text{Ca}^{2+}$  into and out of the SR is responsible for the normal function of cardiac myocytes. As described later, myocardial contraction is dependent on a transient increase in cytoplasmic  $[\text{Ca}^{2+}]$ . The SR serves as the storage site for the bulk  $\text{Ca}^{2+}$  needed for contraction. Studies on the  $\text{Ca}^{2+}$  binding capacity of the SR have supported the role of the SR in myocardial  $\text{Ca}^{2+}$  regulation (57,58).  $\text{Ca}^{2+}$  is stored within the terminal cisternae of the SR complexed with the  $\text{Ca}^{2+}$  binding protein, calsequestrin. This protein binds  $\text{Ca}^{2+}$  with high-capacity and with moderate affinity and has also been shown to interact with the SR  $\text{Ca}^{2+}$  release channel protein (50).

The release of  $\text{Ca}^{2+}$  from the SR is currently believed to be dependent on the influx of  $\text{Ca}^{2+}$  across the SL via L-type  $\text{Ca}^{2+}$  channels. The ryanodine receptor is a calcium-modulated protein which is believed to be responsible for the phenomenon called "calcium-induced calcium release" (51). The  $\text{Ca}^{2+}$  release channel is a oligomeric complex which binds the plant alkaloid, ryanodine, with great affinity (52) This feature has made it possible to purify the receptor in vitro. However, due to its large size ( $M_w=450\text{kD}$ ) it has been difficult to study. Nonetheless studies using ryanodine have shown that myofibril activation and subsequent contraction is dependent on this channel (54). In a study by Tseng, it was shown that contraction does not occur when the ryanodine receptor is inhibited by the presence of ryanodine (5mM). As shown in figure 8, ryanodine inhibits SR  $\text{Ca}^{2+}$  thereby reducing tension

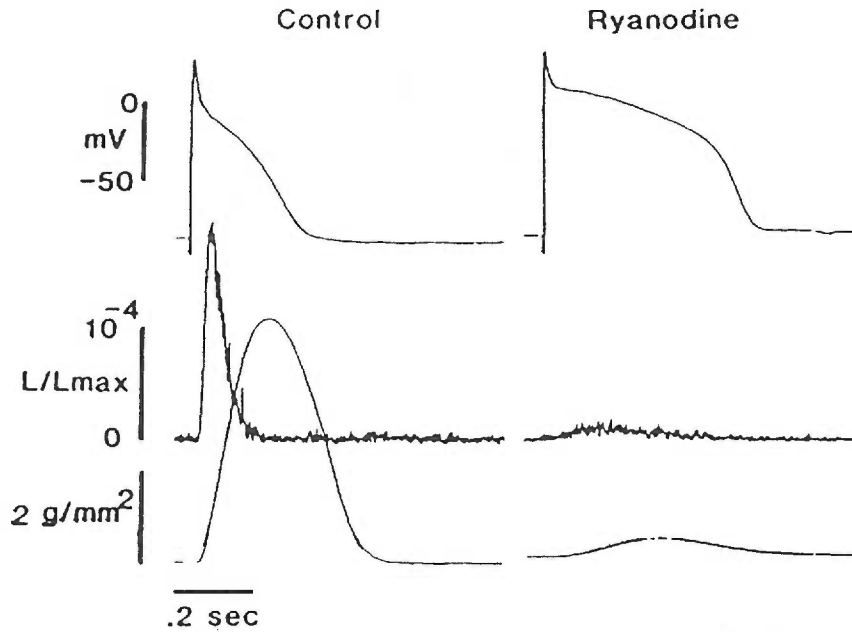


Figure 8: This figure shows the effect of ryanodine (5mM) on action potential (top), aequorin light signal (middle), and force development (bottom) in papillary muscle. In the presence of ryanodine the release of  $\text{Ca}^{2+}$  from the SR is reduced as indicated by the diminished aequorin light signal. As a result of this, the force developed is drastically reduced as well. These findings support the need for SR  $\text{Ca}^{2+}$  release for normal contractile function in cardiac muscle. The action potential in the presence of ryanodine is prolonged due to the lessened inhibition of the inward  $\text{Ca}^{2+}$  current by the low internal  $\text{Ca}^{2+}$ . (From Tseng, 1988)

development. Interestingly, the application of ryanodine appears to prolong the cardiac AP as well. This has been attributed to the lack of  $\text{Ca}^{2+}$ -dependent inactivation of the L-type  $\text{Ca}^{2+}$  channel. With the  $\text{Ca}^{2+}$  channel open for an prolonged period of time the plateau phase of the AP would be extended as shown in fig 8.

Although it is not clear how the protein works, two components of the release channel have been described. The largest part of the protein has been localized to the site where the T-tubule and SR meet. This "foot" protein is thought to serve as a direct connection between the SL and the SR. The actual  $\text{Ca}^{2+}$  channel has been identified at the C-terminal region of the protein. Together, the foot protein and the  $\text{Ca}^{2+}$  channel function as the trigger mechanism for SR  $\text{Ca}^{2+}$  release.

For the cardiac myocyte to contract in a cyclic fashion, the  $\text{Ca}^{2+}$  which was released from the SR at the onset of contraction must be sequestered into the longitudinal SR. The longitudinal SR is juxta-posed to the myofibrils and mitochondria. If ones considers that  $\text{Ca}^{2+}$  is pumped into the SR lumen at the expense of ATP, the location of the mitochondria next to the SR and myofibrils is ideal for efficient EC coupling. The longitudinal SR contains a high-affinity ( $K_m < 0.5 \text{ umol/l}$ )  $\text{Ca}^{2+}$  sensitive ATPase (SERCA). This protein makes up 90% of total SR protein (6, 24). Based on studies of isolated SR membrane vesicles it is now known that the SERCA protein is responsible for the rapid diastolic fall in cytoplasmic  $\text{Ca}^{2+}$  which precedes myofibrillar relaxation. (25, 56, 57,58).

The SERCA is activated by  $\beta$ -adrenergic stimulation via phosphorylation of the regulatory protein, phospholamban (53,59,60). This protein is an integral SR membrane protein which is in a 1:1 molar ratio with the SERCA. Phospholamban is a homotetramer which, when

phosphorylated by cAMP-dependent or calmodulin- dependent protein kinase, stimulates  $\text{Ca}^{2+}$  uptake by the SERCA (61). It is apparent that  $\text{Ca}^{2+}$  movement through the SR is complex and under strict control. Together, the  $\text{Ca}^{2+}$  release channel of the junctional SR and the SERCA of the longitudinal SR regulate the myocyte  $\text{Ca}^{2+}$  cycle in an organized fashion. The combined effects of  $\beta$ -adrenergic stimulation on both the L-type  $\text{Ca}^{2+}$  channel and the SERCA indicate a coordinated and complex system for controlling the dynamic changes in the intracellular  $[\text{Ca}^{2+}]$  during even a single heart beat.

## SECTION II.C: CALCIUM AND MYOCARDIAL CONTRACTION

It is well accepted from the studies performed by Ringer over a century ago that myocardial contraction is dependent on extracellular  $\text{Ca}^{2+}$  (39). To discuss the function of the heart on any level it is important to have at least a basic understanding of the cardiac cycle and how it relates to individual myocytes. Cardiac function has been studied by virtually every discipline in the basic sciences and many definitions have arisen to describe the way the heart works. Physiologists describe the cardiac cycle by measuring arterial pressure and cardiac output over time, while electrophysiologists describe the cardiac cycle by measuring cellular ionic currents. Cell and molecular biologists provide elegant descriptions of how the contractile proteins interact and how the genes which code for these proteins are controlled and expressed. The combined efforts of these disciplines has provided a skeleton of information regarding the mechanisms that underlie the cardiac cycle.

In this section I will discuss the cardiac cycle as a sequence of events which are dependent on transient fluctuations in cytoplasmic  $[\text{Ca}^{2+}]$ . Figure 9 is a modified diagram taken from a classic description of the cardiac cycle by Dr. Carl J. Wiggers (47). In this scheme, all events which can be measured in an intact animal are included; arterial blood pressure, ventricular pressure, ventricular volume, and the electrocardiogram. The first step in understanding the cardiac cycle is recognizing that two main periods or phases exist, systole and diastole.

Cardiac systole can be defined as the period of myocardial contraction. As the ventricle contracts, pressure within it rises until such point where blood is ejected into the great arteries. This is indicated in figure 9 by the pressure and volume tracings. During ejection, ventricular pressure increases while ventricular volume decreases. The period of myocardial relaxation is termed

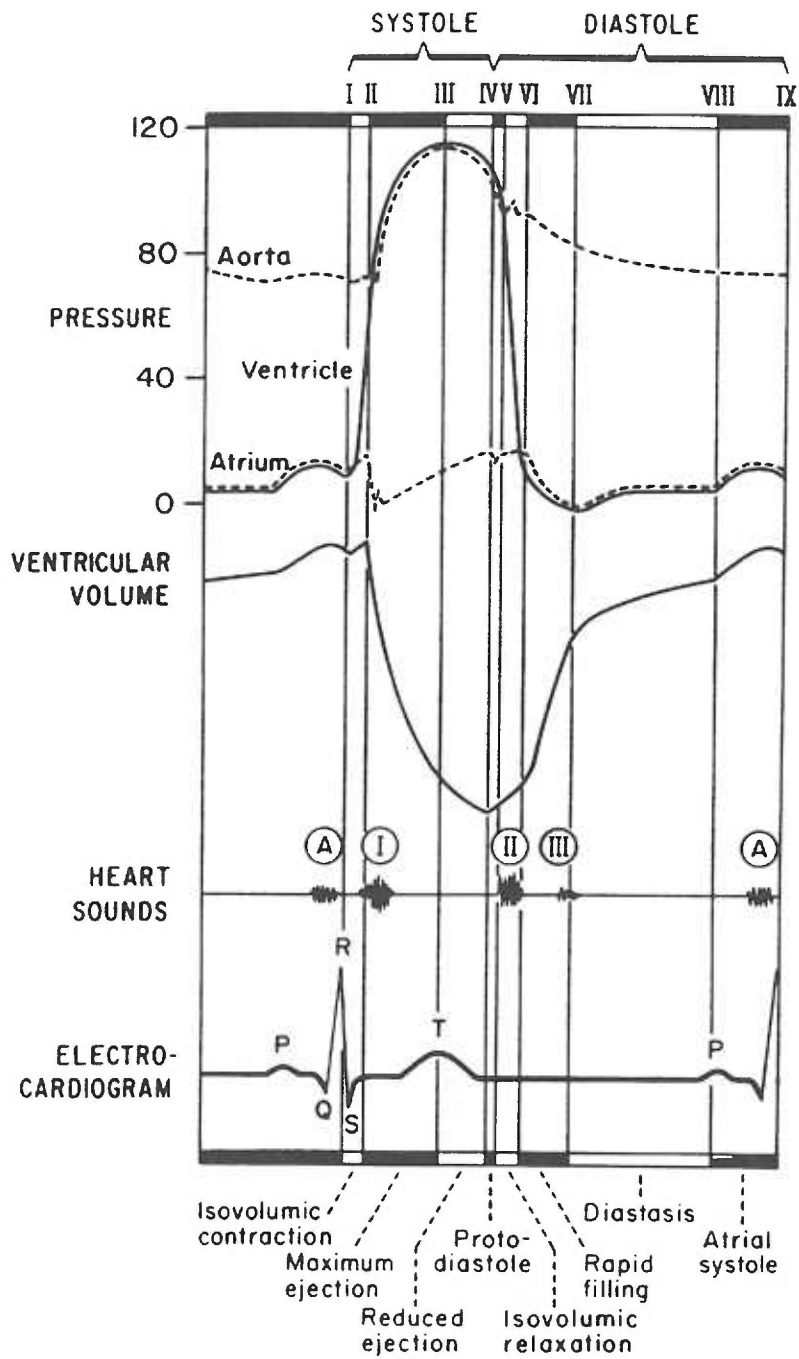


Figure 9: Wiggers diagram, (From Katz, 1992)



diastole. For the heart to function in a rhythmic fashion it must be able to relax to allow the ventricles to refill with blood. This period is also represented in figure 9 by the pressure and volume tracings. In this case, ventricular pressure is falling while ventricular volume is rising. Because the focus of the remainder of this discussion will be on  $\text{Ca}^{2+}$ , I will refer systole as the period during the cycle when intracellular  $\text{Ca}^{2+}$  is at peak levels ( $10\mu\text{M}$ ) and to diastole is the period when intracellular  $\text{Ca}^{2+}$  is at resting levels ( $0.2\mu\text{M}$ ).

The underlying stimulus for myocardial contraction at the cellular level is the action potential which, unfortunately, can not be measured in the intact animal. However, the electrocardiogram (ECG), which is a representation of the electrical activity of the whole heart, can be measured. The ECG is divided into well defined periods which are conserved across mammalian species. Briefly, the first peak or "P-wave", represents atrial depolarization. Because membrane depolarization is the stimulus for myocardial contraction, the atrial pressure rises just following depolarization. The second and most prominent wave is termed the "QRS" complex which represents ventricular depolarization and just precedes ventricular contraction. The most interesting wave for this discussion is, however, the "T-wave". This wave represents ventricular repolarization. During diastole, the ventricular myocardium relaxes and the ventricular chamber fills with blood in preparation for another beat.

How do ventricular contraction and relaxation correspond to the action potential? To answer this, it is necessary to examine the cardiac cycle at a more cellular level. Figure 10 represents the cellular events of each heart beat; a) action potential, b)  $\text{Ca}^{2+}$  transient, c) force development (54). The stimulus for myocardial contraction is the cardiac action potential which is represented in panel "a". The timing of each event is indicated by the vertical marks. The most important event, aside from the action potential, is the rapid rise in cytoplasmic

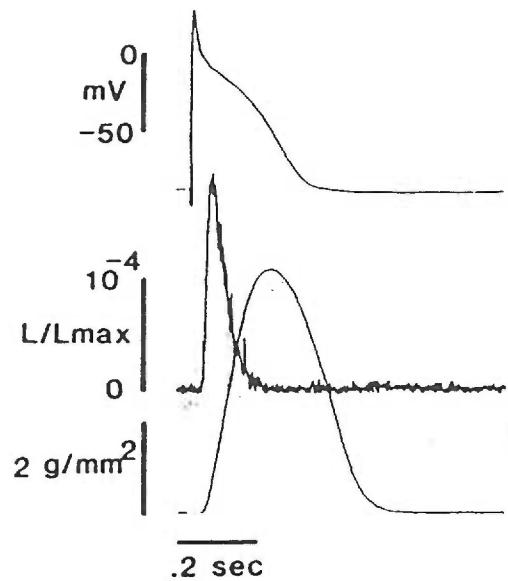


Figure 10: This figure shows the cellular events underlying the cardiac cycle action potential (top), aequorin light signal (middle), and force development (bottom) in papillary muscle. The action potential is the stimulus for myocardial contraction. The  $\text{Ca}^{2+}$  which enters during the action potential stimulates the SR to release its  $\text{Ca}^{2+}$  stores, panel b. As indicated by the vertical mark, the increase in  $[\text{Ca}^{2+}]_i$  is necessary for force development. Recall the studies with ryanodine, (same study, fig 8) supported this. (From Tseng, 1988)

$[Ca^{2+}]_i$  (panel b). This occurs prior to the onset of tension development (panel c), as shown by the vertical marks. Recall that when SR  $Ca^{2+}$  is inhibited by ryanodine contraction does not occur (fig. 8) (54). Together these components represent the major cellular events which underlie the cardiac cycle described above.

### Excitation-Contraction Coupling :

In order for the action potential to stimulate sarcomere shortening the membrane depolarization must be translated into a signal which the myofibrils can respond to. The process by which this translation occurs has been called "excitation-contraction"coupling (EC coupling) (70). To begin this discussion, it is necessary to understand the genesis of the cardiac action potential.

Three main ionic currents underlie action potentials of cardiac myocytes;  $I_{Na}$ ,  $I_{Ca}$  and  $I_K$ . Fig. 11 shows a typical action potential from a ventricular myocyte and the underlying membrane conductances for  $Na^+$ ,  $Ca^{2+}$  and  $K^+$ . The upstroke of the action potential is due to the rapid influx of  $Na^+$  ions through voltage dependent  $Na^+$  channels. With an adequate excitatory stimulus, the  $V_m$  can be depolarized to the threshold potential for the  $Na^+$  channel. The threshold potential is the potential at which  $Na^+$  channels open and allow  $Na^+$  to enter the cell (fig. 11). Following the fast  $Na^+$  current a slower inward current is observed which has been attributed to the flux of  $Ca^{2+}$  via the L-type  $Ca^{2+}$  channel. The influx of  $Ca^{2+}$  carries two positive charges per ion thus contributing to membrane depolarization. Unlike  $Na^+$  channels, L- $Ca^{2+}$  channels are inactivated slowly which results in a plateau phase in the action potential, (Fig.11). The ventricular myocyte action potential is long and can last up to 400ms.

Finally, the repolarization phase is dependent on the outward flux of  $K^+$  ions. By examining the bottom panel of fig.11 it is clear that the slow opening of

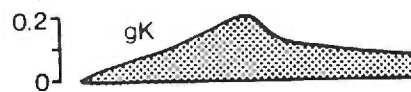
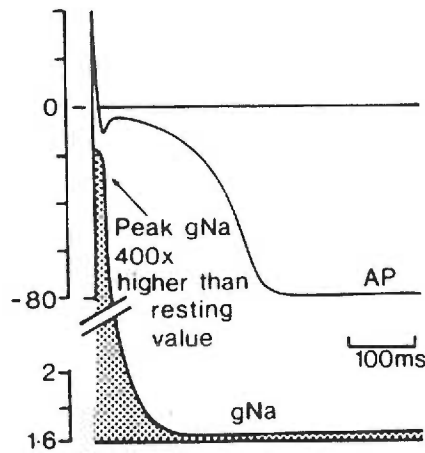


Figure 11: Schematic of a cardiac action potential and the ionic conductances ( $g^X$ ) which are responsible for its shape. The upstroke of the action potential is due to the rapid opening of  $\text{Na}^+$  channels. With a threshold level stimulus the fast  $\text{Na}^+$  channels open, as represented by the increase in  $g_{\text{Na}^+}$ . This channel does not remain open long as it is inactivated by the depolarized membrane potential. Following the upstroke, the L-type  $\text{Ca}^{2+}$  channels open as indicated by the increase in  $g_{\text{Ca}^{2+}}$ . The influx of  $\text{Ca}^{2+}$  gives rise to the plateau phase of the cardiac action potential. During the plateau phase  $\text{K}^+$  channels open slowly as indicated by the gradual increase in  $g_{\text{K}^+}$ . The combination of inactivating  $\text{Ca}^{2+}$  channels and opening  $\text{K}^+$  channels gives rise to the repolarization phase. (Modified from Opie, 1991)

the  $K^+$  channel contributes to the plateau phase. With the slow inactivation of the L-type  $Ca^{2+}$  channel and the activation of the  $K^+$  channel the plateau phase begins to fall off until the membrane potential is back to resting levels. Together these currents make up the action potential which serves as the stimulus for muscular contraction.

The process by which the electrical stimulus (action potential) is translated into a mechanical event (muscle contraction) is called excitation-contraction coupling (EC coupling). Although each muscle type exhibits unique properties with respect to EC coupling, similarities between muscle types do exist. One event common to all muscle types is the need for transient increases in cytoplasmic  $[Ca^{2+}]$  followed by  $Ca^{2+}$  binding to the contractile proteins. In both skeletal and cardiac muscle the predominant source of "activator"  $Ca^{2+}$  is the SR. However, the mechanism by which the  $Ca^{2+}$  stores are released during a contraction differ between the two muscle types.

In skeletal muscle, a direct coupling between membrane depolarization and SR calcium release has been identified. (71) In this system, charge movement within the T-tubule membrane "triggers" the release SR  $Ca^{2+}$  stores. Although the precise "trigger" mechanism has not been identified, pharmacological studies suggest an important role of the L-type  $Ca^{2+}$  channel (72,73). An exciting study by Tanabe and colleagues using dysgenic skeletal myotubes clearly showed a role for the L-type  $Ca^{2+}$  channel in skeletal muscle EC coupling (74). The dysgenic myotube lacks both mechanical activity and a measurable slow-inward current prior to cDNA injection. In myotubes which were injected with cDNA a slow inward current was detected under voltage-clamp conditions. In this study EC-coupling was restored following the expression of cDNA encoding the L-type  $Ca^{2+}$  channel. These results confirmed that functional incorporation of the  $Ca^{2+}$  channel had occurred. In addition, the injected myotubes were observed to

spontaneously contract. Control and injected dysgenic myotubes retained mechanical activity in the absence of extracellular  $\text{Ca}^{2+}$  supporting a depolarization-induced- $\text{Ca}^{2+}$ -release. Together these results support the hypothesis that the L-type  $\text{Ca}^{2+}$  channel serves as the charge sensor responsible for SR  $\text{Ca}^{2+}$  release, although not everyone is convinced.

The mechanism of SR  $\text{Ca}^{2+}$  release in cardiac muscle is much different than that described for skeletal muscle. Unlike skeletal muscle in which  $\text{Ca}^{2+}$  release is triggered by membrane depolarization alone, cardiac SR  $\text{Ca}^{2+}$  stores are believed to be released in response to the influx of  $\text{Ca}^{2+}$  via the L-type  $\text{Ca}^{2+}$  channel (50). Although the L-type  $\text{Ca}^{2+}$  channel has been shown to play an integral role in SR release in striated muscle (74), it functions differently in cardiac muscle.  $\text{Ca}^{2+}$  influx through L-type  $\text{Ca}^{2+}$  channels is not involved in activating SR calcium release in skeletal muscle cells as it appears to be in cardiac muscle cells. (68,75,77). The basis for these cell type differences is not completely clear. The L-type channels in cardiac muscle has faster activation kinetics compared to those in skeletal muscle (76).

In the skinned myocyte preparation, myocytes are mechanically skinned of their sarcolemma while their organelles, including the SR, remain intact (78). Using these skinned cardiac myocytes, Fabiato showed that small quantities of  $\text{Ca}^{2+}$  can stimulate the release of  $\text{Ca}^{2+}$  from within the SR. Thus, the intracellular milieu can be controlled by changing the perfusion solution. Fabiato determined that the rate of  $\text{Ca}^{2+}$  influx triggers the release of SR  $\text{Ca}^{2+}$ . They observed that increasing the calcium concentration at the outer surface of the SR (skinned myocyte) caused  $\text{Ca}^{2+}$  release from the SR when the rate of increase was high, but merely caused  $\text{Ca}^{2+}$  accumulation when the influx rate was low. (79) Analysis of the  $\text{Ca}^{2+}$  current under voltage clamp conditions in the intact myocyte support this suggestion. Two components of the  $\text{Ca}^{2+}$  current have been characterized: a) fast

initial component which inactivates and b) slow component which corresponds to noninactivating channels (141). The fast inactivating phase may serve as the stimulus for SR  $\text{Ca}^{2+}$  release, while the slow phase may contribute to SR loading described above. It is interesting to note that the  $\text{Ca}^{2+}$  channel found in skeletal muscle myocytes do not have a fast kinetic phase (76). This may explain, in part, the lack of  $\text{Ca}^{2+}$ -induced  $\text{Ca}^{2+}$  release in skeletal muscle.

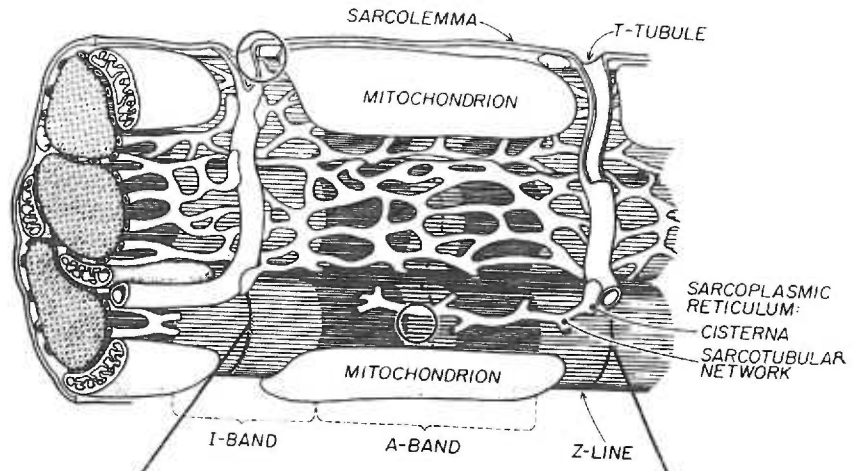
### Contractile Proteins of Muscle:

The proteins which mediate muscular contraction are similar all muscle types. Actin and myosin are the major contractile proteins which make up thick and thin filaments and are responsible for sarcomere shortening in striated muscle. The thin filaments are attached to Z-bodies (Fig. 12.B) that demarcate individual sarcomeres. Thick filaments which are roughly twice the diameter of the thin filaments are interspersed among the thin filaments. A cross-section through the A band, as shown in figure 12.C, shows the microanatomy of the sarcomere. Thick filaments are surrounded by six thin filaments. This arrangement is the optimal configuration for actin-myosin interaction and subsequent tension development.

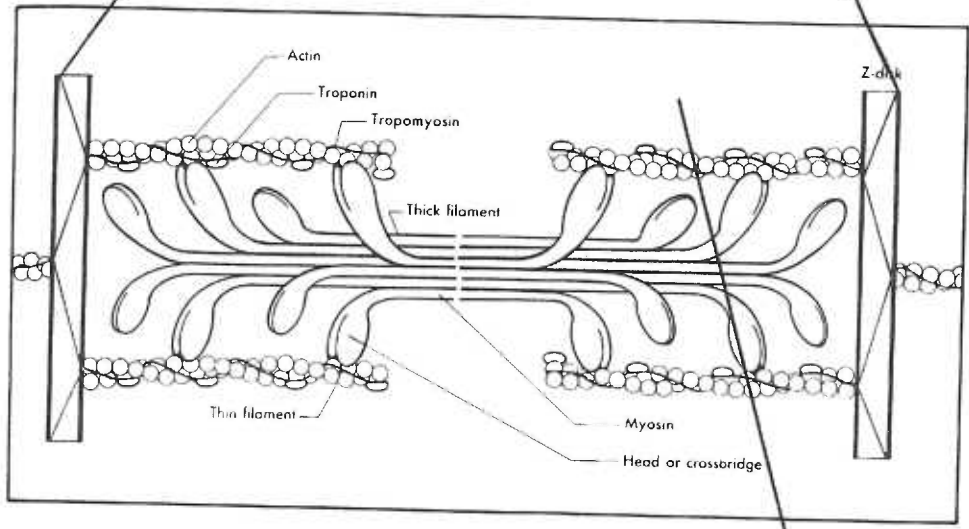
Thick filaments are composed of myosin which is a complex protein made up of 6 different polypeptides, 2 myosin heavy chains (MHC), and 4 light chains (MLC) The MHC are configured together in a rod-like helix with each chain forming a globular domain at the C-terminus. This globular "head" region protrudes from the main myosin body on a hinge like stalk (Figure 13). This head region contains the actin binding sites as well as intrinsic ATPase activity. The myosin ATPase allows the head to cleave ATP and to use the energy derived from the ATP's high energy phosphate bond to energize the contraction process.

Figure 12

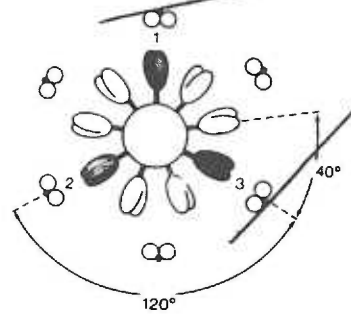
A.



B.



C.





Thin filaments are composed of actin, tropomyosin and troponin. Although actin is the primary contractile protein of the thin filament, tropomyosin and troponin serve key roles as regulators of actin-myosin interaction. Troponin (TPN) is actually a complex of proteins which function together to regulate actin-myosin interaction. TPN is composed of three proteins; TPN-C (calcium), TPN-I (inhibitory), and TPN-T (tropomyosin). Together these proteins interact to control the steric positioning of tropomyosin within the groove of the actin polymer . TPN-C is a  $\text{Ca}^{2+}$  binding protein which, upon binding  $\text{Ca}^{2+}$ , induces a conformational change in tropomyosin (Fig. 13). At rest, tropomyosin resides in the groove of the actin molecule where the myosin head units will bind. Upon  $\text{Ca}^{2+}$  binding to troponin-C, tropomyosin makes a conformational change that alters its position relative to actin such that the myosin binding sites are exposed. This conformational change allows the subsequent actin-myosin interaction to proceed. Subsequent relaxation occurs as a result of cytoplasmic  $\text{Ca}^{2+}$  returning to sub-micromolar levels ( $0.2\mu\text{M}$ ). At rest, cytoplasmic  $\text{Ca}^{2+}$  levels are below the  $K_D$  of TPN-C  $\text{Ca}^{2+}$  and hence the steric inhibition by tropomyosin is established once again.

Actin and myosin interact by way of cross-bridges. The cross-bridges are like loaded springs, which upon releasing energy as a result of ATP hydrolysis, cause the actin and myosin to move in relation to each other. Myosin is a complex protein which has intrinsic ATPase activity. It is this activity which is responsible for releasing the energy required for muscular contraction.

Formation of the actin-myosin complex, via cross-bridge formation, is dependent on the binding and subsequent hydrolysis of ATP by the myosin head. When ATP is bound to the myosin head, there is a weak binding conformation between actin and myosin, and when inorganic phosphate is released, there is a strong binding conformation (Fig. 13) In the presence of elevated  $\text{Ca}^{2+}$

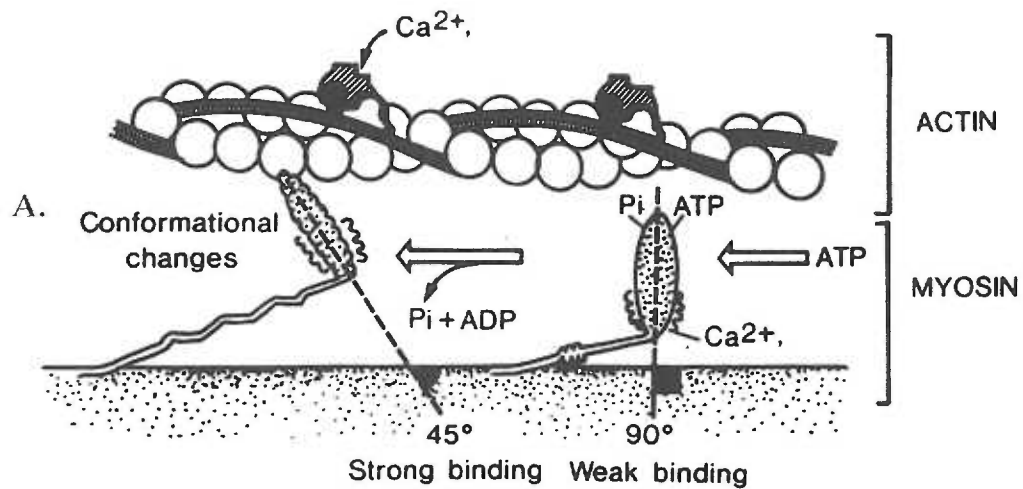
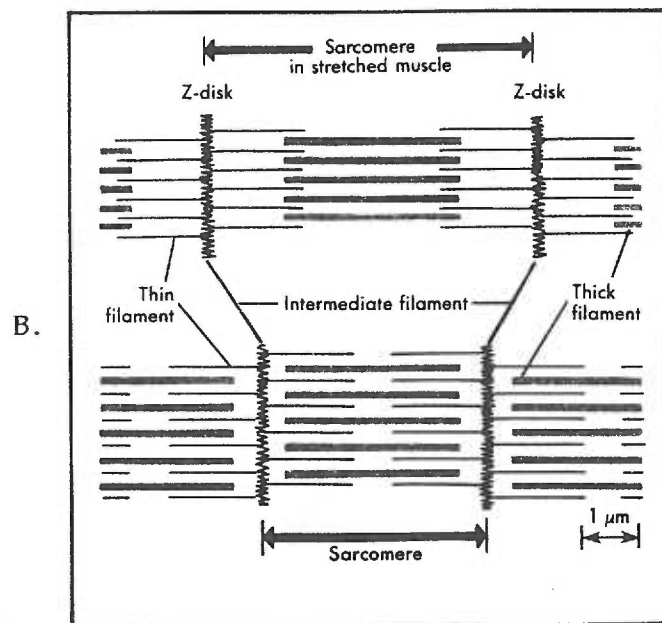


Figure 13: (A) Schematic representation of the actin-filament and the globular head of the myosin-thick filament. The globular head, which contains the ATPase activity protrudes from the main thick filament via a stalk. It is this stalk region which behaves like a spring during sarcomere shortening. The thin filament is shown here as the actin polymer complexed with tropomyosin and troponin. During systole  $[Ca^{2+}]_i$  rises and  $Ca^{2+}$  binds with troponin, as shown in this schematic. This binding induces a conformational change in the thin filament complex which results in the steric inhibition of tropomyosin being removed. In order for the actinomyosin complex to form, ATP must be bound to the myosin head unit. With subsequent ATP hydrolysis by the intrinsic ATPase activity of the myosin head unit, a strong binding affinity of myosin for actin occurs and the final result is the a formation of the actin-myosin bond. The energy for the actual contraction is derived from the release of  $P_i$ . (B) Relationship between the actin-thin filaments and the myosin-thick filaments during sarcomere shortening. (From Ganong, 11989)



(physiological systole) and following ATP hydrolysis the myosin heads go through an oarlike motion from a 90° configuration to a 45° angle with respect to the myosin body. This motion pulls the actin filaments toward the center of the A band resulting in sarcomere shortening. This is depicted in figure 13.b. The lowering of free Ca<sup>2+</sup> ion concentration (physiological diastole) causes the dissociation of the TPN-C-Ca<sup>2+</sup> complex and hence the detachment of crossbridges and the decrease in force.

The cellular mechanisms which lead to the diastolic fall in cytoplasmic Ca<sup>2+</sup> are the subject of this thesis. The interaction of myosin and actin described above applies to immature cardiac myocyte contraction as well as for adults. However, the source of activator Ca<sup>2+</sup> and the mechanism by which cytoplasmic Ca<sup>2+</sup> is sequestered is different at each stage of maturation. As described in section I, the immature cardiac myocyte, by definition, lacks a well developed SR. Considering the importance of the SR in EC coupling it is important to understand how the immature heart functions without it. The following sections will focus on the calcium transport proteins which are responsible for sequestering Ca<sup>2+</sup> and the roles each play during development.

Section III: Calcium Transport Proteins  
and  
Myocardial Relaxation

### SECTION III.A: SARCOPLASMIC RETICULUM Ca<sup>2+</sup> ATPase

#### History:

The sarcoplasmic reticulum (SR) is now known to be the major intracellular Ca<sup>2+</sup> storage organelle in Cardiac myocytes. This, however, was not known until the 1960's when several groups independently discovered that microsomal fractions isolated from skeletal muscle contained membranous vesicles which could actively accumulate Ca<sup>2+</sup> (85,86). Prior to 1960, research on a soluble "relaxing factor" from muscle homogenates was underway. It had been observed that the supernatant from high-speed centrifugations of muscle homogenates had a relaxing effect on actomyosin (87). Two theories were developed to explain this effect. Microsomal mediated relaxation was thought to be due to: a) Ca<sup>2+</sup> binding to specific receptors (86) or b) active Ca<sup>2+</sup> accumulation (85).

Studies on isolated skeletal muscle microsomes by Hasselbach and Makinose, provided the first evidence that relaxation was due to the active transport of Ca<sup>2+</sup> into the microsome (85). In this study, Ca<sup>2+</sup> uptake by microsomes was augmented by the presence of oxalate and dependent on the hydrolysis of ATP. Oxalate acts to precipitate Ca<sup>2+</sup> within the microsome and effectively maintains a low microsomal free [Ca<sup>2+</sup>]. In the presence of oxalate more Ca<sup>2+</sup> is accumulated because the total free [Ca<sup>2+</sup>] within the microsome is reduced, thus enhancing the [Ca<sup>2+</sup>] gradient across the vesicle membrane. Martonosi and Feretos also studied skeletal muscle microsomes, and confirmed the observations of Hasselbach (89). Results from many laboratories indicate that Ca<sup>2+</sup> transport is mediated by a Mg<sup>2+</sup>-dependent, membrane bound ATPase (89,90).

### Biochemistry & Function:

The SR  $\text{Ca}^{2+}$ -ATPase belongs to the "P-type" family of ion transport proteins. This class of proteins include; a) plasma membrane  $\text{Na}^+/\text{K}^+$ ATPase, b)  $\text{Ca}^{2+}$  and  $\text{H}^+$ ATPases also of the plasma membrane, and c)  $\text{Ca}^{2+}$  ATPase of the SR (SERCA). These proteins are included in the P-type class because they form a phosphorylated ("P") intermediate as part of their reaction cycle (80,91). Biochemical studies indicate that the P-type transport proteins are phosphorylated with the  $\gamma$ - phosphate of ATP on a conserved aspartic acid residue in the polypeptide chain (83). Most of the members of this class, ( $\text{Na}^+/\text{K}^+$  ATPase excluded), consist of a single " $\alpha$ " polypeptide chain (70-100kD) and have significant sequence homology. Due to the conserved nucleic acid sequences, members of this class have been hypothesized to come from a common ancestor (81,82).

A schematic showing how  $\text{Ca}^{2+}$  is transported by SERCA is shown in figure 14. The first step in this reaction is the binding of  $\text{Ca}^{2+}$  and ATP to the cytosolic face of the enzyme. The affinity ( $K_d$ ) of the SERCA for  $\text{Ca}^{2+}$  is approximately  $0.5\mu\text{mol/l}$ , which is sufficient to promote binding in the low  $[\text{Ca}^{2+}]_i$  environment. Following the initial binding reaction, the protein undergoes a conformational shift such that bound  $\text{Ca}^{2+}$  is now on the intraluminal face of the enzyme. The energy contained in the acyl-phosphate bond is used to translocate  $\text{Ca}^{2+}$  into the SR lumen. Once the  $\text{Ca}^{2+}$  is released into the SR lumen, inorganic phosphate ( $\text{P}_i$ ) is released and the enzyme returns to its native state, ready to pump more  $\text{Ca}^{2+}$ .

Regulating the rate and extent of  $\text{Ca}^{2+}$  transport into the SR affects changes in myocardial contractility. The force of contraction is dependent on the release of  $\text{Ca}^{2+}$  from the SR. The amount of  $\text{Ca}^{2+}$  released is a function of the amount of  $\text{Ca}^{2+}$  sequestered during the relaxation phase of the previous

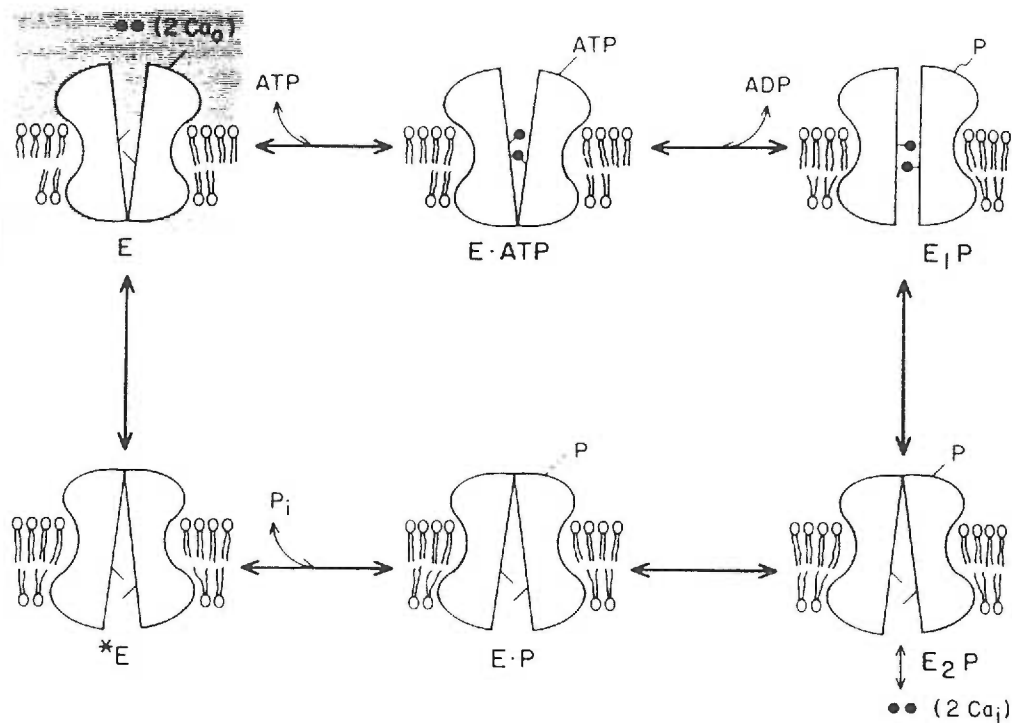


Figure 14: Schematic representation of the mechanism of action of the SERCA. The movement of  $\text{Ca}^{2+}$  across the SR membrane is coupled to the hydrolysis of ATP. Two  $\text{Ca}^{2+}$  ions are shown binding to the cytoplasmic side of the SR membrane followed by subsequent ATP binding, ATP hydrolysis and subsequent  $\text{Ca}^{2+}$  translocation. The energy stored in the acyl-phosphate bond is used to fuel the "uphill" movement of  $\text{Ca}^{2+}$ . Once  $\text{Ca}^{2+}$  is released into the SR lumen the  $\text{P}_i$  is released and the protein "resets" with the  $\text{Ca}^{2+}$  binding site on the cytoplasmic side. (From Katz, 1992)

beat. This amount is dependent on the rate at which the SERCA pumps  $\text{Ca}^{2+}$  into SR. The SERCA is directly regulated by both  $\text{Ca}^{2+}$  and ATP (ADP) via simple enzyme kinetics.  $\text{Ca}^{2+}$  and ATP serve as substrates for the SERCA. When cytoplasmic  $\text{Ca}^{2+}$  is elevated (systole) the SERCA will be stimulated to pump  $\text{Ca}^{2+}$  into the SR. SERCA-mediated  $\text{Ca}^{2+}$  transport is also regulated by the sympathetic nervous system via  $\beta$ -adrenergics stimulation.

Activation of the sympathetic nervous system stimulates the myocardium to increase force of contraction and rate of relaxation (48). This is important during periods of exertion such as physical work or exercise.  $\beta$ -adrenergic stimulation enhances myocardial contraction by modulating the activity of both the L-type  $\text{Ca}^{2+}$  channel and the SERCA. The  $\beta$ -adrenergic effect is mediated by a cAMP-dependent protein kinase A. This protein kinase phosphorylates both the L-type  $\text{Ca}^{2+}$  channel and the SR protein, phospholamban (PLN). Phosphorylation of the L-type  $\text{Ca}^{2+}$  channel enhances the  $\text{Ca}^{2+}$  current, resulting in a larger  $\text{Ca}^{2+}$  influx. Because the magnitude of the  $\text{Ca}^{2+}$  current serves as the trigger for SR calcium release in cardiac myocytes, this effect increases the amount of  $\text{Ca}^{2+}$  released from the SR and thus the force of contraction.

In addition to increasing the amount of  $\text{Ca}^{2+}$  released, the rate of  $\text{Ca}^{2+}$  uptake via the SERCA is enhanced by cAMP dependent phosphorylation of phospholamban. The structure of PLN is similar to the regulatory region of the sarcolemmal  $\text{Ca}^{2+}$ -ATPase (93). Both of these regulatory mechanisms function by inhibiting  $\text{Ca}^{2+}$  transport by interfering with  $\text{Ca}^{2+}$  binding. In the native state, PLN inhibits the SERCA. Thus the SERCA normally has  $\text{Ca}^{2+}$  transporting reserve. Upon phosphorylation of PLN this inhibition is removed and  $\text{Ca}^{2+}$  transport is enhanced. In addition, phosphorylation of PLN increases the  $\text{Ca}^{2+}$  sensitivity of the SERCA. Together, the increased



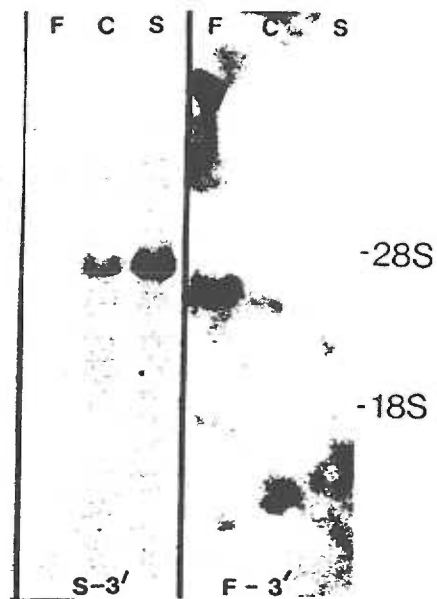
Ca<sup>2+</sup> sensitivity and rate of uptake into the SR results in enhanced myocardial relaxation.

The SERCA exists in several forms and fast-twitch, slow-twitch, cardiac, and non-muscle forms of the enzyme have been identified (94). Biochemical studies support the existence of unique muscle specific SERCA isoforms. Cardiac and skeletal muscle SERCA have been differentiated at the nucleotide level (96) and by the fact that the activity of the cardiac SERCA is regulated phospholamban which has not been detected in fast twitch muscle (55). Although it has been difficult to measure significant biochemical differences between fast twitch and slow twitch muscle isoforms, clinical studies suggest that differences must exist. A genetic basis for different skeletal muscle forms of the ATPases is suggested by Brody's disease (98). This disease, manifesting as a diminished capacity for skeletal muscle relaxation, results from a deficiency of Ca<sup>2+</sup>-ATPase in fast twitch, but not in slow twitch muscle.

#### Molecular Biology:

Much of the work presented in this section was done by D.H. MacLennan and colleagues who were responsible for first purifying the SERCA protein in 1970 (84). The first cloning studies were performed on skeletal muscle using probes designed from partial cDNA sequences which were deduced from amino acid sequences (84). Although the focus of this discussion is the cardiac SERCA, the goal of the original cloning experiments was to characterize the skeletal muscle Ca<sup>2+</sup>-ATPase.

Discovery of the cardiac muscle Ca<sup>2+</sup>-ATPase clone was fortuitous. Using primers designed from previously determined sequence of the fast twitch muscle Ca<sup>2+</sup>-ATPase gene, this group screened a rabbit skeletal muscle



A.

B.

Figure 15: Northern blot analysis of rabbit muscle mRNA. Poly(A) RNA from rabbit fast twitch, slow twitch and cardiac muscle was separated on a 1% denaturing agarose gel and subsequently transferred to solid support for sequential hybridizations. In panel "A", the 3' UTR of the slow twitch skeletal muscle clone was used. Message specific for this clone was detected in cardiac (C) and slow twitch (S) muscle but not fast twitch (F) muscle. In panel "B", the 3' UTR of the fast twitch skeletal muscle clone was used. Message specific for this clone was detected in fast muscle only (F). (From Brandl et al., 1986).

cDNA library. Two cross-hybridizing clones (pFA1 and pCA3) were isolated and their sequences were analyzed for homology to the deduced ATPase amino acid sequence of fast twitch  $\text{Ca}^{2+}$ -ATPase. Clone pFA1 was highly homologous with the fast twitch  $\text{Ca}^{2+}$ -ATPase, whereas clone pCA3 shared only some homology. Clone pCA3 contained 3722 base pairs and coded for a complete protein of approximately 110kD. Although this clone coded for a protein which was slightly smaller than the protein coded for by clone pFA1, the deduced amino acid sequence was 84% homologous. Together these indicated that the clone probably coded for a  $\text{Ca}^{2+}$ -ATPase, although the tissue origin was not known.

The first indication that clone pCA3 coded for a cardiac ATPase isoform came about when a tryptic digest product of rabbit cardiac SR was isolated (156) and sequenced. Trypsin cleaves the  $\text{Ca}^{2+}$ -ATPase into two characteristic peptides between amino acid residues 505 and 506 (87). Near this cleavage site is the binding site for fluorescein isothiocyanate (FITC). The deduced amino acid sequence of the FITC site in clone pCA3 is TSMS which divergent from that of clone pFA1 (AAVGN). The homology between the FITC of clone pCA3 and that from the major trypsin product reported by Briggs was 100%. This provided the first evidence that clone pCA3 may represent the cardiac  $\text{Ca}^{2+}$ -ATPase.

Studies by Brandl et al. suggested that the slow twitch and cardiac muscle  $\text{Ca}^{2+}$ -ATPase may arise from a common gene. Using northern blot analysis Brandl (95) showed that the slow twitch and cardiac  $\text{Ca}^{2+}$ -ATPase transcript were detected with the 3' untranslated region (UTR) of clone pCA3, whereas the fast twitch transcript was not (figure 15.a). Similarly, when the same northern blot was probed with the 3'UTR of clone pFA1 only the fast twitch transcript was detected (Fig. 15.b). Although these results do not prove

that the slow-twitch and cardiac  $\text{Ca}^{2+}$ -ATPase originate from the same gene they do suggest it. Structural and functional similarities exist between slow twitch and cardiac muscle  $\text{Ca}^{2+}$ -ATPase genes/proteins. Immunological studies using antibodies raised against the cardiac  $\text{Ca}^{2+}$ -ATPase detected the protein in both cardiac and nonmuscle tissue but not in fast twitch muscle. Furthermore, antibodies against the regulatory protein PLN have detected the protein in slow and cardiac muscle but not fast twitch muscle. This supports the hypothesis that slow and cardiac muscle may share structure -function similarities.

Subsequent studies have revealed that a common gene (SERCA2) codes for both the cardiac and slow-twitch muscle isoforms and that the alternative splicing is responsible for the two isoforms (140). In summary, three genes encoding five SERCA isoforms have been identified: SERCA1a (adult fast-twitch muscle), SERCA1b (neonatal fast-twitch muscle), SERCA2a (cardiac/slow-twitch muscle), SERCA2b (smooth/nonmuscle), SERCA3 (isoform expressed in muscle and nonmuscle tissues) (134).

### SECTION III.B: SARCOLEMMA SODIUM-CALCIUM EXCHANGER

#### History:

The discovery of the cardiac sodium-calcium exchanger (NCX) occurred in the late 1960's. However, in 1921, pioneering work by Daly and Clark suggested an antagonistic relationship between  $\text{Na}^+$  and  $\text{Ca}^{2+}$  with respect to myocardial contractility. In these early studies, a positive inotropic effect was observed when extracellular  $[\text{Na}^+]$  was reduced. The inotropic effect was similar to that observed when extracellular  $[\text{Ca}^{2+}]$  is increased. By 1960 it was clear that the inotropic response observed in earlier studies (99) was specific for  $\text{Na}^+$  alone and not other monovalent cations (100). This set the stage for rapid discoveries regarding the role of extracellular  $\text{Na}^+$  in  $\text{Ca}^{2+}$  transport across the sarcolemma. Several independent studies observed that isotopic  $^{45}\text{Ca}^{2+}$  uptake by intact hearts or isolated papillary muscle could be enhanced by removing extracellular  $\text{Na}^+$  (61,101-103).

By 1970 the concept of a cardiac sarcolemmal ion transporter specific for  $\text{Na}^+$  and  $\text{Ca}^{2+}$  was becoming accepted, although the details were obscure. Much of the work to define the  $\text{Na}^+$  dependent inotropic response was carried out by Reuter and colleagues. They measured  $^{45}\text{Ca}^{2+}$  efflux from guinea pig atria under varying ionic conditions (104). Figure 16 is a summary of their results. By examining panel "A", it is apparent that as extracellular  $\text{Na}^+$  is reduced, the amount of  $\text{Ca}^{2+}$  in the effluent increases. The bottom trace (a) is the control value ( $[\text{Na}]_o=149\text{mM}$ ). Under conditions when  $[\text{Na}]_o$  is reduced {(b),  $[\text{Na}]_o=81\text{mM}$ , and (c),  $[\text{Na}]_o=47\text{mM}$ } the amount of  $\text{Ca}^{2+}$  in the effluent is increased. Panel "B" represents the dependence of  $\text{Ca}^{2+}$  efflux on the ratio of

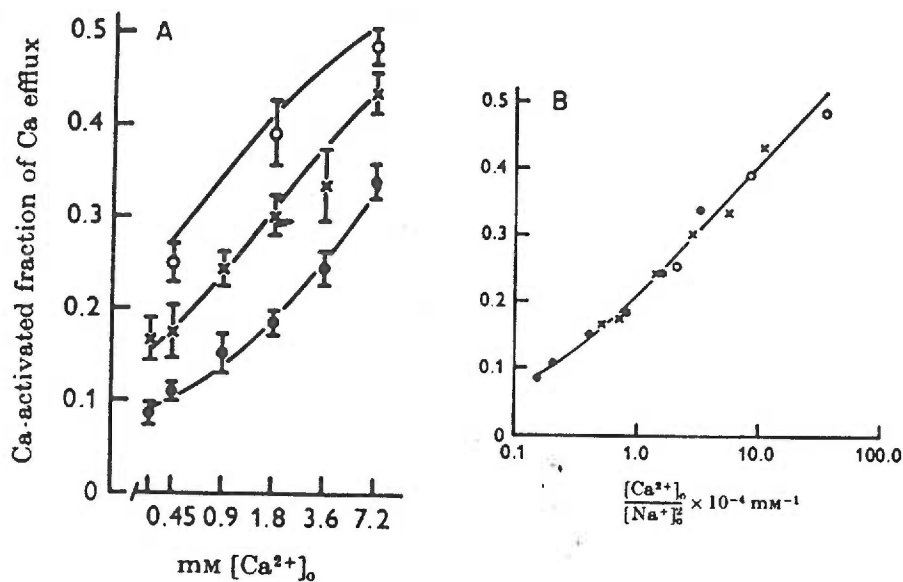


Figure 16: Relationship between Ca<sup>2+</sup>-dependent efflux from guinea pig atria and extracellular [Na<sup>+</sup>]. Panel "a" shows the effect of reducing [Na<sup>+</sup>]<sub>o</sub> on the Ca<sup>2+</sup> efflux, (●) is high Na<sup>+</sup> at 149 mM, (×) is moderate Na<sup>+</sup> at 81mM and (○) is low Na<sup>+</sup> at 47 mM. It is apparent from this figure that as [Na<sup>+</sup>]<sub>o</sub> is reduced the Ca<sup>2+</sup>-activated fraction increases. Panel "b" is a plot of the dependence of Ca<sup>2+</sup> activated efflux on the ratio [Ca<sup>2+</sup>]<sub>o</sub>/[Na<sup>+</sup>]<sub>o</sub><sup>2</sup>. This plot is merely a summary of panel "a". A nearly linear dependence between the Ca<sup>2+</sup>-dependent fraction of Ca<sup>2+</sup> efflux and [Ca<sup>2+</sup>]<sub>o</sub>/[Na<sup>+</sup>]<sub>o</sub><sup>2</sup> the ratio was observed, regardless of variations in the absolute concentrations of either ion over a fairly broad range (b). These data suggest that the two ions may bind to share the same site on the proposed transporter. (From Reuter and Seitz, 1967).

$[Ca^{2+}]_i/[Na^+]_o^2$ . An interesting observation was made regarding the kinetics of the "transporter". The apparent  $K_m$  of the "transporter" for  $Ca^{2+}$  increased with increasing  $[Na^+]_o$ , suggesting a competitive relationship for the two ions with respect to binding to extracellular sites.

With the development of the isolated sarcolemmal vesicle system (105), advances in the understanding of this apparent competitive ion transporter resulted. This model is extremely useful because both intra- and extravesicular compartments can be experimentally manipulated. Using crude cardiac sarcolemmal preparations Reeves and Sutko (106) concluded that the apparent co-transporter was localized to the sarcolemmal. It was Pitts however that further characterized the transporter by measuring  $^{45}Ca^{2+}$  uptake into sarcolemmal vesicles and determining a stoichiometry of  $3Na^+$  to  $1Ca^{2+}$  transported across the sarcolemmal (108). Fig 17 (Fig. 3 from 107) is a representation of this type of study. Briefly, isolated vesicles are first generated that have either high intravesicular  $Na^+$  ( $[Na^+]_i=160mM$ ) or low intravesicular  $Na^+$  ( $[K^+]_i=160 mM$ ) and then  $^{45}Ca^{2+}$  is introduced to the extravesicular medium.  $^{45}Ca^{2+}$  uptake occurs when intravesicular  $[Na^+]_i$  is elevated (Fig X.x, trace "a") but does not occur when  $K^+$  is substituted for the  $Na^+$  (trace "b"). If  $Na^+$  is added to the extravesicular medium as indicated by trace "c" in fig. X.x,  $^{45}Ca^{2+}$  is reduced. This is due to a reduction of the  $Na^+$  gradient across the vesicle membrane. From these studies it is clear that the driving force for  $Ca^{2+}$  uptake is the transsarcolemmal  $Na^+$  gradient.

### Biochemistry and Function:

The stoichiometry of ion exchange for the cardiac NCX has been difficult to determine with confidence. Although it is now well accepted that the cardiac NCX is an electrogenic ion co-transporter; exchanging three  $\text{Na}^+$  for one  $\text{Ca}^{2+}$ , early studies disputed this. Using the isolated vesicle system Pitts and colleagues measured  $^{22}\text{Na}^+$  coupled  $^{45}\text{Ca}^{2+}$  uptake and determined an exchange ratio of 2.9-3.1 (108). Similar conclusions have been made using isolated cardiac myocytes and intact ventricular myocardium (109,110).

During the last decade the cardiac NCX has been purified and subsequently cloned. Purification of this protein was troubled by the lack of a detectable marker during the purification steps as well as its relatively low abundance in tissue (111). Nonetheless, after several inconsistent reports of isolated proteins which retained exchanger activity (112-114), a 120kD protein was purified from canine ventricle which appeared to be the NCX (115). In this study three predominant protein forms were observed, 160kD, 120kD and 70kD molecular weight. All three protein species retain exchanger activity when incorporated in proteoliposomes.

Further analysis under non-reducing conditions suggests that the 160kD protein represents a non-reduced dimer of the 120kD and 70kD proteins (Fig. 18.a). The 70kD protein appears to be the active proteolytic fragment of the 120kD protein (Fig 18.b, 18.c). The protein fraction in lane "b" is prior to treatment with chymotrypsin and lane "c" is the same sample after treatment. Thus it appears that the 70kD protein may be a product of proteolysis. These results have since been reproduced by others.

Two models have been proposed to explain the mechanism of action of the cardiac NCX, "simultaneous" and "consecutive". There is evidence supporting both models, and the question "how does the exchanger



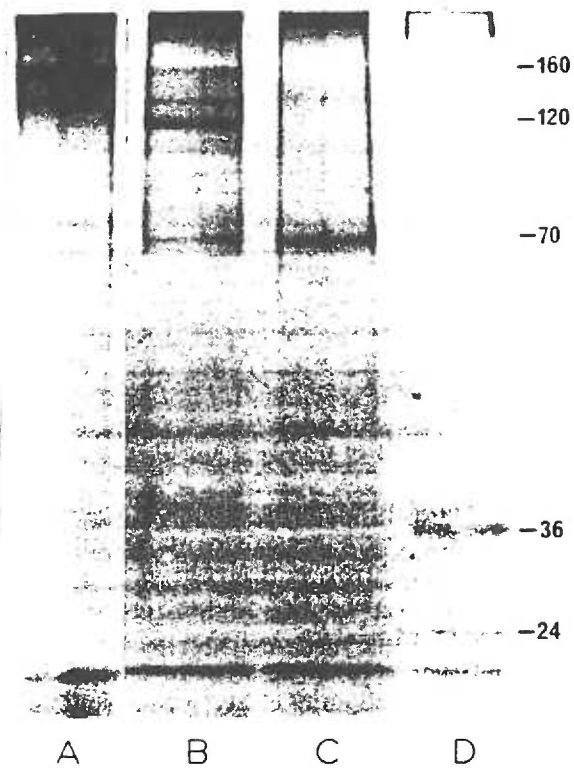


Figure 18: SDS-PAGE of purified the SL NCX protein. In lane "a" the protein is run under non-denaturing conditions which gives a predominant band at 160 kD. Under moderate denaturing conditions, as in lane "b", three characteristic bands are observed, 160kD, 120 kD and 70 kD. The 70 Kd band is believed to be a proteolytic digest product due to the observation that it increases when the sample is pretreated with chymotrypsin (lane "c"). (From Philipson, 1988).

function?" remains open; a brief description of both models will be presented here. The "simultaneous" model suggests that  $\text{Na}^+$  and  $\text{Ca}^{2+}$  bind to the protein and are translocated at the same time. The "consecutive" model on the other hand, requires the binding of  $\text{Na}^+$  and its translocation prior to the binding of  $\text{Ca}^{2+}$  and its subsequent translocation. A major principle to which proponents of both sides agree is that for the exchanger to function by a consecutive mechanism the affinity of the exchanger for  $\text{Ca}^{2+}$  must be dependent on the binding and  $[\text{Na}^+]_o$ . Durkin et al argue against the consecutive model because they have not been successful at observing half-turnover reactions of the exchanger (118). In a consecutive model the complete transport cycle must occur as two events (two half-reactions). Therefore, if the mechanism of action is consecutive then the half-turnover reactions should be detectable. The simultaneous model is supported by studies which have shown that the affinity ( $K_d$ ) of the exchanger for  $\text{Ca}^{2+}$  is independent of  $\text{Na}^+$  binding to the extracellular face of the exchanger (109,116,117).

Using the excised giant patch on ventricular myocytes, Hilgemann found strong evidence for the consecutive model (119). With the giant patch technique it is relatively easy to manipulate the ionic compositions of both cytoplasmic (pipette solution) and extracellular (perfusion solution) spaces. He found that the affinity of the exchanger for both ions was dependent on the concentration of the counter-ion, figure 19. As mentioned above, for a transport reaction to occur in two consecutive steps, the  $K_d$  (dissociation constant) for one ion species should decrease as the counterion concentration decreases (120,121). These studies argue that the consecutive model represents the mechanism of exchanger transport.

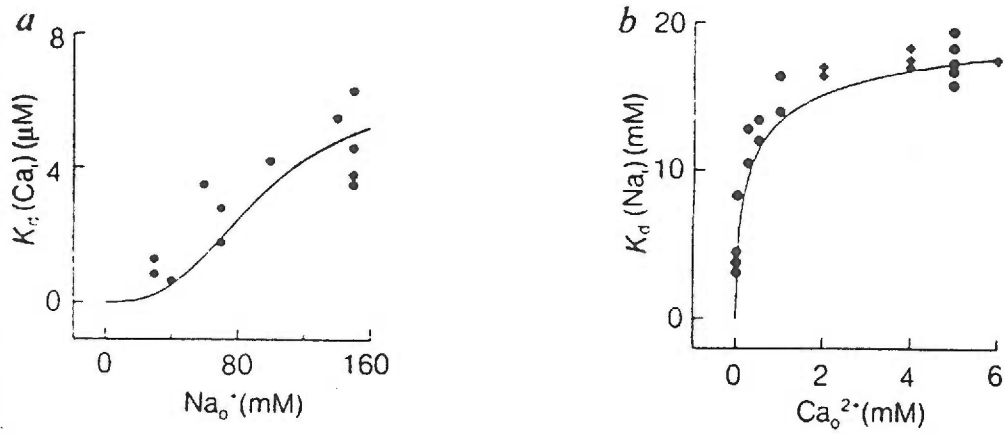


Figure 19: This figure shows that the affinity of the NCX for each ion is dependent on the concentration of the respective counter ion. Panel "a" is a plot of the  $K_d(\text{Ca}^{2+})$  vs. increasing  $[\text{Na}^+]$ . Panel "b" is a plot of the  $K_d(\text{Na}^+)$  vs. increasing  $[\text{Ca}^{2+}]$ . These results show that the binding of one ion is dependent on the presence of the other ion. This supports the suggestion that the NCX operates by a consecutive mechanism. (From Hilgemann et al., 1991)

The cardiac NCX has been shown to be sensitive to  $\text{Ca}^{2+}$ ,  $\text{Na}^+$ , and ATP concentrations. The effect of altering the concentrations of  $\text{Na}^+$  and  $\text{Ca}^{2+}$  are relatively simple to understand. These ions serve as the substrates for the exchanger and thus increasing the concentration of one will result in a displacement of the other, thus driving the reaction in the appropriate direction. For example, when  $[\text{Na}^+]_i$  is elevated as it is during quabain treatment, a positive inotropic response is observed. This response can be attributed to the reduced efflux of  $\text{Ca}^{2+}$  from the cell as  $[\text{Na}^+]_i$  is elevated and the driving force for the exchanger is reduced.

The mechanism of action of ATP on the NCX is not as straight forward. The regulation of NCX activity by MgATP, unlike that of the SERCA, appears to be independent of intracellular kinases (122). In the study by Salow and Briggs, the stimulatory effect of ATP was not blocked by kinase inhibitors or reversed by phosphatases. It was known, however, that the NCX activity is mediated by the lipid environment (123), therefore this group hypothesized that ATP may be involved in maintaining membrane lipid asymmetry. The proposed mechanism of action being aminophospho-lipid translocase, an ATP-dependent enzyme which helps to maintain the lipid asymmetry of the sarcolemma. It was shown that anionic phospholipids enhance exchanger activity whereas cationic phospholipids diminish it (123). In support of the role these phospholipids may play in NCX activity, Langer et al have identified a NCX- dependent exchangeable  $\text{Ca}^{2+}$  pool in intact cells. Analysis of this  $\text{Ca}^{2+}$  pool revealed that it was dependent on the presence of anionic phospholipids in the inner leaflet of the sarcolemma (65,65,66). It is apparent that the regulation of  $\text{Ca}^{2+}$  transport via the NCX is complicated and further studies are required to increase our understanding of its function.

### Molecular Biology:

The cardiac NCX has been cloned from a number of species including; dog, cow, human and rat (123-127). The cardiac NCX cDNA is very well conserved across all these species. Using a polyclonal antibody raised against a partially purified canine NCX protein, Philipson and colleagues (123) screened a  $\lambda$ gt11 expression library, and isolated a 3.2kb clone (A4); it was analyzed further to see if it coded for the cardiac NCX. Northern blot analysis of canine cardiac poly(A<sup>+</sup>) enriched RNA with a probe from clone A4, detected a 7.0 Kb transcript. This suggested that the full length cDNA transcript coding for the NCX was more than two times the size of the first positive clone. However, to test if this clone coded for a functional protein, RNA was synthesized from it and injected into *Xenopus* oocytes. No detectable exchanger activity was observed, suggesting that this clone did not code for the full length protein.

Because the initial clone hybridized to a single transcript on northern blot it was used to screen a canine heart oligo(dT) primed cDNA library. Positive clones were subsequently characterized by sequence and restriction endonuclease analysis. These clones were approximately 6.0 Kb in length and extended more 3' than clone A4. However, none of the clones had a poly(A<sup>+</sup>) tail (signifying the end of the protein). One clone, TB11, looked promising because it had the longest 5' extension, suggesting that it may carry the initiation site. To test this, RNA was synthesized from clone TB11 and injected in *Xenopus* oocytes. Six days following injection, [Na<sup>+</sup>]<sub>i</sub>-dependent exchanger activity was detectable, figure 20. Thus, it was apparent that this group had successfully cloned and expressed the canine cardiac NCX.

By cloning the cDNA which codes for the cardiac NCX it was now possible to analyse the protein's structure. The deduced amino acid sequence

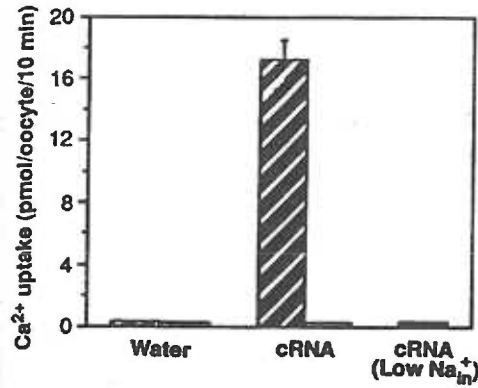


Figure 20:  $^{45}\text{Ca}^{2+}$  uptake studies using *Xenopus* oocytes. Lane "a" represents the basal uptake by oocytes following injection with sterile water. Lane "b" represents the NCX mediated  $^{45}\text{Ca}^{2+}$  by oocytes injected with cRNA for the NCX. Lane "c" confirms that the enhanced  $\text{Ca}^{2+}$  uptake is mediated by the NCX because the uptake is reduced to control levels in the absence of intracellular  $\text{Na}^+$ . (From Nicoll et al, 1990).

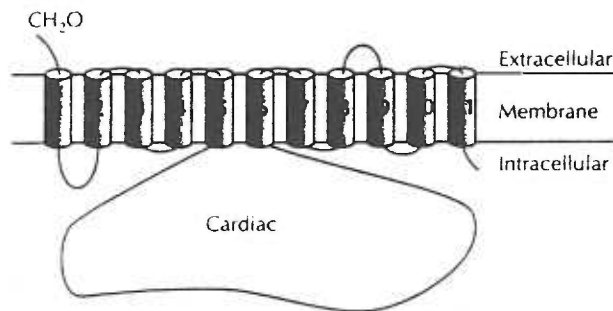


Figure 21: Topography of the cardiac NCX as determined from the deduced amino acid sequence from clone TB11. (From Philipson and Nicoll, 1992).

from the combined cDNA sequences of overlapping clones was determined. The coding region of the cDNA was 2910 bases in length and coded for a protein of 970 amino acids with an apparent molecular weight of 108 kD. Topography analysis of the deduced amino acid sequence indicates that the mature cardiac NCX contains 11 transmembrane domains with a large, 520 amino acid, hydrophilic intracellular domain (Fig. 20).

Native proteins in myocytes and expressed proteins in oocytes share similar regulatory properties suggesting that regulation is intrinsic to the protein and not due to accessory intracellular proteins. As described above, such regulatory properties include  $\text{Na}^+$ ,  $\text{Ca}^{2+}$ , and ATP dependent regulation. In addition, a region (20 amino acids) of the intracellular loop has been shown to have homology to a calmodulin-binding domain. When a synthetic peptide homologous to this region is added to the cytoplasmic face of giant membrane patches exchanger activity is attenuated (128). The effect of this "exchanger inhibitory peptide" (XIP) is specific and relatively potent. Because XIP is homologous to a calmodulin binding domain it is thought to act by interfering with a  $\text{Ca}^{2+}$  binding site of the NCX.

To investigate the potential role of the intracellular loop, mutant clones which all or part of the loop deleted were engineered and expressed in Xenous oocytes. Interestingly enough, the clones still had exchanger activity. However, the regulation of the mutants was different compared to the wild types. Figure 22 is a summary of the results obtained with the mutant clones. The index of exchanger activity in this study was the exchanger current associated with the electrogenic pumping mechanism. It is apparent that regulation of the NCX by the proposed exchanger inhibitory peptide is dependent on some regions within the intracellular loop (top trace). The exact function of this calmodulin-binding domain has not been defined to

date, but these studies support the hypothesis that the NCX is regulated by intracellular accessory proteins, such as calmodulin.



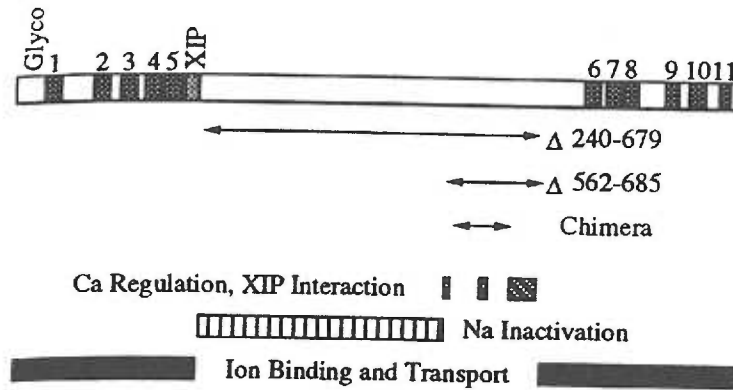


Figure 22.a: Schematic of the deletion mutant engineered to study the role of the large cytoplasmic hydrophilic domain of the cardiac NCX. The top sequence represents the native cDNA sequence with the regions of interest defined in the lower portion of the figure. The mutants are labelled as  $\Delta$  with the number of the base pairs corresponding to the region deleted listed. For example  $\Delta 240-679$  represents a mutant which had base pairs 240-679 deleted. Using these mutant clones this group was able to characterize region of the NCX protein which are responsible for a) ion binding and transport, b)  $\text{Ca}^{2+}$  regulation, c)  $\text{Na}^{+}$  inactivation, and d) XIP interaction. ( From Matsuoka, 1993).

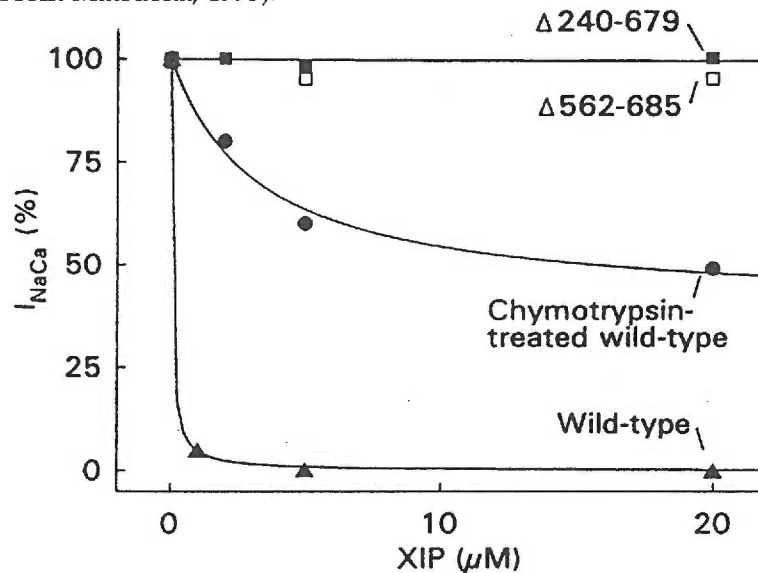


Figure 22.b: Data from the study of the mutant clones depicted in figure 20.a. In this figure, NCX activity is measured as the current associated with the movement of  $\text{Ca}^{2+}$  across the membrane. XIP, when applied to the cytoplasmic face of the NCX, attenuates NCX activity. In this study deletional mutants were made which removed part or all of the coding sequence for cytoplasmic loop of the NCX. These mutants, when expressed can be studied for functional differences compared to wild-type clones. In this figure, the lower trace is the wild-type clone which shows significant attenuation of the NCX in the presence of the XIP peptide. The middle trace shows that the inhibiting effects of XIP can be reduced with prior chymotrypsin treatment of the wild-type protein. The top trace is the activity of the mutants in the presence of the XIP peptide. These results indicate that the regulatory site of the XIP peptide resides in the hydrophilic loop domain corresponding to the coding sequence of base pairs 562-685.

### SECTION III.C: DEVELOPMENT OF THE SERCA AND NCX

Morphological studies on developing cardiac myocytes have shown a developmental pattern for the sarcoplasmic reticulum (Section I). The SR content is lower in the immature cardiac myocyte than in the mature cell (18-24). These observations have led investigators to search for an understanding of how the immature heart functions without a well developed SR. The question "how is  $\text{Ca}^{2+}$  controlled during the cardiac cycle?" is most interesting. To address this question, investigators have studied  $\text{Ca}^{2+}$  transport using models including the intact heart, isolated papillary muscle, and membrane vesicles from hearts of increasing gestational ages. In addition, studies have been performed to understand the expression patterns of SERCA and NCX during development. This section will review pertinent findings.

#### SERCA studies:

Some investigators have used the intact heart or isolated papillary muscle to examine developmental changes in myocardial function (Section I). However, such models are not adequate to study  $\text{Ca}^{2+}$  transport across cellular membranes. Therefore, isolated membrane vesicles have been used to study the functional aspects of the  $\text{Ca}^{2+}$  transport proteins (130-133). These studies indicate that all species studied follow a similar developmental pattern although on different time lines. Nayler and Fassold showed that preterm rabbits and guinea pigs have significantly lower SERCA activity compared to the adult (130). Similarly, studies in the fetal sheep have indicated that the immature SR has lower SERCA activity (131-133).

A complete description of the development of the cardiac SERCA was presented by Lynn Mahony (142). Experiments with isolated SR vesicles from hearts of various ages corroborated earlier descriptions of developmental changes in the SERCA made by others (132, 133). Briefly, cardiac SR vesicles isolated from fetal sheep accumulate less  $\text{Ca}^{2+}$  than those from adult sheep. Fig 23 represents the time course of  $\text{Ca}^{2+}$  uptake by the SR vesicles in this study. To determine if the reduced  $\text{Ca}^{2+}$  uptake was based on the density of active pumps, the radiolabeled acylphosphate intermediate was quantitated in each sample. Similar findings have been reported more recently in the developing rabbit heart (137).

During the transport of  $\text{Ca}^{2+}$ , the pump can phosphorylated with radiolabeled  $\gamma\text{-}^{32}\text{P}$ phosphate of ATP. This step allows individual pump molecules to be tagged, thus allowing the total number of active pumps to be quantified. The reduced  $\text{Ca}^{2+}$  uptake of the fetal hearts could be explained by fewer pump protein molecules. In postnatal hearts, the number of pump protein molecules was not reduced, although  $\text{Ca}^{2+}$  uptake was still low. Therefore, the efficiency of the SERCA at each age was determined. The coupling ratio of mol  $\text{Ca}^{2+}$  transported /mol ATP hydrolyzed was calculated (Fig. 24. In this figure the vesicles from the immature hearts are observed to pump  $\text{Ca}^{2+}$  inefficiently. Thus reduced  $\text{Ca}^{2+}$  uptake by the isolated vesicle may be due to the expression of a particular SERCA isoform with lower activity or perhaps the expression of specific regulatory proteins in the mature heart.

David MacLennan's group addressed the developmental expression pattern of SERCA isoforms in rabbit heart (134). Recall that this group first purified the SERCA protein and cloned it from rabbit heart. Using Northern blot analysis of total RNA from rabbit hearts of increasing age they showed

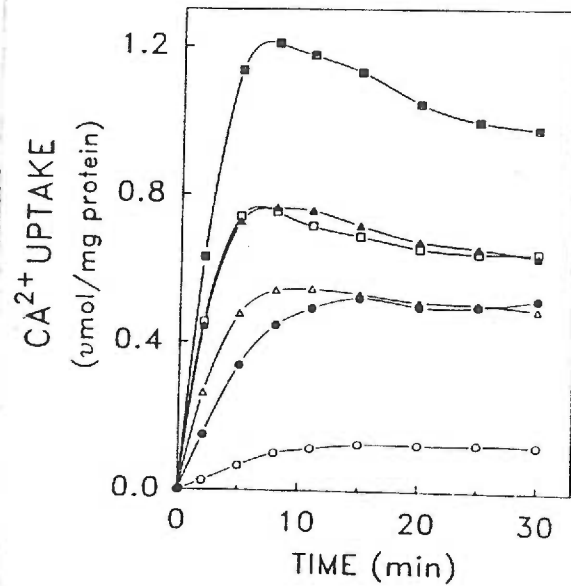


Figure 23: Ca<sup>2+</sup> uptake by SR vesicles isolated from sheep hearts of various developmental ages (fetal 100-105 (°), fetal 128-132 (•), newborn (Δ), postnatal 4 weeks (◻), postnatal 8 weeks (▴), maternal (■)). From this figure it is apparent that as the heart matures Ca<sup>2+</sup> uptake by the SR increases. This description agrees with morphological data which show a low density of SR in immature myocytes. (From Mahoney, 1988).

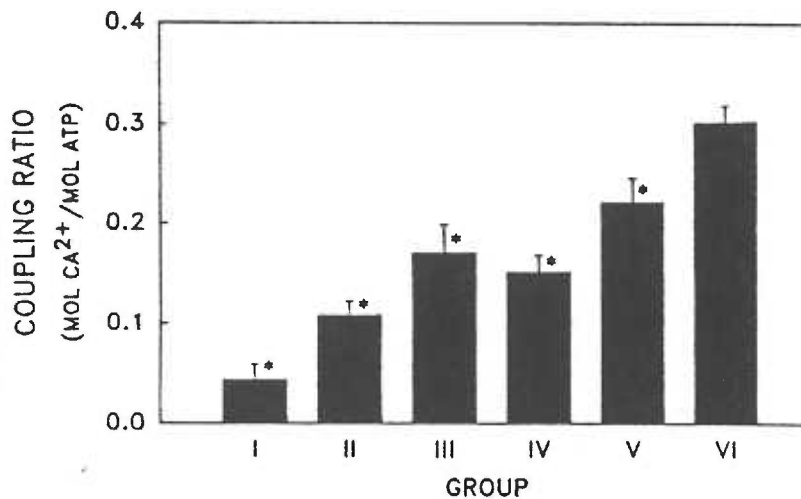


Figure 24: Developmental profile of the coupling efficiency of isolated SR vesicles from sheep hearts of various developmental ages (same as in figure 23). The coupling ratio is lowest in the SR vesicles from the most immature hearts and appears to increase with development. This suggests that the SERCA in the immature hearts may be pumping less efficiently than the SERCA in the adult hearts. This may be due to regulatory proteins, and or expression of different isoforms. (From Mahoney, 1988).

that the SERCA2a gene (cardiac/slow twitch) increases throughout gestation with peak levels in the adult rabbit heart. In contrast, the expression of SERCA2b (smooth nonmuscle) was low in the rabbit heart and did not change significantly throughout development (Fig 25). The results from the morphological, physiological, and molecular studies on the SR and its components described here support the hypothesis that another mechanism is responsible for Ca<sup>2+</sup> cycles in immature cardiac myocytes.

#### NCX Studies:

Although developmental studies of the cardiac NCX are limited, the recent cloning of the cardiac NCX gene greatly advanced the progress in this area (124). However, even now, less is known about the developmental regulation of NCX than of the cardiac SERCA. Using sarcolemmal vesicles isolated from the hearts of neonatal and adult mongrel dogs, Hanson et al studied Na<sup>+</sup>-dependent Ca<sup>2+</sup> uptake (136). The NCX mediated uptake was greater in vesicles isolated from neonatal hearts compared to those from adult hearts. These results support the hypothesis that the NCX is more active in the immature cardiac myocyte, possibly compensating for inadequate SERCA activity.

Artman and colleagues provided the first evidence that expression of the NCX gene is upregulated in the fetal rabbit heart (137). This study correlated Na<sup>+</sup>-dependent Ca<sup>2+</sup> uptake by isolated SL vesicles with western blot analysis of the NCX protein (Figure 26). The essential findings from this study agreed with the hypothesis that the NCX is relatively more active in the immature heart than the adult. Chen et al performed an elegant study looking at the localization of the rabbit cardiac NCX during development in the rabbit (138). Monoclonal antibodies were used to localize the NCX in

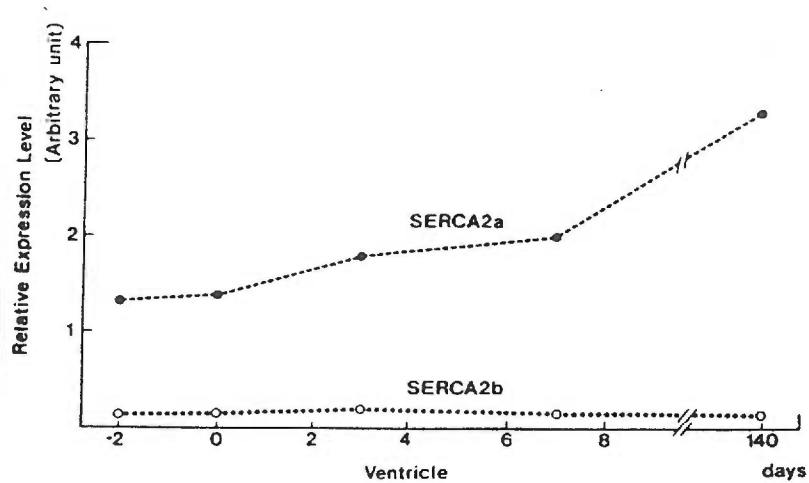


Figure 25: Developmental expression of the SERCA2a and SERCA2b genes in rabbit heart. The SERCA2b gene, which codes for the smooth/ non-muscle isoform is shown to not change over the course of development in the heart. The SERCA2a gene, which codes for the slow/cardiac isoform, however is expressed at increasing levels as the heart matures. (From Arai, 1992).

isolated rabbit ventricular myocytes of increasing gestational ages. During development the localization of the NCX shifts from widely distributed throughout the sarcolemma in the very immature myocyte to the T-tubules in the adult myocyte. Although the results of this study were not quantitative, they showed that the immature myocyte has abundant NCX protein and thus may rely heavily on it for normal EC coupling.

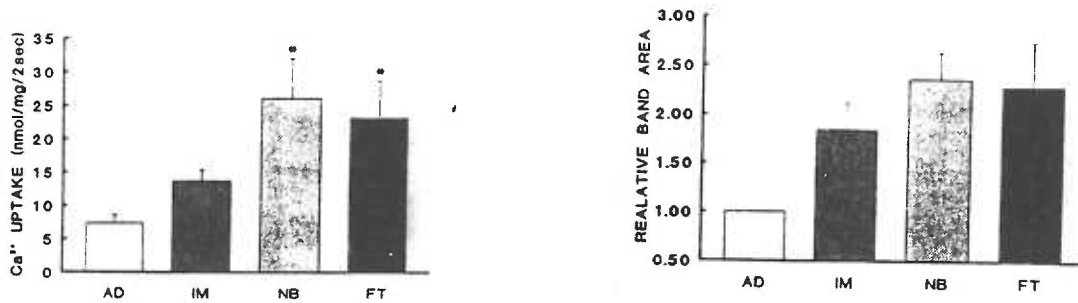


Figure 26: Panel "a" shows the results of  $^{45}Ca^{2+}$  uptake assays using isolated SL vesicles from rabbit hearts of various developmental ages (FT= fetal, NB= newborn, IM=juvenile, AD=adult). From these studies it is apparent that NCX activity, as measured by  $Na^{+}$ -dependent Ca uptake, is greater in the immature rabbit heart than the adult rabbit heart. Panel "b" is summary of slot-blot analysis of NCX protein abundance in SL vesicles from the same groups of animals. The greatest immunoreactivity was observed in the immature hearts. These findings correlate well with the  $^{45}Ca^{2+}$  uptake data. (From Artman, 1992).



Chapter II: Ca<sup>2+</sup> Transport Proteins in the  
Developing Sheep Heart

The idea that all mammalian species follow a predetermined set of developmental events during heart development has been set forth in the preceding sections. Such developmental events include the maturation of the SR and T-tubules concomitant with an increase in myocyte size. Combined with the development of these membrane systems is the development of the calcium transport proteins, including the SERCA and the SL-NCX. The work presented has led to the theory that the immature myocyte lacks a well developed SR and is thus more dependent on the SL-NCX for Ca<sup>2+</sup> extrusion during diastole. Much of this work has been done using the rabbit, a small altricial mammal. I have proposed that more studies need to be performed on a larger mammalian model which may give a better insight into the breadth of biological mechanisms across species and may represent the development of the human heart more closely. The developing fetal sheep heart has been suggested to be such a model for human development (17).

The fetal sheep is a valuable model for studying the cardiovascular system for several reasons including, the 150 day gestation period and the large size of the fetus. Studies from the Thornburg lab have taken advantage of these properties to perform chronic studies which are impossible in smaller animal models. For example, this lab has successfully characterized the response of the fetal coronary bed to hypoxia (143). This was an important study because we observed that the fetal coronary bed has the capacity to dilate beyond what was previously predicted from adult studies. In this study we showed that the dilatory hypoxic response of the coronary bed is mediated in part by nitric oxide. This study would have been difficult to do in the small mammal because of the technical difficulties associated with instrumenting the heart with coronary artery and coronary sinus catheters. To further

our understanding of the events which take place during development of the heart I have proposed to study the maturation of the Ca<sup>2+</sup> transport proteins in the sheep heart. Many laboratories have studied the fetal sheep heart so that new information can be placed in the context of normal sheep heart function. However, there is a large gap in our knowledge of the maturation of the myocyte in sheep, except for a general description of the myocyte size changes during development. The integration of calcium transport protein expression with heart development is still understudied. Therefore, I have performed the proposed project for the following reasons to: a) gain new information regarding the development of the heart in a large mammal, and b) use this information as the basis for future studies in the fetal sheep heart under chronic experimental conditions. The following sections focus on the experiments I have performed during the course of my study of this subject. In order to characterize the maturation of the SERCA and SL-NCX the project has been divided into three main sections, a) cloning of the sheep SL-NCX gene, b) maturational expression of the SERCA and SL-NCX genes, and c) western blot analysis of these proteins during development.

## Materials and Methods

## Section IV: General Techniques

## SECTION IV: GENERAL TECHNIQUES

### IV.1 Preparation of *E. coli* Competent Cells:

The first step in this molecular based study was to generate stable stocks of complementary DNA which were specific for the genes of interest. Thus it was necessary to make bacterial cells *competent* to receive plasmid DNA. This was done by submitting the bacteria to ionic and cold shock treatment. Briefly, a single loop from a stock of *E. coli* strain JM 101 was cultured overnight at 37°C in Luria Broth (LB). The following day an aliquot was subcultured into LB at 37°C with vigorous aeration until an optical density (OD) of 0.3-0.5 was reached. Cells were then pelleted by centrifugation at 2500x g at room temperature for five minutes (Beckman, Accuspin FR), decanted, and resuspended in 2.4 ml of 50mM calcium chloride in a sterile 50ml conical tube (Stardstedt). The cell suspension was then brought up to 1/2 the original culture volume with ice cold 50mM CaCl<sub>2</sub> and left on ice for 30 minutes. Following the incubation on ice the cells were pelleted at 2500x g at 4°C. At this point the cells were "competent" and ready to be "transformed" with plasmid DNA. Competent cells were then aliquoted and snap-frozen in N<sub>2</sub>liq and stored at -80°C for future use.

### IV.2 Transformation of *E. coli* Competent Cells:

200µl of aliquoted competent cells in an eppendorf tube were placed on ice and allowed to thaw partially. 100ng of plasmid DNA was added to the

competent cells and mixed by gentle stirring with the pipette tip. The cells were then incubated on ice for thirty minutes, heat shocked 45 seconds at 42° C, then incubated two minutes on ice. 200µl of LB medium was added and the cells were incubated, with shaking, for 45 minutes at 37° C. Following this incubation, 10µl, 50µl, and 100µl aliquots were plated out on individual LB agar plates containing 50µg/ml ampicillin and incubated at 37° C overnight.

#### IV.3 Plasmid Extraction:

Our lab has been successful extracting plasmid DNA using the method provided by the QIAGEN plasmid kits. Briefly, single recombinant colonies were used to inoculate 1-500ml of LB medium containing 100µg/ml ampicillin. The cultures were allowed to grow to log phase (5-12 hours) at 37°C with vigorous aeration. Following the incubation period the cells were pelleted by centrifugation at 4000 rpm for 10 minutes. The plasmid DNA was then isolated following the protocol from the manufacturer. The final plasmid was resuspended in 50-500µl Tris EDTA (TE).

#### IV.4 Phenol:Chloroform Extraction and Ethanol Precipitation:

Prior to using plasmid DNA for sequencing or other manipulation which requires a clean template, the DNA was extracted twice with phenol:chloroform (1:1) followed by a single extraction with chloroform. One volume of the phenol:chloroform solution was added to the DNA solution and vortexed for thirty seconds. The suspension was then centrifuged at 14,000 rpm in a bench top centrifuge (Eppendorf Model#5402) for two minutes at room temperature. The top aqueous layer was transferred

to a clean tube and the extractions were repeated as described. The DNA in the final aqueous phase collected was then precipitated with 0.1 volume 3M sodium acetate pH 5.2 and 2.5 volumes ice-cold 100% ethanol, and incubated at -80°C for a minimum of thirty minutes. The DNA was then pelleted by centrifugation at 14,000 rpm at 4°C in a refrigerated table top centrifuge (Eppendorf). The DNA pellet was subsequently washed with 1.0ml ice-cold 70% ethanol, recentrifuged and dried under vacuum. The DNA pellet was resuspended in sterile water, and the concentration and purity of the DNA in solution was determined by measuring the optical density (OD) at 260 nm and 280 nm (151).

#### IV.5 Isolation of Total RNA:

The method used to isolate quality total RNA from whole tissues was based on the single-step acid-phenol method (154). One gram of tissue was homogenized in 10ml of Solution D in a sterile 50ml RNase free Nalgene tube (28.7x103). The tissue was homogenized using a polytron on medium speed until the tissue was entirely dispersed. To the homogenate the following were added in order; (a) 0.1 volume 2M sodium acetate, pH 4.0, (b) 1.0 volume water saturated phenol, pH < 4.0, and (c) 0.33 volumes chloroform:isoamyl alcohol (24:1). The sample was vortexed following each addition and placed on ice for fifteen minutes. The sample was then centrifuged at 10,000 rpm for twenty minutes in a Beckman JA-20 rotor. The aqueous phase was carefully removed to a clean RNase free 50 ml Nalgene tube; the RNA was precipitated by adding 1.0 volume of cold isopropanol and incubating the tube at -20°C for 1 hour. The RNA was then pelleted by centrifugation as described above. The RNA pellet was subsequently



resuspended in one-third the original volume (3.33ml) of Solution D. The RNA was precipitated again with an equal volume of isopropanol and pelleted as described above. The pellet was then washed with 1ml of 70% ethanol (DEPC), centrifuged for five minutes at 10,000 rpm and allowed to air-dry; the RNA was then resuspended in 1.0 ml of DEPC-treated H<sub>2</sub>O. The concentration and purity were determined by measuring the OD at 260 nm and 280 nm. The RNA was generally precipitated again with 0.1 volume 3 M sodium acetate and 2.5 volumes 100% ethanol at -80°C overnight. This final precipitation was necessary to obtain a stock RNA solution of approximately 5mg/ml. To determine the integrity of the RNA a 5µl aliquot was electrophoresed on a formaldehyde denaturing gel (1% agarose (w/v), 1.2M formaldehyde, 1X mops). The RNA was denatured prior to electrophoresis by adding 1.0 volume of RNA sample buffer-1 and heating at 65°C for 5 minutes. To the denatured RNA 0.1 volume 10X RNA loading buffer was added. The RNA was electrophoresed in 1X MOPS running buffer at a constant voltage of 100 volts until the dyes had separated sufficiently. RNA integrity was determined to be good when, by visual inspection, the 28S ribosomal band appeared at least twice as intense as the 18S band.

#### IV.6 Preparation of Northern Blots:

RNA was denatured by the addition of an equal volume of RNA sample buffer-1 and heating at 65°C for five minutes. The RNA was immediately placed on ice and 0.1 volume of 10X RNA loading buffer was added to the sample. The RNA was electrophoresed on a formaldehyde denaturing gel (1% agarose (w/v), 1.2M formaldehyde, 1X mops), for 2-4 hours at a constant voltage of 75 volts in 1X MOPS running buffer. When the

RNA had run a sufficient distance, the gel was rinsed in DEPC-treated H<sub>2</sub>O to remove residual formaldehyde. While the gel was rinsing, a piece of Genescreen Plus was cut to the same dimensions as the gel and allowed to wet by capillary action in dH<sub>2</sub>O. Meanwhile two pieces of 3MM filter paper were also cut to the same dimensions as the gel and wetted with Northern transfer buffer. The blotting apparatus was the same as that described by Sambrook et al (151). Briefly, the gel is arranged on top of a piece of 3MM filter paper which was suspended over the transfer buffer by a glass support. The Genescreen Plus membrane was then laid carefully on the gel, eliminating all bubbles. Next, a layer of two wet 3MM filters were placed on the membrane followed by a stack of absorbent paper towels. As buffer is drawn into the towels, the separated RNA is transferred from the gel to the membrane by capillary action (blotting). To facilitate transfer, a moderate weight is placed on top of the paper towels. Transfer is allowed to proceed for approximately sixteen hours. When transfer was complete, the membrane was wrapped in plastic wrap (polyvinyl-chloride) and the RNA was cross-linked to the membrane by brief exposure to UV light (Hoeffer Mighty Brite). The membrane was stained with methylene blue. Because this stain is fully reversible it does not interfere with subsequent hybridization steps. Methylene blue is specific for RNA and can be used to determine the efficiency of transfer, as well as the integrity and the relative amount of RNA in each lane. The membrane was immersed in methylene blue solution for three minutes at room temperature and then rinsed with DEPC-treated water until the background was low. The methylene blue was then completely removed by rinsing the membrane in the primary wash solution at 65°C for 10 minutes with gentle agitation. The blot was then probed with radiolabeled cDNA fragments or stored at -20°C.

#### IV.7 Low Melt Extraction:

Restriction endonuclease digested plasmid DNA was electrophoresed on a 1% low melting point agarose gel in order to isolate and subsequently purify the desired cDNA fragment. A gel slab containing the DNA fragment of interest was cut out with a clean razor blade and transferred to a 1.5ml eppendorf tube. To this tube an equal volume of TE buffer, pH 8.5 was added. The tube was then heated at 65°C for five minutes and then vortexed. The tube was then frozen quickly at -80°C for five minutes. Next the sample was thawed out by placing the tube at 42°C. While the sample was thawing, the tube was "flicked" several times in order to disrupt the agarose matrix. The agarose was then pelleted by centrifugation at 14,000 rpm (Eppendorf) for ten minutes at room temperature. The supernatant containing the desired DNA was then transferred to a clean 1.5ml eppendorf tube and stored at -20°C until needed. Generally, a 10µl aliquot was tested on a 1.0% agarose (w/v) gel to confirm that the extraction was successful.

#### IV.8 Radiolabeling DNA Fragments:

Our lab has been successfully using the Random Primed Labeling Kit from Boehringer Mannheim. Briefly, 100ng of template DNA was transferred to a 1.5ml eppendorf tube denatured by heating at 95°C for ten minutes, and then rapidly chilled on ice. To the DNA the following was added: 2.0µl of reaction mixture, 1.0µl of each dNTP (specifically dATP, dTTP, and dGTP), 5.0µl of  $\alpha$ -<sup>32</sup>P-dCTP (Dupont Easytides 10µCi/µl), and 1.0 µl Klenow enzyme

(2U/ $\mu$ l). All of the reagents, except for the  $^{32}\text{P}$ -dCTP were supplied in the kit. The tube was then centrifuged briefly to collect contents at the bottom and then incubated for at least one hour at 37°C. At the end of the incubation period, the reaction was stopped by placing the tube on ice. The radiolabeled probe was precipitated with 40 $\mu$ g of tRNA, 12 $\mu$ l of 7.5M ammonium acetate and 100 $\mu$ l of 100% ethanol, incubated at room temperature for ten minutes, and then pelleted by centrifugation at 14,000 rpm for ten minutes at room temperature in a bench top Eppendorf centrifuge. The DNA pellet was then resuspended in 400 $\mu$ l of 2X SSC and total radioactivity in 1.0 $\mu$ l was determined with a liquid scintillation counter (Beckman LS6000SC). The radiolabeled probe was then stored at -20°C.

#### IV.9 Probing of Northern Blots:

Northern blots were hybridized with radiolabeled probes according to the method described by Sambrook et al (151). The membrane was prepared as described in section 4.6 and then prehybridized in 15ml of hybridization solution for one to sixteen hours at 37°degrees in a rotating incubator, Hybaid (Mini Hyb Oven). Following the incubation period, denatured radiolabeled DNA was added directly to the hybridization solution and was allowed to continue hybridizing for a minimum of twelve hours at 42°C. When hybridization was complete, the hybridization solution was transferred to a sterile 50ml Sarstedt conical tube and stored at -20°C. The hybridization solution when stored in this manner can be used repeatedly until the isotope has decayed 2 half-lives. The membrane was washed repeatedly in approximately 100ml wash solution to reduce non-specific binding. First, the membrane was rinsed quickly in primary wash solution to remove excessive

hybridization solution, then gently agitated for twenty minutes in fresh wash solution at room temperature. The membrane was then washed with approximately 100ml of secondary wash solution at the hybridization temperature for 20 minutes. Washing was continued with the secondary wash solution until the background was reduced to approximately 2000 counts per minute. The blot was exposed overnight at -80°C to X-ray film with two intensifying screens; the film was subsequently developed with an automated film processor.

#### IV.10 Western Blot Background:

Western blotting was used to substantiate the gene expression patterns observed with the northern blots. Antibodies specific for SERCA and NCX were commercially available. A mouse monoclonal antibody against the SERCA protein was obtained from Affinity Bioreagents Inc. This antibody was positive for cross-reactivity with the sheep SERCA. A rabbit polyclonal antibody against the canine NCX was obtained from SWant Inc. This antibody was also positive for cross-reactivity with the sheep NCX.

In order to draw a complete picture of the developmental expression of the calcium transport proteins it was important to determine whether or not the genes being expressed were actually representing the amount of protein present in a particular age group. The western blot technique is useful for this purpose because it detects the total amount of antigen present in a particular population of proteins. Because each protein is present on a different cellular membrane and in such different amounts two protein isolation protocols were employed. The SERCA is present in much greater abundance relative to the NCX and a crude protein extraction was sufficient for antigen detection.

The NCX protein is present at much lower concentrations therefore a more purified membrane preparation had to be employed for appropriate antigen detection.

#### IV.11 Crude Protein Extraction for SERCA:

Whole tissue was gently homogenized in 10 volumes (e.g. 1g/10 ml) of protein extraction Solution I with a Brinkman Polytron. Homogenization was complete when the tissue appeared evenly dispersed. The homogenate was then boiled for five minutes after which time the DNA was sheared by passing the homogenate through a 26 gauge needle several times. Any remaining debris was pelleted by a one minute centrifugation at 14,000 rpm in an eppendorf bench top centrifuge at room temperature. The supernatant was removed and the protein concentration was determined using a protein assay kit (Sigma) which was based on the method of Lowry. The proteins were stored at -80°C.

#### IV.12 Sarcolemmal Protein Extraction for NCX:

Whole tissue was gently homogenized in 10 volumes of protein extraction Solution II with a Brinkman Polytron. Homogenization was complete when the tissue appeared evenly dispersed. The homogenate was centrifuged in a Beckman JA-20 rotor at 8500x g for fifteen minutes at 4 C. The supernatant was then centrifuged in a Beckman Ultracentrifuge (Becman L8-M) at 100,000x g for sixty minutes at 4°C. The pellet was resuspended in 50ml of protein extraction Solution II. The protein concentration was

determined using a protein assay kit (Sigma) which was based on the method of Lowry. The proteins were stored at -80°C.

#### IV.13 Electrophoresis of Proteins:

Sodium dodecyl sulfate polyacrylamide gel electrophoresis (SDS-PAGE) was employed to separate the isolated protein on a size basis. I followed the method described by Laemmli for discontinuous gels. Generally, a 4.0% stacking and 7.5% separating gels were cast and run in a Tris, glycine buffer. Briefly, the 7.5% separating gel (Hoeffer Scientific) was poured and a small amount of 0.01% SDS was overlaid to facilitate polymerization, approximately 30 minutes. The 0.01% SDS was removed and the stacking gel was rinsed with sterile deionized water. The 4.0% stacking gel was then poured on top and allowed to polymerize, approximately 15 minutes. Twenty to thirty mg of total protein was transferred to a 1.5ml eppendorf tube and an equal volume of 2X sample buffer followed by boiling for five minutes. The sample buffer contains 100mM dithiothreitol which serves reduce disulfide bonds in the proteins. Boiling the protein helps disaggregate proteins such that separation is enhanced. The protein samples were then loaded into the wells and electrophoresed at a constant amperage of 25mA until the leading dye front reached the bottom of the gel. Generally, proteins were run in duplicate so that half of the gel could be stained with 0.1% Coomassie Blue for total protein detection and the other half could be transferred for subsequent immunoblotting. The gel to be stained was soaked in a 0.1% Coomassie Blue for 1 hour and destained for 2 hours to overnight. The longer the destaining process the greater the resolution of proteins.

#### IV.14 Transfer of Proteins: Electroblothing:

Electroblotting (BioRad) was used as an efficient method for transferring proteins from a polyacrylamide gel to a solid nitrocellulose support (BioRad). Prior to electroblotting, two 3MM filters, and a piece of nitrocellulose were cut to the same dimensions as the gel and soaked, along with the gel, in transfer buffer (25mM Tris, 190mM glycine) for five minutes. The blotting apparatus was then set-up as follows: (a) support pad (BioRad), (b) 3MM filter paper, (c) gel, (d) nitrocellulose membrane, (e) 3MM filter paper, (e) another support pad. The key to setting up the blot was to ensure that no air bubbles were trapped between the layers and that the nitrocellulose membrane was on the anode side of the gel. The proteins were transferred for eight to 12 hours in the cold room. In addition to transferring in the cold room an internal ice pack was included to in order to prevent the apparatus from overheating. When transfer was complete the apparatus was disassembled and the nitrocellulose membrane was marked to orient the proteins later. The membrane was then ready for immunoblotting.

#### IV.15 Immunoblotting:

The nitrocellulose membrane containing the proteins of interest was first incubated in a blocking solution for one hour with gentle agitation at room temperature. This incubation serves the purpose to block non-specific binding sites on the nitrocellulose membrane. The membrane was then washed two times for five minutes with gentle agitation at room temperature with 1X TBST. The membrane was then incubated for one hour as described above in 1X TBST containing the primary antibody. The optimal primary



antibody titer was determined by trial and error and was different for each antibody studied. The polyclonal rabbit anti-canine SLEX antibody worked well when diluted 1:3500, whereas the monoclonal mouse anti-SERCA antibody worked well at a 1:3000 dilution. Following the primary antibody incubation the membrane was then washed four times for five minutes each with 1X TBST as described above. The membrane was then incubated in 1X TBST containing the secondary antibody (1:3000) for forty-five minutes to one hour at room temperature with gentle agitation. The secondary antibodies were, (a) Horse anti-mouse IgG for the mouse monoclonal antibody (Vector Labs), and (b) Goat anti-rabbit IgG for the rabbit polyclonal antibody (BioRad). Each of these secondary antibodies has been conjugated with alkaline phosphatase, which is used for colorimetric detection of the antibody in subsequent steps. Following the incubation with the secondary antibody the membrane was washed with 1X TBST as described above.

Colorimetric detection of antibody-antigen complex is accomplished by incubating the membrane in a solution containing substrate for alkaline phosphatase. In the presence of bromochloroindolyl phosphate/nitro blue tetrazolium (BCIP/NBT) substrate alkaline phosphatase generates a black-purple precipitate at the enzyme site. Just prior to developing the blot 10ml fresh alkaline phosphatase buffer was made up and 66 $\mu$ l of NBT (Promega) and 33 $\mu$ l BCIP was added and the solution was mixed well. The blot was then incubated in this developing solution for up to thirty minutes with gentle agitation. It was important to keep an eye on the blot as the color developed so that the reaction could be stopped once the band of interest was detected. The reaction was then stopped by the addition of 20mM EDTA in 1XTBST. The membrane was photographed to obtain a permanent record since the color faded with time.

Section V: Polymerase Chain Reaction  
Amplification and Cloning of the  
Sodium-Calcium Exchanger

## SECTION V: POLYMERASE CHAIN REACTION AMPLIFICATION AND CLONING OF THE SHEEP SODIUM-CALCIUM EXCHANGER GENE

### V.1 Design of Primers:

In order to amplify a cDNA fragment coding for the sodium-calcium exchanger gene using PCR, I designed primers which would define a particular region of the known exchanger sequence. I performed a search of the Gene Data Banks using a PC based search protocol to obtain sequence information on the sodium-calcium exchanger. The homology of sequences from several species (human, bovine, and canine) was between 91% and 93%, suggesting that the gene is well conserved. Nonetheless, the hybridization levels on sheep RNA by Northern blot was poor using a probe from the cDNA fragment coding for the guinea pig Na<sup>+</sup>-Ca<sup>2+</sup> exchanger (donated by Dr. Philipson). I therefore decided to amplify the gene from sheep heart cDNA using PCR. Specific oligonucleotide primers which defined region (+2566-+2925) of the canine sodium-calcium exchanger sequence (124) were designed and synthesized. The nucleotide sequence corresponding to the sense primer was 5'-CCAGACACATT GCAAGCAAAG-3', and the nucleotide sequence corresponding to the antisense primer was 3'-CCTGTGAAATTCCAGGAA-5'. The concentration of primers in the stock solutions was determined by measuring the O.D. at 260 nm by spectrophotometry. Working primer solutions (25mM) were made and all primers were stored at -20°C.

## V.2 cDNA Synthesis:

cDNA was synthesized from adult sheep heart total RNA using reverse transcriptase (RT). Five micrograms of total RNA was resuspended in 9 $\mu$ l of sterile distilled water and to this 1.0 $\mu$ l of 10X random hexamer solution was added (Boehringer-Manheim). The RNA was denatured by heating at 70°C for ten minutes and then quickly chilled on ice. To the sample the following was also added: 4.0 $\mu$ l 5X RT buffer, 2.0 $\mu$ l 0.1M DTT stock, 1.0 $\mu$ l 10mM dNTP stock, and 1.0 $\mu$ l sterile water. The sample was mixed well, briefly centrifuged, then heated at 37°C for two minutes. 1.0 $\mu$ l of RNase inhibitor (Promega 28U/ $\mu$ l) and 1.0 $\mu$ l of Superscript RT were added and the sample was incubated at 37°C for one hour. The template RNA was then removed by incubating the sample with 1.0 $\mu$ l of RNaseA (10mg/ml) at 37°C for an additional thirty minutes. The single strand cDNA was then stored at -20°C.

## V.3 PCR Amplification

The PCR reaction mixture contained the following: 1.0 $\mu$ l sheep heart cDNA (0.1mg/ml), 10.0 $\mu$ l 10X buffer, 4.0 $\mu$ l 50mM MgCl<sub>2</sub>, 16 $\mu$ l 10mM dNTP mixture, 4.0 $\mu$ l 25mM sense primer, 4.0 $\mu$ l 25mM anti-sense primer, 60.5 $\mu$ l sterile water, and 0.5 $\mu$ l  $\Delta$ Taq polymerase. The sample was overlaid with 50 $\mu$ l of mineral oil prior to starting the PCR to prevent evaporation. The thermal profile for the PCR reaction was an initial denaturation at 94°C for two minutes; 30 cycles of alternate annealing at 55°C for two minutes, extension at 72°C for three minutes and denaturation at 94°C for one minute; a final extension at 72°C for five minutes (Biometra Personal Cycler). When the PCR was complete, the mineral oil was carefully removed and the sample

was extracted with 50 $\mu$ l of chloroform to remove any residual oil. The sample was vortexed and the aqueous layer containing the DNA was transferred to a clean 1.5ml eppendorf tube. Ten  $\mu$ l of the PCR reaction was combined with 0.1 vol 10X DNA loading buffer and was electrophoresed through a TAE 3% agarose (w/v) gel containing 0.5mg/ml ethidium bromide. A single band of approximately 350 base pairs indicated the PCR product was correct and the reaction was then stored at -20°C.

#### V.4 Subcloning of Sodium-Calcium Exchanger cDNA:

In order to generate a permanent stock of the PCR amplified cDNA which encoded a portion of the sheep sodium-calcium exchanger I subcloned the PCR product into a plasmid vector. For this purpose I used the TA Cloning Kit available from Invitrogen and followed the manufacturers suggested protocol. With this kit I was able to subclone the PCR product directly from the PCR reaction mixture without further modification, since the random hexamers provided in the kit (which were used for the PCR amplification step) have linkers which facilitate the cloning of the PCR product directly into the plasmid vector. The ligation reaction was set up as follows: 1.0 $\mu$ l of PCR reaction mixture, 5.0 $\mu$ l of sterile water, 1.0 $\mu$ l of 10X buffer (supplied in the kit), 2.0 $\mu$ l of PCR vector (supplied in the kit), and 1.0 $\mu$ l of T4 DNA ligase. The sample was then allowed to incubate overnight at 16°C.

The sample was collected by brief centrifugation in a bench top Eppendorf centrifuge. Two  $\mu$ l of 0.5M  $\beta$ -mercaptoethanol was added and the sample was mixed gently by flicking the tube. One  $\mu$ l of the ligation reaction was then used to transform *E. coli* cells as described in Section 4.2. The

transformed cells were plated out on LB plates containing 100µg/ml ampicillin, 40µg/ml X-gal, 40µg/ml IPTG and allowed to grow overnight at 37°C. The following day colonies which appeared white on the plate were picked as positive recombinants.

The multiple cloning site of the PCR vector supplied in the TA Cloning Kit is located within the *LacZ* gene of the vector. This gene encodes for β-galactosidase and is expressed in the presence of the inducer IPTG. With the substrate X-gal and the inducer IPTG present in the growth media, transformed cells containing the intact *LacZ* gene will metabolize X-gal and take on a blue color. However, cells which have been transformed with plasmids containing DNA sequences inserted at the multiple cloning site will not express the *LacZ* gene. The ligated PCR product disrupts the coding sequence of the *LacZ* gene thus generating white colonies in the presence of X-gal and IPTG.

Twenty positive recombinants were picked and individually cultured in LB media, and plasmid was extracted as described in section 4.3. Plasmid DNA was digested at the ligation site with EcoR1, to release the insert. The digestion mixture contained 8.0µl of the plasmid DNA prep, 1.0µl of 10X One-Phor All buffer (Pharmacia), and 1.0µl EcoR1 (Pharmacia, 10U/µl). The reaction was incubated at 37°C for one hour, after which it was terminated by the addition of 0.1 vol of 10X DNA loading buffer. The digest was then examined on a 1% agarose (w/v) TAE gel. Clones containing the 350 bp insert were identified and subsequently cultured in 500ml of LB media overnight at 37°C with shaking. Large quantities of plasmid DNA were isolated with the QIAGEN kit as described in section 4.3 and extracted twice with phenol:chloroform as described in section 4.4. The DNA was stored at -20°C.

## V.5 DNA Sequencing :

The amplified cDNA PCR product was sequenced by the dideoxy chain termination method (152) using  $\Delta$ Taq Version 2.0 (USB) kit with  $\alpha$ -<sup>35</sup>S-dATP. This method utilizes dideoxy-nucleotide derivatives (ddNTP's) which, when incorporated into a DNA sequence prevent further chain elongation, and allow single bases to be resolved on a polyacrylamide gel. Sequencing was performed from both directions using the sense and antisense primers described earlier for the PCR reactions. The double-stranded plasmid DNA (5 $\mu$ g) was first denatured with an alkali solution containing 0.4M NaOH and 0.4M EDTA at 37°C for ten minutes. The DNA was then chilled on ice for 5 minutes and precipitated with 0.2 volumes 2M sodium acetate, pH 5.2 and 4 volumes ice-cold ethanol. The DNA was precipitated at -80°C for a minimum of thirty minutes and then pelleted by centrifugation at 14,000 rpm at 4°C for thirty minutes in a table top Eppendorf refrigerated centrifuge. The DNA was washed with 500ml of 70% ice-cold ethanol, centrifuged again as described above, and dried under vacuum (Savant). The DNA pellet was then resuspended in 50 $\mu$ l of sterile water. A 9.0 $\mu$ l aliquot of the denatured DNA was transferred to a 1.5ml eppendorf tube on ice, and the remaining denatured DNA was stored at -20°C.

The annealing reaction was initiated by the addition of 2.0 $\mu$ l of the sense primer (25mM) and 2.0 $\mu$ l Taq reaction mixture (supplied in the kit) to the tube. A second tube containing 9.0 $\mu$ l of the denatured DNA was set up for the antisense primer. The samples were then heated at 75°C for five minutes and then allowed to cool slowly to room temperature for 25 minutes. Once the annealing reaction was complete, the sample was placed on ice. The chain extension reaction was initiated by addition of 2.0 $\mu$ l labeling mix which

includes the deoxy-nucleotriphosphates (dNTP's), 0.75 $\mu$ l  $^{35}$ S dATP (10 $\mu$ Ci/ $\mu$ l), 0.25 $\mu$ l *Taq* polymerase (32U/ $\mu$ l) and dH<sub>2</sub>O to a final volume of 17.5 $\mu$ l. The tubes were incubated at 45°C for five minutes. Termination of chain elongation was achieved by the addition of ddNTP's to the sample. The extension reaction was divided among four eppendorf tubes containing 4.0 $\mu$ l of termination mix which correspond to each of the four bases, (e.g. ddGTP, ddATP, ddTTP, ddCTP). The samples were then heated to 70°C for 10 minutes and placed on ice. Four  $\mu$ l of stop solution was added to each sample and they were placed on ice.

The sequencing reactions were analyzed by separating them on a 21x50cm polyacrylamide gels composed of 5% (v/v) Long Ranger gel solution (AT Biochem), containing 8M Urea and 1.2X TBE. Samples were heated at 80°C for 5 minutes and placed on ice prior to loading. The sequencing gel was run in 0.6X TBE at a constant power of 110W and maintained at 50°C for a period of two to eight hours. When the electrophoresis was complete, the gel was transferred to Whatman 3MM paper, covered with plastic wrap and subsequently dried at 80°C under vacuum for 1 hour. The dried gel was then exposed to X-ray film overnight at room temperature.

#### V.6 Generation of ExoIII Deletions:

Unidirectional deletions were made in plasmid based clones using a protocol based on the Erase-a-base system (Promega) which employed Exonuclease III and S1 nuclease.

Two micrograms of the plasmid DNA was digested with two different restriction enzymes, both unique to the polylinker site of the plasmid vector, but not within the insert. One of the enzymes had to generate a four base 3'



overhang to be resistant to the activity of the Exonuclease III; this protects the sequence primer binding site. The second enzyme had to leave a 5' overhang or blunt end, making it vulnerable to Exonuclease III digestion. After digestion, the DNA was purified using Magic Clean-up resin (Promega). The DNA was eluted off the column in a volume of 54 $\mu$ l to which was added 6 $\mu$ l of 10 x ExoIII buffer. 800U of Exonuclease III was added to a reaction tube, prewarmed for two minutes at 37°C. 5 $\mu$ l aliquots were removed at 30 second intervals to 1.5 ml Eppendorf tubes on ice, containing 7.5 $\mu$ l of S1 nuclease mix. After all of the time point samples were removed, the S1 tubes were incubated at room temperature for thirty minutes. 2 $\mu$ l of S1 stop buffer was then added and the S1 nuclease inactivated by heating at 70°C for ten minutes. To determine the extent of the Exonuclease III digestion, 2 $\mu$ l aliquots were removed from each time point and analyzed on a 1% (w/v), 1xTBE agarose gel. If a sequential reduction in size of the linearized plasmid was observed, then 1 $\mu$ l of Klenow mix was added to each remaining sample and the reaction was allowed to proceed for five minutes at 37°C. 1 $\mu$ l of dNTP mix (0.125 mM of all four dNTPs) was added and incubated for another ten minutes. The samples were then transferred to room temperature and 50 $\mu$ l of ligase mix was added and the tubes were incubated at room temperature for one hour. The entire sample volume was then used to transform 200 $\mu$ l of competent XL-1B cells (section 4.2). Ten recombinants, from each time point, were picked and the rapid plasmid mini-preparation method (section 4.3) was used to prepare plasmid DNA. The recombinants were sized by running 10 $\mu$ l aliquots of the plasmid sample in a 1% (w/v), 1X TBE agarose gel, along with the full size undelated clone as a size reference point. Plasmids were then chosen from each time point that gave the correct

size range of overlapping clones. Clones were then sequenced as described in section 5.5.

#### V.7 Construction of fetal sheep heart cDNA library:

The cDNA library was constructed with the ZAP-cDNA synthesis kit from Stratagene according to the manufacturers recommended protocol; unless stated specifically, all the buffers and enzymes were provided in the kit. Total RNA was extracted from 2.0g of 130 day fetal sheep heart as described in section 4.5. Two milligrams of the total RNA was further purified by poly (A+) isolation, using the oligo-dT chromatography based kit from Promega. The integrity of the message enriched RNA was determined by spectrophotometry as well as visually, by ethidium bromide staining on a 1% agarose (w/v) TAE gel. Five micrograms of the poly (A+) RNA was pelleted by centrifugation at 14,000 rpm at 4°C for 30 minutes in a table top refrigerated centrifuge. The RNA pellet was washed with 500µl of ice-cold DEPC treated 75% ethanol, recentrifuged, dried under vacuum, and resuspended in 36.5µl of DEPC treated water (0.1%). The first strand cDNA synthesis reaction contained 5.0µl 10X first strand synthesis buffer, 3.0µl first strand methyl-dNTP mix, 2.0µl linker-primer solution (1.4 mg/ml), 1.0µl RNase inhibitor, and 36.5µl poly (A+) RNA (5µg). The RNA was heat denatured at 65°C for 10 minutes and rapidly chilled on ice. The annealing of the primer-linkers to the RNA occurred during a ten minute incubation at room temperature. cDNA synthesis was initiated by the addition of 2.5µl (100U/ml) Stratascript RNase H- reverse transcriptase. To monitor the quality and quantity of cDNA synthesis 5.0µl of the reaction mixture was transferred to a tube containing 0.5µl of  $\alpha$ -<sup>32</sup>P-dATP (800µCi/mmol). Both samples were

incubated at 37°C for one hour after which time the control tube containing the radiolabeled cDNA was stored at -20°C and the remaining cDNA was placed on ice.

Second strand cDNA synthesis was initiated by combining 40.0µl of 10X second strand buffer, 6.0µl of second strand dNTP mix, 288.1µl sterile water, 2.0µl  $\alpha$ -<sup>32</sup>P-dATP (800µCi/mmol), 5.7µl of RNaseH (1.1U/ml), and 13.2µl of DNA polymerase I (7.6U/ml). The reaction tube was incubated at 16°C for 2.5 hours. The DNA was extracted once with 1.0 volume phenol:chloroform (1:1) and once with 1.0 volume chloroform. The aqueous layer was transferred to a clean tube and the DNA was precipitated as described in Section 4.4. To determine the quality and quantity of cDNA synthesized, 5.0µl aliquots of each reaction mixture were separated on a 1% alkaline gel. Following electrophoresis the gel was wrapped in plastic wrap and dried under vacuum. The dried gel was exposed to X-ray film (Dupont) for 2 hours and then the film was developed with an automated developer. The cDNA was visible as a smear throughout the length of the lanes of the gel, indicating a good cDNA synthesis reaction.

#### V.8 Ligation of Adapters to the cDNA:

To facilitate the ligation of cDNA into the vector, EcoR1 adapters were ligated to the ends of the cDNA. These adapters provide a cohesive end to the cDNA which is also present in the vector, thus making ligation between cDNA and the uni-ZAP II vector easier. The protocol was provided by the manufacturer, so only a brief description will be given in this section. In order to ligate the EcoR1 adapters, the cDNA had to first be modified by blunting the ends. The blunting reaction contained 42.0µl cDNA prep, 5.0µl

10X buffer #3, 2.5µl blunting dNTP mix and 1.0µl Klenow fragment (1U/µl). The blunting reaction was performed at 37°C for thirty minutes. To stop the reaction, an equal volume of sterile water was added and the DNA was subjected to a single phenol:chloroform (1:1) extraction, followed by one extraction with chloroform. The DNA was precipitated for a minimum of thirty minutes on ice with 7.0µl of 3M sodium acetate and 226.0µl of 100% (v/v) ethanol. The DNA was pelleted by centrifugation at 14,000 rpm at 4°C for sixty minutes. The pellet was washed briefly with 800µl of 80% (v/v) ethanol, recentrifuged, dried under vacuum and resuspended in 7.0µl of the EcoR1 adapter solution. The ligation reaction contained 1.0 µl 10 X buffer #3, 1.0 µl of 10 mM dATP, 1.0 µl of T4 DNA ligase (4 Weiss U/µl), and 7.0 µl of the cDNA adapter mix. Ligation was performed overnight at 4°C. The following day the ligase was inactivated by heating at 70°C for thirty minutes. The sample was collected by a brief centrifugation and allowed to cool to room temperature for five minutes.

To facilitate ligation of the cDNA into the vector the adapters were phosphorylated using T4 polynucleotide kinase. The kinase reaction contained 1.0µl of 10X buffer #3, 2.0µl of 10mM dATP, 6.0µl of sterile water, 1.0µl of T4 polynucleotide kinase (10.0U/µl), and the previous ligation reaction. The tube was incubated for thirty minutes at 37°C. The kinase was then inactivated by heating for thirty minutes at 70°C. The sample was collected by a brief centrifugation and allowed to cool to room temperature for five minutes, then digested with Xho1 to release the EcoR1 adapter from the 5'-end of the cDNA strand. The result of this modification is the directional cloning of the cDNA into the ZAP vector. To the sample 28.0µl of SHO1 buffer supplement and 3.0µl of SHO1 (40U/µl) were added. The digestion was

performed at 37°C for 1.5 hours. Following the incubation period the sample was cooled to room temperature.

#### V.9 Size Fractionation cDNA:

The EcoR1 adapters which were not ligated to the cDNA were then separated from the cDNA by size fractionation through Sephacryl S-400 spin columns (supplied in the kit). To the sample 5.0µl of 10X STE buffer was added and the sample was applied to the spin column. The sample was centrifuged in a table top centrifuge at 400x g for two minutes. The first fraction was collected and set aside. A second fraction was collected by the addition of 60µl of 1X STE and centrifuged as described above. A final fraction was then collected with the addition of another 60µl of 1X STE and centrifugation. The cDNA fractions were extracted once with phenol:chloroform (1:1) and once with chloroform alone. The DNA was precipitated on ice for sixty minutes by adding an equal volume of 100% (v/v) ethanol. The DNA was pelleted by centrifugation at 14,000 rpm for sixty minutes at 4° C as described earlier. The pellet, which contained the majority of counts, was washed briefly with 80% (v/v) ethanol, recentrifuged and dried under vacuum. The pellets were then resuspended in 10.5µl of sterile water. The cDNA concentrations in each fraction were determined using an ethidium bromide plate assay (Stratagene) with known standards.

#### V.10 Ligation of cDNA into the Uni-ZAP Vector:

Ligation reactions were set up for each fraction collected. The ligation reactions contained 100ng of cDNA, 0.5µl of 10X buffer #3, 0.5µl of 10mM

rATP, 1.0µl of the Uni-ZAP vector (1mg/ml), and sterile water to a final volume of 4.5µl. To this, 0.5µl of T4 DNA ligase (4Weiss U/ml) was added and ligation was performed at 12°C overnight.

#### V.11 Packaging of the cDNA Library:

Packaging is the step when the cDNA vector construct is introduced into the host phage. Prior to packaging, the library host cells (XL1-blue MRF') had to be prepared. A single colony of SL1-blue cells was picked from a plate (LB-tet, (12.5µg/ml) and used to inoculate 50ml of LB medium containing 0.2% (v/v) maltose and 10mM MgSO<sub>4</sub>. The cells were grown for four to six hours (OD<sub>600</sub><1.0). The cells were then pelleted by centrifugation at 2000 rpm for 10 minutes at room temperature in a table top centrifuge. The pellet was resuspended in 0.5 volumes of 10mM MgSO<sub>4</sub>. The final cell concentration was adjusted to an OD<sub>600</sub> of 0.5 with 10mM MgSO<sub>4</sub>. The library was packaged using the Gigapack II packaging extract (Stratagene) following the manufacturers protocol. The packaging reaction was performed for two hours at room temperature, after which 500µl of SM buffer was added to the tube and the sample was mixed gently. To this, 20µl of chloroform was added and the sample was again mixed gently, then centrifuged. The supernatant, which contained the packaged library, was then stored at 4°C.

#### V.12 Titrating the cDNA Library:

Serial dilutions of the packaging reaction were performed in order to titrate the library. To titer the library, the supernatant was diluted (1:10, and 1:100) with SM buffer and 1.0µl of this dilution was added to 200µl of XL1-blue

cells (OD<sub>600</sub> of 0.5) The phage was allowed to adhere to the bacteria for twenty minutes at 37°C. After this incubation the following was added to the cell-phage suspension: 5ml NZY top agar at 48°C, 15µl of 0.5M IPTG (in water), and 50µl of X-gal (250 mg/ml in DMF). The cells were plated immediately onto NZY plates, and allowed to set for ten minutes, and then incubated at 37°C for 8-12 hours. The total number of plaques was counted and the efficiency (plaque forming units (pfu/µg) of the packaging was calculated with the formula:

$$\frac{\text{Number of plaques} \times \text{dilution factor} \times 1000\mu\text{l}}{\text{total } \mu\text{g packaged} \times \text{total ml plated}}$$

In addition to titering the library, an estimate of the quality of the cDNA library was made by comparing the number of recombinant plaques to the number non-recombinant plaques. It was estimated that greater than 95% of the plaques were recombinants, suggesting that a high quality library had been generated.

### V.13 Amplification of the cDNA Library:

The primary library had to be amplified in order to obtain a more stable stock before screening. To amplify the library, 20 aliquots of the primary library containing 50,000 pfu were combined with 600µl of XL1-blue cells (OD<sub>600</sub> of 0.5) per plate, which would amplify a total of 1x10<sup>6</sup> pfu for subsequent screenings. The tubes were incubated at 37°C for 20 minutes to allow the phage to adhere to the bacteria. To each tube 5.0ml of NZY top agar was added and the cells were mixed by inversion and then plated out on dry

150mm NZY plates. The plates were left at room temperature until the top agar set, then incubated at 37°C until the plaques were visible, approximately six to eight hours. The plates were then overlaid with 10ml of SM and placed at 4°C overnight. This step allows the phage to diffuse out into the buffer. The following day the SM was transferred to a 15ml conical tube (Sarstedt) and chloroform was added to a final concentration of 5% (v/v). The sample was mixed well by inversion and left at room temperature for fifteen minutes. The cell debris was pelleted by centrifugation at 500x g for ten minutes. The supernatant was then transferred to a sterile 15ml conical tube and chloroform was added to a final concentration of 0.33% (v/v). The amplified library was retitrated and stored at 4°C.

#### V.14 Plating Out the cDNA Library:

A total of  $1 \times 10^6$  pfu were plated out onto twenty 150mm NZY plates. Each plate contained 50,000 pfu. Plating of the library was similar to that described for the amplification step. Instead of allowing the phage to diffuse into the SM buffer, the phage DNA was lifted onto a solid support for subsequent screening. After the plaques were visible the plates were placed at 4°C for a minimum of four hours to prevent the top agar from sticking to the nylon membrane during the lifting procedure. Plaques were lifted in duplicates onto 137mm discs of Colony/Plaque Screen (NEN research products). A disc was carefully laid on top of the plaques and left on for two minutes. During this time, the disc was oriented by asymmetrically marking the membrane and plate using a 2ml syringe containing indelible ink (Higgins, Black India drawing ink). After the plaques were lifted, the disc was placed plaque side up onto 3MM filter paper which had been saturated with



0.5M NaOH for two minutes. The disc was then transferred to a second 3MM filter also saturated with 0.5M NaOH for another two minutes, then neutralized by transferring it to 3MM filter paper which had been saturated with 1M Tris/HCl pH 7.5 for five minutes. A duplicate disc was placed on the dish and oriented with the same marks and treated as the first for each plate. All filter discs were left at room temperature to dry, then sealed in a plastic bag and stored at 4°C. The stock agar plates were overlaid with 10ml of Hogness medium, covered with a fresh filter, and stored at -20°C.

#### V.15 Screening of the cDNA Library:

The sheep specific probe for the sodium-calcium exchanger described earlier was used to screen the fetal sheep heart cDNA library. A total of forty library filters were prehybridized in 300ml solution containing 1M NaCl, 1% (w/v) SDS, 10% PEG 3350 (Sigma) and 100µg/ml denatured salmon sperm DNA. The filters were prehybridized overnight at 60°C with gentle agitation. The first radiolabeled sheep probe was generated by performing four reactions as described in section 4.8. After the prehybridization step, the filters were removed and the denatured  $\alpha$ -<sup>32</sup>P-labeled sheep SLEX probe (2000cpm total) was added to approximately 200ml of the prehybridization solution. The filters were placed in the hybridization solution one at a time and were hybridized overnight at 60°C. The following day the filters were washed once in 1X SSC/1% (v/v) SDS for thirty minutes at 60°C, once in 0.5X SSC/0.5% (v/v) SDS for thirty minutes at 60°C, and finally twice in 0.1X SSC/0.1% (v/v) SDS for 30 minutes at 60°C. The filters were blotted dry and wrapped in plastic wrap, then organized with their respective duplicates, and exposed

overnight to X-ray film (Dupont) with an intensifying screen at room temperature.

The following day films were developed with an automated film developer. Positive clones were identified as those which were identical between the duplicate filters. The filters were then aligned with their parent dish, and positive clones were isolated by removing a 1cm plug from the agar dish using a cork bore. The agar plug was transferred to a sterile tube containing 1ml of SM buffer and chloroform was added to a final concentration of 0.3%. The tube was mixed by inversion and the phage was allowed to diffuse into the buffer for a minimum of five hours at room temperature. Serial dilutions ( $10^{-2}$ ,  $10^{-3}$ ,  $10^{-4}$ ) of the phage containing SM buffer were made, and these were plated out on 100mm NZY plates and incubated overnight at 37°C. The resulting plaques were lifted onto 82mm Colony/Plaque Screen (NEN Research) filter discs and screened with the sheep specific SLEX probe as described above. This routine of screening, picking, plating, and screening again, was repeated until single positive clones could be identified on the agar plate. The final single positive clone once obtained, was stored at 4°C in SM buffer.

#### V.16 In Vivo Excision of pBluescript Phagemids from the Uni-Zap Vector:

The Uni-Zap vector (Stratagene) has been engineered to facilitate the recovery of the cloned cDNA as a phagemid in very few steps. The in vivo excision process removes the cDNA insert from the Uni-ZAP vector arms and results in a phagemid which can recircularize with the cDNA inserted into the multiple cloning site. The protocol recommended by the manufacturer was followed with slight modification. In a 50ml sterile conical

tube, 200µl of XL1-blue plating cells, 200µl of recombinant phage stock ( $>1 \times 10^5$  phage particles), and 10µl of ExAssist helper phage (Stratagene) were combined. The phage was allowed to infect the bacteria by incubating at 37°C for twenty minutes. 3mls of LB were added to the cells, and the incubation was continued for an additional three hours at 37°C with shaking. The sample was then heated at 70°C for fifteen minutes and the cell debris was pelleted by centrifugation at 4000x g for fifteen minutes in a table top centrifuge. The supernatant which contained the excised pBluescript phagemid packaged as filamentous phage particles was carefully transferred to a fresh sterile 50ml conical tube. This stock is stable for two months at 4°C. To isolate the phagemid containing the cDNA, 10µl of phagemid stock was combined with 200µl of SOLR cells, OD<sub>600</sub> +1.0 (Stratagene) and incubated for 15 minutes at 37°C. After this 10µl and 100µl of the phagemid-cell suspension were plated out on LB plates containing ampicillin (100µg/ml). The plates were incubated overnight at 37°C. Any resulting colonies represent recombinant pBluescript double-stranded phagemid. The phagemid was stored at -20°C

## SOLUTIONS:

### Bacterial Strains :

XL1-Blue:

### Growth Media (for 1 litre)\*:

LB: 10g Bacto-tryptone, 5g Bacto-yeast extract, 10g NaCl.

LB-agar: as above plus agar to 1.5% (w/v).

NZYCM: 10g NZ-Amine, 1g Casamino acids, 5g Bacto-yeast extract, 5g NaCl, 2g MgSO<sub>4</sub>·7H<sub>2</sub>O, pH7.5.

NZYCM  
agar: as above plus agar to 1.5% (w/v).

NZYCM-  
TOP: NZYCM medium plus Agarose 15 (Sigma) to 0.7% (w/v).

Hogness: 3.6mM K<sub>2</sub>HPO<sub>4</sub>, 1.3mM KH<sub>2</sub>PO<sub>4</sub>, 2mM Sodium citrate,  
1mM MgSO<sub>4</sub>·7H<sub>2</sub>O, 15% glycerol (w/v).

\*All media was sterilized by autoclaving, liquid cycle, 30 minutes\*

### General:

20xSSC: 3M NaCl, 0.3M Sodium citrate.

20xMOPS: 400mM Na.MOPS, 100 mM Sodium acetate, 20 mM Na<sub>2</sub>EDTA.

10xTBE: 0.9M Tris-borate, 0.02M Na<sub>2</sub>EDTA pH 8.0.

50xTAE: 2M Tris base, 6% glacial acetic acid, 0.05M EDTA pH 8.0.

TE Buffer: 10mM Tris.HCl,pH 8.0, 1mM Na<sub>2</sub>EDTA.

dNTP's: 10mM dGTP, 10mM dTTP, 10mM dATP.

### Nucleic Acid Preparation and Manipulation:

Solution D: 4M Guanidine isothiocyanate, 0.02M Sodium citrate, 0.02M N-Lauroylsarcosine, 0.7%  $\beta$ -ME.

#### 10x DNA Loading

Buffer: 0.25% (w/v) Bromophenol Blue, 0.25% (w/v) Xylene cyanol, 15% (w/v) Ficoll 400, 0.2M EDTA.

#### Methylene blue

Stain: 0.03% (w/v) Methylene blue, 0.3M Sodium Acetate.

FDB: 50% (v/v) formamide, 6% (v/v) formaldehyde, 1xMOPS.

#### 10xRNA Loading

Buffer: 50% (v/v) glycerol, 1mM Na<sub>2</sub>EDTA, 0.25% (w/v) Bromophenol blue, 0.25% (w/v) Xylene cyanol FF.

#### Transfer

Solution: 10x SSC.

#### Hybridization

Solution: 50% (v/v) formamide, 0.25mM Na<sub>2</sub>HPO<sub>4</sub> pH7.2, 0.5M NaCl, 1mM EDTA, 7% (w/v) SDS, 10% (w/v) Dextran sulphate, 400 $\mu$ g/ml yeast tRNA.

1° Wash: 2xSSC/0.1% SDS.

2° Wash: 1xSSC/0.1% SDS.

### Protein Preparation and Manipulation:

Solution I: 2% SDS, 0.1M DTT, 60mM Tris, pH 6.8.

Solution II: 0.5mM EDTA, pH 8.0, 160mM KCl, 20mM MOPS, 100 $\mu$ g/ml PMSF, 2 $\mu$ g/ml Aprotinin, 2 $\mu$ g/ml Leupeptin.

#### 2x Sample

Buffer: 100mM Tris, pH 6.8, 200mM DTT, 4% SDS, 0.2% bromophenol blue, 20% glycerol.

#### Coomassie

Blue: 0.1% Coomassie blue in 40% methanol, 10% glacial acetic acid.

Destain: 40% methanol, 10% glacial acetic acid.

Transfer  
Buffer: 25mM Tris, 190mM glycine.

10xTBS: 8g NaCl, 0.2g KCl, 25 ml 1M Tris.HCl pH7.5.

Blocking  
Solution: 5% nonfat milk, 1x TBS, 0.5% Tween-20.

Alkaline Phospatase  
Buffer: 100mM NaCl, 5mM MgCl<sub>2</sub>, 100mM Tris, pH9.5.

SM: 0.1M NaCl, 8mM MgSO<sub>4</sub>·H<sub>2</sub>O, 50mM Tris.HCl pH7.5,  
0.01% (w/v) gelatin.

Phage  
Solution: 3.75M ammonium acetate, 20% (v/v) PEG 8000.

STE  
Buffer: 100mM NaCl, 20mM Tris, pH7.5, 10mM EDTA.

## Section VI: Results and Conclusions

## SECTION VI: RESULTS AND CONCLUSIONS

### VII. Cloning of Sheep :

Using PCR based cloning I amplified a sheep specific cDNA probe for the cardiac NCX, pBNCX1 (figure 27.a). The amplified cDNA was approximately 300-400 bp in length as expected from the target sequence. Sequence and northern blot analysis of the PCR product confirmed that it coded for a region of the cardiac NCX. Figure 28 is a sequence comparison between the sheep cDNA probe and the region of interest within the canine cardiac NCX cDNA sequence showing high degree of homology. Figure 27.b is a northern blot analysis of 129 day fetal sheep heart poly(A+) RNA probed with clone pBSlex1. A single band is visible at approximately 7.0kb which agrees with the previously NCX transcript size.

Clone pBSlex1 was subsequently used to screen a fetal sheep cDNA library which I generated (Section 5.7). A total of  $1 \times 10^6$  pfu were screened under stringent conditions. Eight clones were picked and analyzed by restriction endonuclease analysis. Four, (pBSlex2-pBSlex5), out the eight were unique with respect to the restriction analysis and were characterized further. Clones pBSlex2-4 were similar and appeared to vary only in the 5'end. Because the native NCX cDNA is approximately 7.0 kb in length, I selected the largest clones to characterize.

Clone pBSlex5 was unique and contained an Ecor1 restriction site in the 5'end that was not found in the other clones. This was of particular interest because sequence analysis of the other clones revealed that they were lacking the complete 5' coding region. To analyze this, I subcloned the 5'-end and subsequent sequence analysis revealed no homology with the cardiac NCX coding sequence. A search of various DNA databases also revealed no



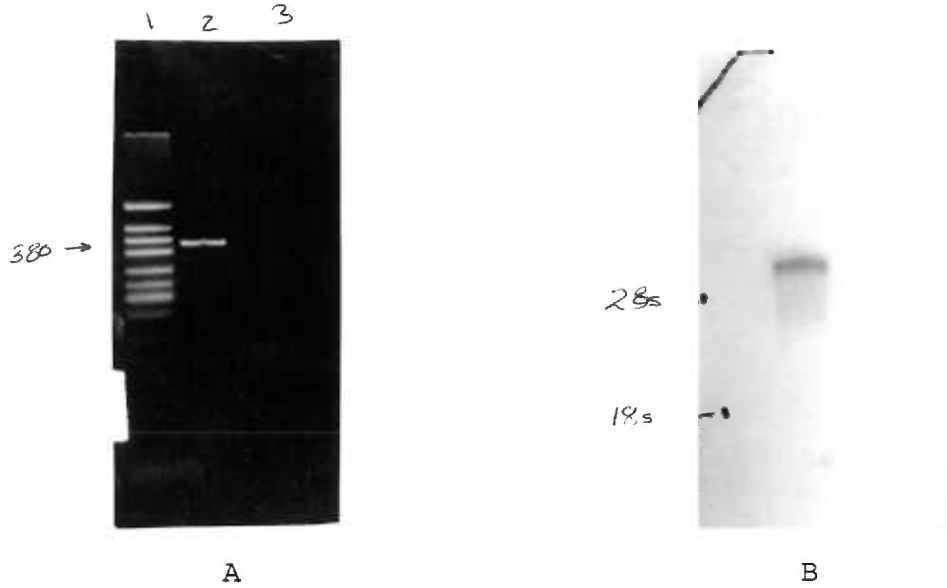


Figure 27: Panel A is a photograph of an agarose gel with the PCR product stained with ethidium bromide. Lane 1 is a standard size ladder , lane 2 is the amplified product, and lane 3 is negative control. Panel B is a northern blot of 129 day fetal sheep RNA probed with the PCR product, pBSlex1.

```

CCAGACACAT TTGCAAGCAA AGTGGCCGCC ACCCAGGACC AGTATGCGGA TGCATCCATA GGTAACGTCA
|||||      |||||      ||||| |||  |||||      |  |||||      ||  |||||      |||||      |||||
CCAGACACAT TTGCAAGCAA AGTGGCAGCC ACCCAGGATC AGTATGCAGA CGCGTCCATA GGTAACGTCA

CAGGCAGCAA CGCGGTGAAC GTCTTCCTGG GCATCGGTGT GGCCTGGTCC ATCGCCGCCA TCTACCACGC
|  |||||      |||||      |||||      |||||      |||||      |||||      |||||      |||||
CTGGCAGCAA CGCGGTGAAC GTCTTTCTGG CCATCGGCCT GGCCTGGTCC ATCGCTGCCA TCTACCACGC

GGCCAACGGG GAACAGTTCA AAGTGTCCC TGGCACGCTA GCTTTTCTG TCACTCTCTT CACCATTTT
|||||      |||||      |||||      |||||      |||||      |||||      |||||      |||||
GGCCAACGGG GAACAGTTCA AAGTGTCCC TGGCACGCTA GCTTTCTCTG TCACTCTCTT CACCATTTT

GCTTTCATCA ATGTGGGGT GCTGCTGTAT CGGCGGAGGC CAGAAATT-G GAGGTGAGCT GGGTGGGCCC
|||||      |||||      |||||      |||||      |||||      |||||      |||||      |||||
GCTTTCATCA ATGTGGGGT GCTGCTGTAT CGGCGGAGGC -AGAAATTCG GAGGTGAGCT GGGTGGGCCC

CGGACTGCCA AGCTCCTCAC ATCCTGCCTC TTTGTGCTCC TGTGGCTCTT GTACATTTTC TTCTCCTCCC
|||||      |||||      |||||      |||||      |||||      |||||      |||||      |||||
CGGACTGCCA AGCTCCTCAC ATCCTGCCTC TTTGTGCTCC TGTGGCTCTT GTACATTTTC TTCTCCTCCC

TGGAGGCCTA CTGCCAC
|||||      |||||
TGGAGGCCTA CTGCCAC

```

Figure 28: Sequence comparison of PCR amplified product (bottom sequence) and bovine cardiac NCX sequence (top sequence). Underlined segments represent the primers used to for the PCR.

significant matches. Therefore, clone pBSlex5 had what I believe to be a splicing artifact, created during the synthesis of the cDNA library. This was confirmed when the linker-adapter sequence was found at the 3'end of the clone.

Clones pBSlex3, and pBSlex4 were identical throughout most of their length except for two major discrepancies: clone pBSlex3 had a 500 bp 5' extension which was not homologous to any reported NCX sequence to date. It also had a 105 bp insert adjacent to the poly(A) tail. Unlike clone pBSlex5, this clone did not have the "linker-adaptor" sequence in it. Instead it appeared that a second gene had been spliced onto the 5' end of a portion of the NCX coding sequence. This is shown in figure 29. The splice site is apparent where the homology matches the bovine coding sequence at basepair #1330 (underlined in fig. 29).

On a search of the DNA database (GenBank) with the 500bp sequence of clone pBSlex3 no significant matches were found. Therefore I determined it to be a splice artifact of unknown origin which occurred during the cDNA library synthesis. It is likely that the artifact was related to an error of the reverse transcriptase. This is a reasonable explanation considering the length of the clone (5.5kb). This finding was discouraging because I had invested more than 6 months of time and was still 1.3 kb short of the complete coding sequence.

Some type of cloning error or artifact was found in each clone studied. I have attributed this to the large size of primary transcript. Every clone was truncated near basepair #1330 (+/-50 bases), suggesting that the reverse transcriptase had "difficulty" transcribing such a large RNA species into cDNA. Therefore to complete the cloning project I had to design new protocols for cloning the 5' end of the coding sequence. My first attempt

```

5' -CGGGCTG CAGGAATCG GCACGAGCAG GTGCCCCACG AACGTGCGGT GCGTGACGGG
CGAGGGGGCG GCGCCTTTCG GGCCCGGCCG CGGGTCCCGG GACGAAGGGC TCTCCGCACC
GGACCCCGGT CCCGACGCGC GCGGGGGGCG CGCCGCGGCC GCGCCCCCGG GGGGGGACGC
GGGGACGGC CCGCCGGCGG GGACGGGGGG GGACCGGCTA TCCGAGGCCG ACCGACGGCT
CCCGCGGCGC TCGCGTATCG GTTCGGCCTT GCGCGATTTC TGACTTAGAG GCGTTCAGTC
ATAATCCCAC AGATGGTAGC TTTGCCCCAT TGGGCTCCTC AGCCAAGGAC ATACACCAA
TGTCGAACC TCGGTTCTCT CTCGTACTG AGCAGGATTA CCATGGCAAC AACACATCAT
CAGTAGGTA AACTAACCT GTTCACGACG GTCTAAACCC ATTGACCAA-//...3'
                ^ bp #1330 in bovine NCX
                sequence

```

Figure 29: Sequence of the 468 bp 5' extension of clone pbSlex3. The underlined segment corresponds to the site where homology begins with the bovine cardiac NCX sequence. From this point on the homology is very high.

involved PCR amplification and sequencing directly from the unamplified and amplified cDNA library using PCR based cycle sequencing. I designed a new antisense primer based on my ovine sequence and used the universal T3 primer for the sense primer. As I had feared, these experiments were not successful because the cDNA library which I had made was lacking the full length cardiac clone.

I then designed new primers from the canine cardiac and the ovine sequences using primer design software. These primers were used to amplify the 5' coding sequence from genomic sheep DNA, using the PCR. Although I was originally reluctant to use genomic DNA as the template due to the possibility of complicating introns, these cloning efforts were successful. A PCR amplification product was detected which corresponded to the anticipated cDNA size. Figure 30 is a photograph of the PCR product, which is approximately 1400 bp in length. Subsequent subcloning and sequencing of this product revealed that it coded for the cardiac NCX, and did not contain introns. With this new clone corresponding to the 5' coding region I have successfully cloned and sequenced the complete coding sequence for the ovine gene including the 3' untranslated region (UTR). Figure 31 is the complete sequence of this gene including a comparison with the bovine sequence. The shared identity is approximately 96%.

The gene is well conserved across all species studied to date, including the ovine gene. Homologies range from 92%-98% at the nucleotide level and the similarity of proteins are equally conserved. The deduced amino acid sequence appears to code for a protein with 11 transmembrane domains and a large hydrophilic intracellular loop (153). Fig. 32 is the translated ovine sequence compared to the bovine sequence. The conserved transmembrane

domains are underlined. The similarity between the two proteins is remarkable, and is consistent with other species studied. The only significant

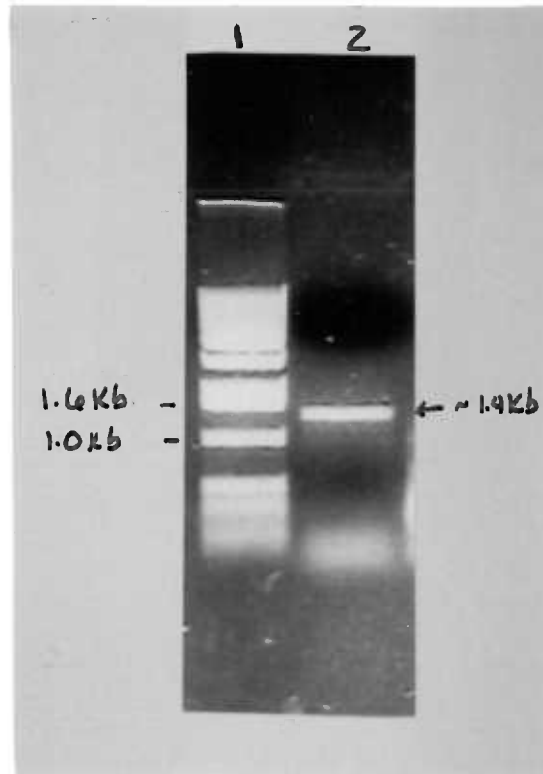


Figure 30: Photograph of agarose gel with ethidium bromide stained PCR product. Lane 1 is a standard molecular size marker. Lane 2 shows the 1400bp PCR product.



CTACCCGCCT GATGACCGGA GCAGGCAACA TTTTAAAGAG GCATGCAGCA GACCAAGCCA GGAAAGCTGT CAGCATGCAT  
|||||?||| ||?||||| ||||||| ||||||| ||||||| |||||||?||| |||||||  
CTACCCGCCT GATGACTGGA GCGGGCAACA TTTTAAAGAG GCATGCAGCA GACCAAGCCA GGAAAGCCGT CAGCATGCAT  
  
GAGGTCAACA CGGAAGTGGC TGAAAATGAC CCTGTGAGTA AGATCTTCTT TGAACAAGGG ACATATCAGT GTCTGGAGAA  
|||||?||| ||||||| ||||||| ||||||| ||||||| ||||||| ||||||| |||||||  
GAGGTCAACA CGGAAGTGGC TGAAAATGAC CCTGTGAGTA AGATCTTCTT TGAACAAGGG ACATATCAGT GTCTGGAGAA  
  
CTGTGGCACA GTAGCCCTGA CCATTATCCG CAGAGGTGGT GATTTGACCA AACTGTGTT TGTGACTTC AGAACAGAGG  
|||||?||| ||||||| ||||||| ||||||| |||||||?||| ||||||| |||||||  
CTGTGGCACA GTAGCCCTGA CCATTATCCG CAGAGGTGGT GATTTGACCA AACTGTGATT TGTGACTTC AGAACAGAGG  
  
ATGGCACAGC CAATGCTGGA TCTGATTACG AATTTACCG- AAGGAACTGT GGTCTTTAAG CCTGGTGAGA CCCAGAAGGA  
||||?||| ||?||| ||||||| |||||||: :||| ||||||| ||||||| |||||||  
ATGGTACAGC CAACGCTGGA TCTGATTACG AATTTACCGG AA-GAACTGT GGTCTTTAAG CCTGGTGAGA CCCAGAAGGA  
  
AATCAGAGTT GGCATCATTG ATGATGACAT CTTTGAGGAG GATGAGAATT TCCTTGTGCA TCTCAGCAAC GTCAAAGTAT  
|||||?||| ||||||| ||||||| ||||||| ||||||| ||||||| ||||||| |||||||  
AATCAGAGTT GGCATCATTG ATGATGACAT CTTTGAGGAG GATGAGAATT TCCTTGTGCA TCTCAGCAAC GTCAAAGTAT  
  
CTTTGGAAGC CTCGGAAGAC GGCATCCTGG AAGCCAGTCA TGTCTCTACC CTGCTTGCC TGGGATCCCC CTCCACTGCC  
|||||?||| |||||||? |||||||? |||||||? |||||||? |||||||? |||||||?  
CTTTGGAAGC CTCGGAAGAT GGCATCCTGG AAGCCAGTCA TGTCTCTACC CTGCTTGCC TGGGATCTCC GTCCACTGCC  
  
ACCGTACTA TTTTGTGTA TGACCATGCT GGCATCTTTA CTTTGTAGGA ACCGGTGACT CATGTGAGTG AGAGCATTGG  
|||||?||| |||||||? |||||||? |||||||? |||||||? |||||||? |||||||?  
ACCGTACTA TTTTGTGTA TGACCACGCT GGCATCTTTA CTTTGTAGGA ACCCGTGACT CATGTGAGTG AGAGCATTGG  
  
CATCATGGAG GTGAAAGT-T CTGAGAACAT CTGGAGCAGC TGGAAATGTT ATCGTTCCT ATAAGACCAT TGAGGGGACC  
|||||?| ||||?|:| :||?||| ||||||?| ?|?||| ||||||| |||||||?| |||?|||?  
CATCATGGTG GTGAAGGTAT -TGCGAACAT CTGGAGCTCG AGTAAATGTT ATCGTTCCT ATAAGACCGT TGAAGGGACT  
  
GCCAGAGGTG GAGGGGAGGA CTTTGTAGGAC ACATGCGGAG AGCTCGAGTT CCAGAATGAC GAAATTGTCA AAACAATATC  
|||||?||| ||||?||| ||||?||| ||||?||| ||||||| ||||||| |||||||  
GCCAGAGGTG GAGGAGAGGA CTTCGAGGAC ACATGTGGAG AGCTCGAGTT CCAGAATGAC GAAATTGTCA AAACAATATC  
  
AGTCAAGGTA ATTGATGATG AGGAGTATGA GAAAAACAAG ACCTTCTTCC TTGAGATTGG AGAGCCCCGC CTGGTGGAGA  
|||||?||| ||||||| ||||||| ||||||| ||||||| ||||||| ||||||| |||||||  
AGTCAAGGTA ATTGATGATG AGGAGTATGA GAAAAACAAG ACCTTCTTCC TTGAGATTGG AGAGCCCCGC CTGGTGGAGA  
  
TGAGTGAGAA GAAAGCCCTG TTATTGAATG AGCTTGGTGG CTTCAACAATA ACAGGGAAT ACCTGTATGG CCAGCCTGTC  
|||||?||| ||||||| ||||||| ||||||| ||||||| ||||||| ||||||| |||||||  
TGAGTGAGAA GAAAGCCCTG TTATTGAATG AGCTTGGTGG CTTCAACAATA ACAGGGAAT ACCTGTATGG CCAGCCTGTC  
  
TTCAGGAAAG TTCATGCTAG AGAACATCCA CTCCCCTCTA CTATAATCAC CATCGCAGAT GAATATGATG ACAAGCAGCC  
|||||?||| ||||||| ||||||| ||||||| ||||||| ||||||| ||||||| |||||||  
TTCAGGAAAG TTCATGCTAG AGAACATCCA CTCCCCTCTA CTATAATCAC CATCGCAGAT GAATATGATG ACAAGCAGCC  
  
ACTGACCAGC AAAGAGGAGG AAGAGAGGCG CATTGCGGAA ATGGGGC-GC CCCATTCTGG GAGAGCACAC CAGACTGGAG  
|||||?||| |||||||? |||||||? |||||||? |||||||: :||| |||||||?||| |||||||  
ACTGACCAGC AAAGAAGAGG AAGAGAGGAG CATTGCGAAG ATGGGGCTG- CCCATTCTGG GAGAACACAC CAGACTGGAG  
  
GTGATCATTG AAGAATCCTA CGAGTTCGAG AGTACCGTGG ACAAACTGAT TAAGAAGACA AAC-CTAGCC CTCGTGGTTG  
|||||?||| |||||||? |||||||? |||||||? |||||||? |||||||: :||| |||||||  
GTGATCATTG AAGAATCCTA TGAGTTCGAG AGTACCGTGG ACAAACTGAT TAAGAAGACA AACTC-AGCC CTCGTGGTTG  
  
GGACGAACAG CTGGAGAGAG CAGTTCATCG AGGCGATCAC TGTCAGTGCT GGGGAAGATG A---CGA--- TGACGACGAA  
||||?||| |||||||? |||||||? |||||||? |||||||? |||||||: :|||: :||| |||: :|||: :|||  
GGACTAACAG CTGGAGAGAA CAGTTCATTG AAGCCATCAC TGTCAGTGCT GGGGAAGATG ATGACGACGA TGA-----A  
  
TGTGGGGAGG AGAAGCTGCC CTCCTGTTT GACTACGTGA TGCACCTTCT GACTGTGTTC TGGAAGGTCC TCTTCGCCTT  
|||||?||| |||||||? |||||||? |||||||? |||||||? |||||||: :||| |||||||  
TGTGGGGAGG AGAAGCTGCC CTCCTGTTT GATTACGTGA TGCACCTTCT GACTGTGTTC TGGAAGGTCC TCTTCGCCTT





```

TGGCATAATC CTAACCCGAT TTTTTCTGAA GATTTATTTA ATGCAAAAAGC TAGCCTAGAAA CACCAAGTAA ATAGTCAAGG
GATATGAGTT GTTTAAACAT TAGAAAGACTT TGCACCTTCTT TCTAGCTATA TTTGGAATGTT AATGAYCCCA TAGCAAATTT
CACAGAGGAT GTTAAGAAAT CTTTACCGTTG GTCAATTTCA ATTTCAAAGC TTTTGGTTTG TTTGCTTTTT AAATTTTCAT
GTTATAGAGA AAATATGATT CTGGTTGTTCA GGGTTGTTTT AGTAATTATA GTCATGTAAAA TTATTTTCAT TTGATTATTT
TATTTTGTGT GAATTGTGCA CAGCTTAGGGG GGAGGTACAC TAATTGTGCT GTTCCTTATAA ATGGTACACA TTATTGACAC
AGACAAATAA AGTTTCTAAT GATTTCTGATT TAATCACTAG TGATCCAGCA TATCTGTATG GAATGTTTTC TCTCTTCTCA
TTGTCATCTA CTTTCATCTTT TGTTTTTCATGT TTTGAAGAAA TAAAGACCT AAAAGGTTTTT +6013

```

Figure 31: Comparison of the cDNA sequences of the bovine and ovine cardiac NCX genes. The upper sequence is that of the bovine gene (Bv) and the lower is for the ovine gene (Ov). Homology is very high throughout the coding sequence. The bovine sequence extends 240 bp further in the 5' direction. This is due to the incomplete cloning of the ovine sequence. The "ATG" start codon is conserved between the two sequences and is in bold type. It is likely that a significant degree of homology would exist in the 5' untranslated region, but those studies have not been done. The only major discrepancy is the site of the T(A/G)A stop codon. The ovine coding sequence extends approximately 60bp further than the bovine coding sequence. The complete 3' untranslated sequence of the ovine sequence is also shown in this figure. The full bovine 3'UTR is not available for sequence comparison. (Legend: |=identical base, ?=mismatch base, - = introduced gap)

difference between the two protein sequences is the termination site. This is denoted by a period (.) in figure 32. The ovine NCX protein extends 26 amino acids further at the C-terminus.

In addition to sequencing the complete coding sequence of the ovine gene I have made a preliminary analysis of the 3'UTR. The 3'UTR of the gene is about 3.0 kb and is rich in "AT" domains (Fig. 33). This region has not been studied in depth in any species to date and should be valuable in understanding how the gene is regulated. Of note, however, are 5 conserved Shaw-Kamen pentamer sequences (ATTTA) in the 3'UTR. Although the significance of these sequences are not known, they have been shown to possibly play a role in mRNA instability (144).

Analysis of clones pBSlex3 and pBSlex4 revealed unique 3' end sequences. Although both clones had intact poly(A<sup>+</sup>) tails, clone pBSlex4 was missing a 105 bp portion adjacent to the tail (Fig. 34). Two explanations for this discrepancy are possible; 1) a splicing artifact and/or 2) alternative splicing. I have ruled out a splicing artifact because the poly(A<sup>+</sup>) tail is the initiation site for the cDNA synthesis, thus mispriming of the oligo-d(T) primer would have generated a completely separate cDNA species. This was not the case since homology with clone pBSlex3 begins just after the poly (A<sup>+</sup>) tail (fig 34). In addition, at the site where homology begins a conserved Shaw-Kamen pentamer sequence is observed. This sequence may provide some insight to the regulation of the expression of the NCX gene.

Furthermore, the poly(A<sup>+</sup>) tail of clone pBSlex4 was more than 20 bases in length, suggesting that the priming site contained more than two adenine residues which are all that are present adjacent to the poly d(T) primer sequence. Although a splicing artifact could be the unlikely explana-

Figure 32: Translated Bovine vs. Translated Ovine cDNA sequences  
 Top: Bovine amino acid sequence  
 Bottom: Ovine amino acid sequence

MLQFSLSP T L S M G F H V I A M V A L L F S H V D H I S A E T E M E G E G N E T G E C T G S Y Y C K K G V I L P I W E P Q D P S F G D  
 |||  
MLQFSLSP T L S M G F H V L A M V A L L F S H V D H I S A E T E M E G E G N E T G E C T G S Y Y C K K G V I L P I W E P Q D P S F G D  
 |||  
K I A R A T V Y F V A M V Y M F L G V S I I A D R F M S S I E V I T S Q E K E I T I K K P N G E T T K T T V R I W N E T V S N L T L M A L G  
 |||  
K I A R A T V Y F V A M V Y M F L G V S I I A D R F M S S I E V I T S Q E K E I T I K K P N G E T T K T T V R I W N E T V S N L T L M A L G  
 |||  
S S A P E I L L S V I E V C G H N F T A G D L G P S T I V G S A A F N M F I I I A L C V Y V V P D G E T R K I K H L R V F F V T A A W S I F  
 |||  
S S A P E I L L S V I E V C G H N F T A G D L G P S T I V G S A A F N M F I I I A L C V Y V V P D G E T R K I K H L R V F F V T A A W S I F  
 |||  
A Y T W L Y I I L S V S P G V V E V W E G L L T F F F F P I C V V F A W A D R R L L F Y K Y V Y K R Y R A G K Q R G M I I E H E G D R P  
 |||  
A Y T W L Y I I L S V S P G V V E V W E G L L T F F F F P I C V V F A W A D R R L L F Y K Y V Y K R Y R A G K Q R G M I I E H E G D R P  
 |||  
S S K T E I E M D G K V N S H V D S F L D G A L V L E V D E R D Q D D E A R R E M A R I L K E L K Q K H P E K E I E Q L I E L A N Y Q V  
 |||  
S S K T E I E M D G K V N S H V D S F L D G A L V L E V D E R D Q D D E A R R E M A R I L K E L K Q K H P E K E I E Q L I E L A N Y Q V  
 |||  
L S Q Q K S R A F Y R I Q A T R L M T G A G N I L K R H A A D Q A R K A V S M H E V N T E V A E N D P V S K I F F E Q G T Y Q C L E N C G  
 |||  
L S Q Q K S R A F Y R I Q A T R L M T G A G N I L K R H A A D Q A R K A V S M H E V N T E V A E N D P V S K I F F E Q G T Y Q C L E N C G  
 |||  
T V A L T I I R R G G D L T N T V F V D F R T E D G T A N A G S D Y E F T E G T V V F K P G E T Q K E I R V G I I D D D I F E E D E N F L V  
 |||  
T V A L T I I R R G G D L T N T V F V D F R T E D G T A N A G S D Y E F T G R T V V F K P G E T Q K E I R V G I I D D D I F E E D E N F L V  
 |||  
H L S N V K V S L E A S E D G I L E A S H V S T L A C L G S P S T A T V T I F D D D H A G I F T F E E P V T H V S E S I G I M E V K V L R T  
 |||  
H L S N V K V S L E A S E D G I L E A S H V S T L A C L G S P S T A T V T I F D D D H A G I F T F E E P V T H V S E S I G I M V V K V L R T  
 |||  
S G A R G N V I V P Y K T I E G T A R G G G E D F E D T C G E L E F Q N D E I V K T I S V K V I D D E E Y E K N K T F F L E I G E P R L V E  
 |||  
S G A R V N V I V P Y K T V E G T A R G G G E D F E D T C G E L E F Q N D E I V K T I S V K V I D D E E Y E K N K T F F L E I G E P R L V E  
 |||  
M S E K K A L L L N E L G G F T I T G K Y L Y Q P V F R K V H A R E H P L P S T I I T I A D E Y D D K Q P L T S K E E E E R R I A E M G R  
 |||  
M S E K K A L L L N E L G G F T I T G K Y L Y Q P V F R K V H A R E H P L P S T I I T I A D E Y D D K Q P L T S K E E E E R S I A E M G L  
 |||  
P I L G E H T R L E V I I E E S Y E F K S T V D K L I K K T N L A L V V G T N S W R E Q F I E A I T V S A G E D D D D E C G E E K L P S C  
 |||  
P I L G E H T R L E V I I E E S Y E F K S T V D K L I K K T N S A L V V G T N S W R E Q F I E A I T V S A G E D D D D E C G E E K L P S C  
 |||  
F D Y V M H F L T V F W K V L F A F V P P T E Y W N G W A C F I V S I L M I G L L T A F I G D L A S H F A C T I A L K D S V T A V V F V A L  
 |||  
F D Y V M H F L T V F W K V L F A F V P P T E Y W N G W A C F I V S I L M I G I L T A F I G D L P S H F G C T I G L K D S V T A V V F V A L  
 |||  
G T S V P D T F A S K V A A T Q D Q Y A D A S I G N V T G S N A V N V F L G I G V A W S I A A I Y H A A N G E Q F K V S P G T L A F S V T L  
 |||  
G T S V P D T F A S K V A A T Q D Q Y A D A S I G N V T G S N A V N V F L A I G V A W S I A A I Y H A A N G E Q F K V S P G T L A F S V T L  
 |||  
F T I F A F I N V G V L L Y R R R P E I G G E L G G P R T A K L L T S C L F V L L W L L Y I F F S S L E A Y C H I K G F .  
 |||  
F T I F A F I N V G V L L Y R R R Q K F G G E L G G P R T A K L L T S C L F V L L W L L Y I F F S S L E A Y C H I K G F I Y G R C S S K F I  
 |||  
 Y I Y I Y I Y I K S I M N R G N .

Figure 33:

**BOVINE 3' Untranslated Region:** 5'.....//.....TATAATGAAC AGAGGAAACT  
 |||||? |||||

**Ovine 3' Untranslated Region:** 5'.....//.....TATAATGAAT AGAGGAAACT

GGCATTTGTC ATGTCCACCC ACCTGCTGATG GAATCCAGCT TCAAGAGCAGA CTCTGTACTA GGGCCCGAGA GAGAAGGCAT  
 |?|||?|| ||||| ||||| ||||| ||||| ||||| ||||| |||||? |||||

GACATTTCTC ATGTCCACCC ACCTGCTGATG GAATCCAGCT TCAAGAGCAGA CTCTGTACTA GGGCCCGAGT GAGAAGGCAT

CACCTCCCGT TTCCCAGGGG CGTTCGTCTTG TTGAACCAGG CATGGAGGCAG GGCCATCTTT ACCTCAGCTC AGCCAGAAG  
 ||||| |||||? |||||? ||||| ||||| |||||? |||||? |||||? |||||

CACCTCCCGT TTCCCAGGGG A--TCGTCTTG TTGAACCAGG CAT----- -CTTT GCAGCC--TC AGCCAGAAG

CGGTGTGTTT TCCCAGGGTT CATAAATCCTT AAGTTCTTTG ATTTGTTTTCT GTTTTGCTT GTTTGGGTC GGGTAGGGA  
 ?|||? |||||? |||||? |||||? |||||? |||||? |||||? |||||? |||||?

GGCTGTGTTT TCCCTGGGTT CATAAATCCTT AAGT-CCTTG ATTTGTTTTCT GTTTTGCTT GTTTGGGTC GGGTAGGGA

GGTGGTTGAT GTTAGGGTTT GGTTTTGGTTT TGCAGGGGA AGATCAGGGTT TGTGGTCTC TTGTGGGAGG TGATGTCCAA  
 ||||| ||||| |||||? |||||? |||||? |||||? |||||? |||||? |||||?

GGTGGTTGAT GTTAGGGTTT GGTTTTGTTC TGCAGGGGA GGATCAGGGTT TGTGCTTCTC TTGTGGGAGG TGATGTCCAA

TCTCAATGGT AAAAATGGAA ATCAGGAAGAT GACTCTCCCT TTGCCAAAA ACTTTAAAA TTATTTTGA GTAAGAAAGG  
 |||||? |||||? |||||? |||||? |||||? |||||? |||||? |||||? |||||?

TCTCAGTGGT AAAAATGGAA ATCAGGAAGAT GATTCTCCCT TTGCCAAAA ACTTTAAAA TTATTTTGA GGAAGAAATG

AAACGGGCAT GGAAGAAGAA AGAAGCATGTC TTCACCATAT TACTAAATTC ATGCCTTATC TCTGGAGTGG GAGCAGAGGT  
 ????? ||||| ||||| ||||| ||||| |||||? ||||| ||||| |||||

----GGCAT GGAAGAAGAA AGAAGCATGTC TTCACCATAT TACTAAATTC ATGC--TTATC TCTGGAGTGG GAGCAGAGGT

GAAGTCTCC CTCCAAGAAG AAACAGGGGAG CTGGAATGGA GCCAAGAAGAG TCATGGTTCT AGATACAGTC TGATGTTAA  
 |||||? |||||? |||||? |||||? |||||? |||||? |||||? |||||? |||||?

GAAGTCCCC C-CCAAGAAG AAACATGGGAG CTGGAATGGA GCTAAGAAGAG TCATGGTTCT AAATACAGTC TGATATTTA

AGATACATCG CTGCCTGGCA CCCTGTGTTCA ACAGGTACAAA AACAACATGCC TAGATTCCCA GGAACGCACA AAGTCTTTT  
 |||||? |||||? |||||? |||||? |||||? |||||? |||||? |||||? |||||?

AGATACTAGG ---CCTGGCA CCCTGTGTTCA ACAGGTACAAA AACAACATGCC TAGATTCCCA GGAACATACA AAGTCTTTT

TTATCTCTTC AGCGCTGGAC TGTGATTAGC AAGGCCCTGAT TCTGATGTTCT ACACCCGCTG ATTCCCAGC CCTCCCATCC  
 |||||? |||||? |||||? |||||? |||||? |||||? |||||? |||||? |||||?

TTATCTCTTT AGCGCTGGAC TATGATTAGC AAGGCCCTGAT TCTGATGTTCC ACACCCGCTG ATTCCCAGC CCTCCCATCC

CAAACCCCTT CTCCGGACCC TTTACCCCTC GTACAAACAGG AAGAATAACTC CATTCAAAA GCACACCATC CTTTCCATTC  
 |||||? |||||? |||||? |||||? |||||? |||||? |||||? |||||? |||||?

CAAACCCCTT TFCCTG-CCC TTTACCCCTC ATACAAACAGG AAGAATAACTC CATTCAAAA GCACATCATC CTTTCCATT

-GCATCTGCC TGGGATGTCC ATCAGTTCTG TTTTCCAAGG CATCTACGGCC TGCACACTCC TGTTCAGTC ATGAGGGAACA  
 ?|||? |||||? |||||? |||||? |||||? |||||? |||||? |||||? |||||? |||||?

TGCATCAGTC TGTGTCCCAT GTTGCTATCC TCTTTCATCT GCCTGTTGGG AATGTTGTTG TGATAACCTG TTACACAGTGC

TTTGCT  
 ?????  
 ATGGATGA AAACATAAC AAAACAAAGC

GTATCTGTAT ATAGTAGAGT ATAGCATATA CTGTTCTCCCA TTTGGCGACAT TGATTGGACA TTGAAGACAT AAGTGAGTTT

TCTTTTACC TGAGTTGTAA CTTTTGTGTT GTTATTGAGTT TGATTAGGGAT AAAAGGAGAA AATGGCTTAT TGTTTCATGGAT

CTGCAGGTTT ATTTCTAAGA AACAATAACT GTTACGTGGGA GTTAAAGCTAT TGAGAGGACA GTGGACACGC GACAAAGTATC

TTCAAGGAAA ATTAGCCATG TGGTGCATTT CGAAGCCTTGA AAACACCTG TTGGTTCAGG AGGGCCGAGG AGAAGGGCTGT  
 GTAGAGAAGG GTGCACGTTA GATGTGCCTG GGCTCTGAAA CCTCCGTTCTT GGAACACCCC GCCCCCAAAGT **ATTTA**TTTCA  
 CATCTGCTCT GTCTGGCACA GATGGTAGAT AGTGCTGGTTT TTTCATTTTAT TTTTTATGTA AAAGGCTATT CAGAGCCCCAT  
 TTGTTACCCG TCCACACCCC TCTGATAGTA TCTGCAGTTC TGAGGAGAAAA GAAGCCACGG TGAGCAACAG GCCTTCTCTAC  
 GTAGGGCTAA GGAGGAAGTG ATTAAAATGA GAGTGCCTCTC ATAGGACTACT CTGGGAGGTT TTTAACCCCTG GAAATGGAATG  
 GCTCTATTTC ACAATATCAA AGAGTATGAT AAACCCAACAT TCCAAAGCTGT GAGTCCACAA ATGAGGAAAA ATGGAATGACT  
 TAGGTCCCCCT CTCAGACATT TCTCTATCCA TAAAGAATCCC AGGCCGGAGAC ACCCCTAAGC CCTCTGTGTT GATTCAAAGAT  
 ACTTAACTGA TAATAATTTT CATTTCTTAT TTTCTCTTCT CCACCTAGTAA TCACAATCAT TCATC**ATTTA** ATAAACACTGG  
 GTGACTGAAC AAATGAGTAA ATGCTGAGCA CCCACTCAATC TGCCAGTACT GTGCTAGCAC TCGGGGACTA CACACGCACCA  
 GACAGCCCAG ATCCCTATCC TGAGGGGGTC CACAGTTAATC CCTGAGTAACA GTTAACACAG CCACATGGAG ACAGTGTGATC  
 TTACAAGAAA AACACAATG CTGAAATTAT CTTGCCTAGAT GTCCAAGATTT TCTTGATCTG AGAGAGTACA AGGCACAGGGT  
 AGGAGCAGCC GTCTGTATCC TGAGCCAATC TTGCAGATCTG TACACCTTTCC ATTTTAAACC AAGTAAGGAA ATCCTGTGAT  
 GACCCAGCTG TCTGAGAAAT CCCAATTAAT CCAAATTTTTA TCTTCAGCTGA TCTTTGTTGG ACAGCAGTAC TTTTCCATGCC  
 CCCTGCAGCT ATAATTTCTC ACATCTCCTG GAGCCTCCGCC CTGACCTGTCA TGGCCCAACG TGCTGGTGGC ATAATCCTAAC  
 CCGATTTTTT TCTGAAGATT **TATTTA**ATGC AAAAGCTAGCC TAGAAACACCA AGTAAATAGT CAAGGGATAT GAGTTGTTTAA  
 ACATTAGAAA GACTTTGCAC TTCTTTCTAG CTATATTTGGA ATGTTAATGAT CCCATAGCAA ATTTACAGA GGATGTTAAGA  
 AATCTTTACC GTTGGTCAAT TTCAATTTCA AAGCTTTTTGG TTTGTTGCTT TTTAAATTTT CATGTTATAG AGAAAATATGA  
 TTCTGGTTGT TCAGGGTTGT TTTAGTAATT ATAGTCATGTA AAATATTTTCA TTTTCATTAT TTTATTTTGT GTGAATGTGC  
 ACAGCTTAGG GGGGAGGTAC ACTAATGTG CTGTTCCCTTAT AAATGGTACAC ATTATTGACA CAGACAAATA AAGTTTCTAATG  
 ATTTCTG**AT TTA**ATCACTA GTGATCCAGC ATATTCTGTAT GGAATGTTTC TCTCTTCTCA TTGTCATCTA CTTTCATCTTTT  
 GTTTTCATGT TTTGAAGAAA **TAA**GACCCT AAAAGCTTTTT 6013

Figure 33: Nucleotide sequence comparison of full-length ovine cardiac NCX 3'UTR and partial bovine cardiac NCX 3'UTR. Homology is very well conserved between the two species in the region which has been reported. The 3'UTR of both sequences is rich in "AT" residues, which is common in the 3'UTR of many genes. Significant nucleotide sequences have been underlined. These include the ovine stop codon (TGA) at the start of the sequence. The polyadenylation signal sequence is also underlined (AAATAA) near the end of the sequence. Of particular interest are the multiple Shaw-Kamen petamer sequences (ATTTA) throughout the 3'UTR (bold and underlined).

### 3' untranslated region sequence comparison

```
pBSlex3: 5'-...//.....ATTATTGACA CAGACAAAATA AAGTTTCTAAT GATTTCTGAT TTAATCACTA GTGATCCAGC
           ||| ||| ||| ||| ||| ||| ||| ||| ||| ||| ||| ||| ||| ||| ||| ||| ||| ||| ||| ||| ||| |||
pBSlex4: 5'-...//.....ATTATTGACA CAGACAAAATA AAGTTTCTAAT GATTTCTGAT TTA-----
           ||| ||| ||| ||| ||| ||| ||| ||| ||| ||| ||| ||| ||| ||| ||| ||| ||| ||| ||| ||| |||

ATATTCTGTAT GGAATGTTTTC TCTCTTCTCA TTGTCATCTA CTTTCATCTTT GTTTTCATGT TTTGAAGAAA TAAGACCCTA
-----

AAAGCTTTTT      6013
   ||| |
-----TTTTT      5908
```

Figure 34: Comparison of unique 3'UTR sequences from clones pBSlex3 and pBSlex4. Underlined sequences represent putative poly-adenylation signals. Bold and underlined sequences represent a putative Shaw-Kamen element. (|= conserved nucleotide, - = introduced gap).

tion for this finding, I believe alternative splicing is a more likely. This idea is bolstered by a recent study by Nadia Gabellini reporting multiple alternative splice sites within the 3'UTR of the canine cardiac NCX gene. This will undoubtedly be an exciting area of research in the near future.

The most powerful evidence for splicing is the recent report showing that the 3' end of the human cardiac cDNA is homologous to the sequence of the two clones described above (126). This confirms that both clones code for the cardiac NCX, however the question of why clone pBSlex4 is missing 105 bp remains unanswered. Gabellini suggested that the first cardiac sequence (pTB11) reported by Nicoll et al (124) was truncated at the 3' end, including poly(A<sup>+</sup>) tail. Expression of this clone in *Xenopus* oocytes was poor and could only be seen when the 3'UTR and poly(A<sup>+</sup>) of the glucose transporter was spliced to it. It appears that the native 3' end and poly(A<sup>+</sup>) tail may be involved in mRNA stabilization and needed for appropriate expression. Clone pBNCX4 may be similar to clone pTB11 in that it may represent a relatively low copy number transcript in comparison to clone pBNCX3 which was more readily pulled up from the cDNA library. The 105 bp sequence adjacent to the poly(A<sup>+</sup>) tail was present in three of the four clones sequenced. I conclude that there is alternative splicing in the sheep heart .

#### VI.2: Northern blot analysis of calcium transport proteins:

I have studied the expression pattern of the genes encoding , SERCA2a and the ryanodine receptor (ryr-2) during development of the sheep heart. Northern blot analysis of total RNA from 80 day fetal heart (gestation is 147 days) and adult heart is shown in figure 35.a. Ten micrograms of total RNA

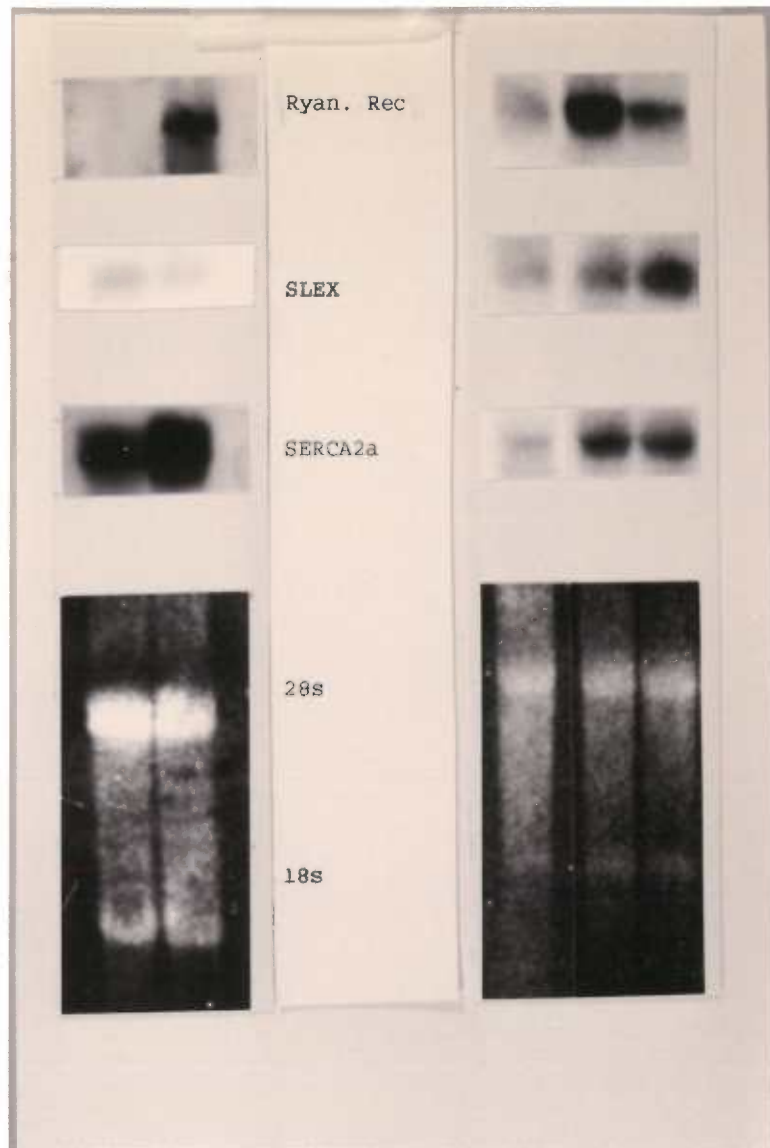


Figure 35: Northern blot analysis of total RNA extracted from sheep hearts of various ages. Panel A contains 10 $\mu$ g of total RNA extracted from 80 day LV (lane 1) and adult LV. The blot was probed sequentially with cDNA probes specific for the NCX (SLEX), SERCA2a, and ryanidine receptor genes. The top blot shows the hybridization of the ryr-2 cDNA probe. The expression of this gene is very low in the 80 day heart and strong in the adult. The middle blot shows the hybridization of the pBSlex1 cDNA probe. The expression of the NCX gene is similar between the two ages. Finally the bottom blot shows the hybridization intensity of the SERCA cDNA probe. Although this blot was over exposed it is apparent that the expression of this gene is greater in the adult heart compared to the 80 day fetal heart. Panel B is arranged similarly, but includes total RNA (10 $\mu$ g) extracted from a non-pregnant adult heart (lane 3). In addition to substantiating the results observed in panel A, some interesting findings are observed with respect to the gene expression in the pregnant sheep heart. The expression pattern of the ryanidine receptor gene appears to be reduced during pregnancy. Not quite as dramatic are the expression levels of the NCX and SERCA2a genes. However, it appears that the NCX gene may be upregulated in the heart during pregnancy. The SERCA2a gene, on the other hand may be downregulated. More studies are necessary to substantiate these findings. The lower half of each panel is a photograph of the ethidium bromide stained RNA to show equal loading of RNA.



from each sample was probed sequentially with cDNA probes specific for each of these genes.

I hypothesized that the NCX expression would be greater in the more immature fetal sheep heart even though morphological studies indicate that SR is present as early as 50 days gestation. The expression levels of the NCX gene between the 80 day fetal heart and adult heart were not visibly different, as indicated by hybridization with the SLEX probe(Fig. 35). This finding was unexpected based on the data from small mammals. Previous studies in rabbits indicate that the expression is greater in the fetal heart relative to the adult heart.

Northern blot analysis of SERCA2a expression show that the 80 day fetal sheep heart has detectable levels of SERCA2a message. The expression pattern of the SERCA2a gene in sheep is similar to findings in rabbit. The SERCA2a gene is expressed at low levels in the immature cardiac myocyte and increases as development progresses (Fig. 35). In agreement with this progression is the expression pattern of the gene encoding the ryanodine receptor, another SR related protein (Fig. 35). The expression of the ryr-2 gene is low in the 80 day fetal heart and increases throughout development to reach peak values in the adult heart.

Figure 35 is northern blot data also showing the developmental expression of the NCX and SERCA2a genes. This blot is more clear, but is missing the Ryr-2 data. Panel A shows the SERCA2a hybridization intensity in 80 day fetal heart, 5 day newborn, and adult heart. The SERCA2a is expressed in the immature heart and increases as development proceeds. Panel B is the same blot probed with the pBSlex1 cDNA. Here the hybridization intensity between the 80 day fetal heart and the adult are comparable. An interesting observation was made with respect to NCX

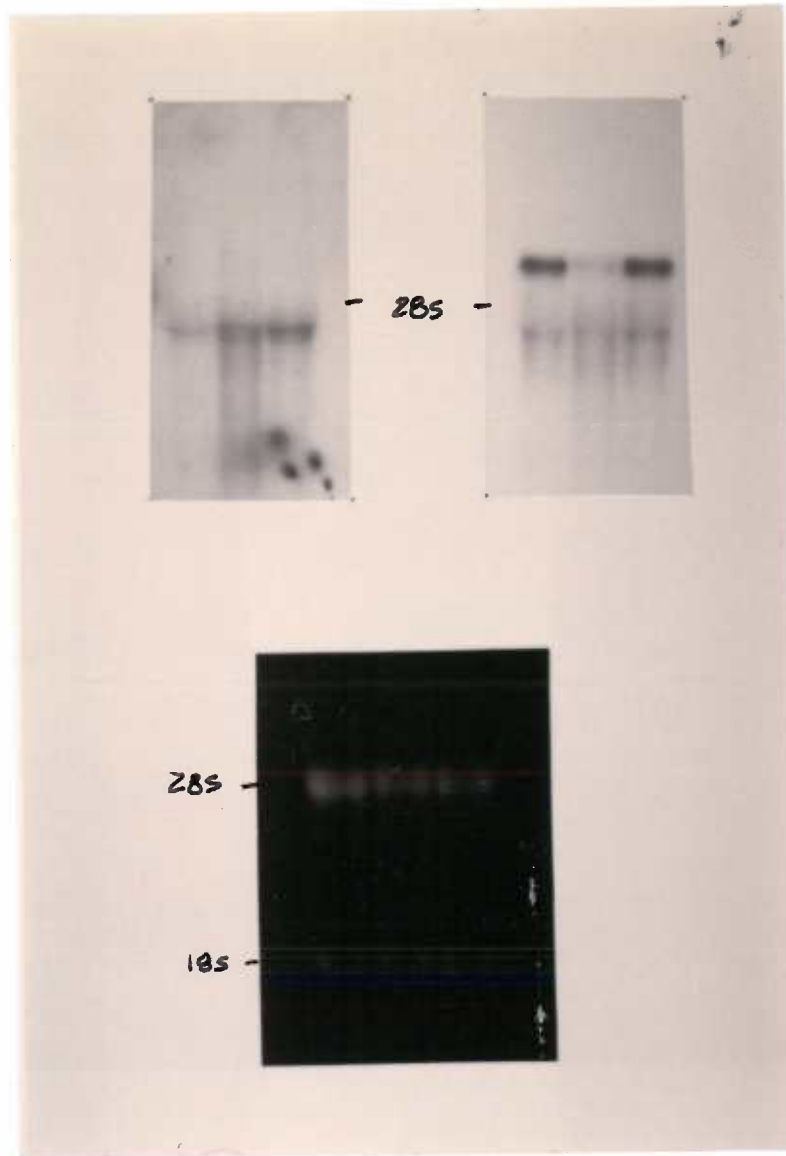


Figure 36: Northern Blot analysis of total RNA extracted from sheep hearts of various ages. The northern blot contains 10  $\mu$ g of total RNA extracted from 80 day LV (1), 5 day newborn RV (2), and maternal LV (3). The blot was probed sequentially with cDNA probes specific for the NCX (SLEX) and SERCA2a genes. Panel A shows the hybridization intensity of the SERCA cDNA probe. The expression of the SERCA2a gene increases during development as indicated by the previous blots (fig. 35). Panel B shows the hybridization intensity of the pBSlex1 cDNA probe. The expression of the NCX gene is comparable between the 80 day and adult heart, however it drops in the 5 day newborn heart. This was an unexpected finding which needs to be further studied. The 5 day total RNA sample appears to be intact due to the hybridization of the SERCA cDNA probe and the ethidium bromide staining (bottom). Panel C is a photograph of the ethidium bromide stained RNA. This is used to estimate the quality and equivalence of sample loading.

expression in the 5 day newborn heart. NCX expression decreased to extremely low levels. This is a preliminary finding and needs to be substantiated with further studies. However, previous studies in the developing heart have shown similar findings in the postnatal heart (155, 156).

For these studies the maternal heart has been used as the mature heart. I was interested in how the expression of these genes might differ between the pregnant and non-pregnant female hearts so I compared their respective message levels. Figure 35, panel B, lane c represents gene expression in the non-pregnant female sheep heart. Expression of the ryanodine receptor is clearly enhanced in the non-pregnant animal tested. Although this finding needs to be confirmed with more animals, it is suggestive that there might be differences between the pregnant and non-pregnant heart with regard to ryanodine receptor regulation. It is included here as an interesting sideline but is not part of the conclusions of this thesis.

### VI.3: Western Blot analysis of Calcium Transport Proteins:

Western blot analysis was performed on proteins extracted from hearts of different developmental ages. These studies were done in order to determine if changes in message levels detected in northern blots correlate with protein levels. The protein was comparable across all ages studied (fig. 37). It is difficult to make a quantitative estimate of the protein content using western blot analysis due to multiple bands for the protein. The NCX protein is consistently observed as two or more bands on western blots due to the different states of the native protein. Characteristic bands are observed (fig. 38). The native protein is said to be approximately 108 kd in size, although the 108 kD band is never detected alone. The band at about 160 kd is reported

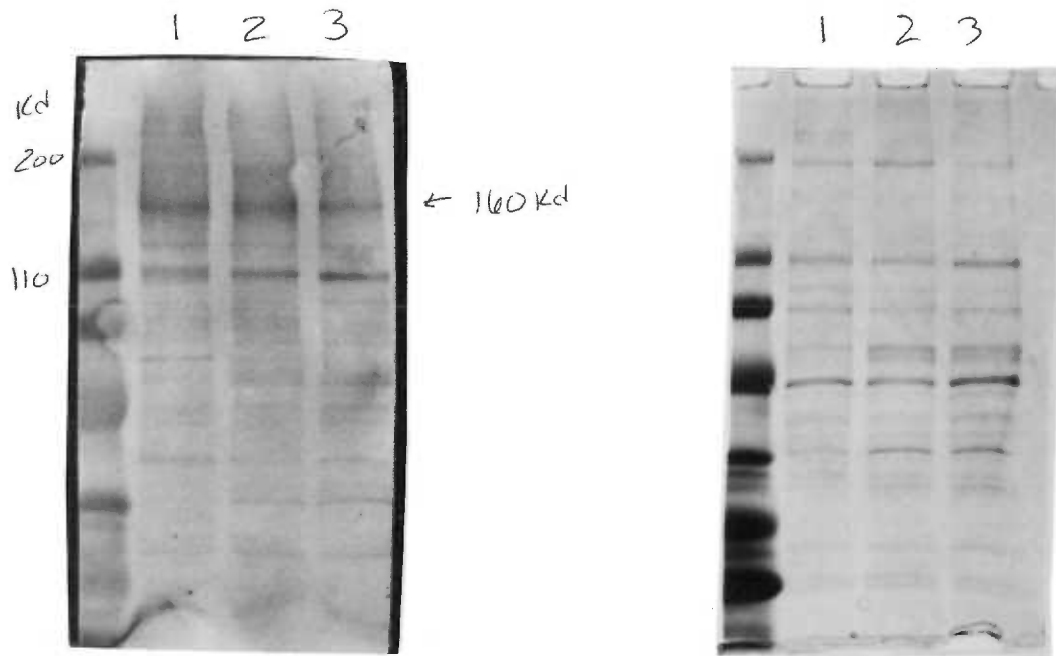


Figure 38: Western blot analysis of sarcolemmal (SL) enriched protein fractions isolated from sheep heart of various ages. Panel A is a western blot of SL proteins extracted from 80 day LV (lane 2), 5 day newborn LV (lane 3), and adult LV (lane 4). A polyclonal antibody which was raised against a partially purified NCX protein was used for these studies. The 160 kD band is most prominent and similar across the ages in this blot. This correlates well with the northern blot data for the 80 day fetal and adult sheep heart. Panel B is a duplicate gel which has been stained with Coomassie blue. This is used to show comparable loading of the samples.

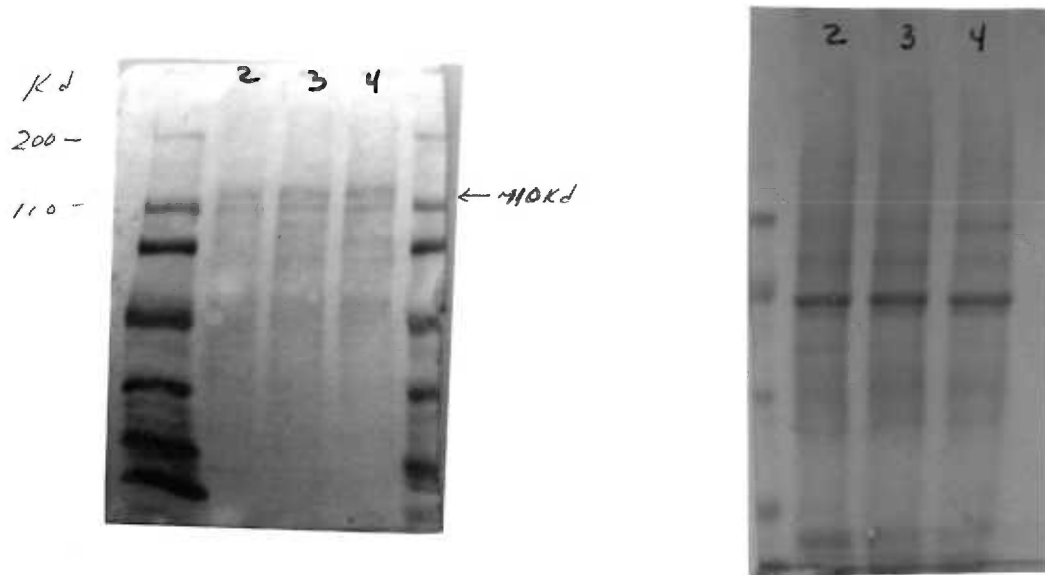


Figure 39: Western blot analysis of crude proteins isolated from sheep hearts of various ages. Panel A is a western blot of crude proteins extracted from 80 day LV (lane 2), 5 day newborn LV (lane 3), and adult LV (lane 4). A monoclonal antibody raised against the SERCA protein was used for these studies. The 110 kD protein corresponds to the SERCA protein. The SERCA is lower in abundance in the 80 day heart compared to the more mature hearts. This correlates well with the northern blot data presented earlier (fig 36). Panel B is a similar gel which has been stained with Coomassie blue. This is used to show comparable loading of the samples.

to be the non-reduced form of the protein since it has been observed to disappear under strong reducing conditions (115). There is not a dramatic difference in the amount of detectable protein between the ages studied (80 day fetus, 5 day lamb, and adult). These findings correlate well with the message levels detected on northern blots.

Western Blot analysis of the crude proteins extracted from hearts of different developmental ages (80 day fetus, 5 day lamb, adult) using a monoclonal antibody against the SERCA2a protein was also performed. Figure 39 is a representative western blot, the results of which support the findings of the northern blot analysis. The SERCA2a protein is present in the immature heart but increases in abundance as the heart matures. This finding agrees with the observations that the amount of functional SR increases as the heart matures.

## Section VII: Discussion

## SECTION VII: DISCUSSION

### Expression Studies:

From the results presented here it is apparent that the sheep heart develops in a fashion similar to the postnatal rabbit with respect to the SR. I have shown that the genes which encode the SR related proteins are expressed at lower levels in the fetal sheep heart when compared to the adult heart. This supports the hypothesis that the SR develops as the size of the myocyte increases during development. In the immature cardiac myocyte the surface area/volume ratio (SA/V) is larger than it is in the adult myocyte (24). This facilitates the transfer of activator  $Ca^{2+}$  to the myofibrils. In addition the myofibrils have been shown to be located peripherally in the immature sheep myocyte (Fig 1). Thus with this arrangement the immature cardiac myocyte does not rely solely on the SR for contractile function.

In the immature rabbit myocyte NCX activity has been shown to be enhanced relative to the adult myocyte. Based on the studies reported here, this is not the case for the sheep cardiac myocytes. In this study I compared the amount of detectable NCX message and protein in fetal and adult hearts and found no measurable difference. However, with respect to the western blots, I used total membrane proteins alone for this comparison. Thus, during development the amount of NCX protein relative to SL membrane proteins does not change significantly. If however, I were to compare the amount of NCX protein relative to total cellular proteins including contractile proteins it is likely that the NCX may have been more abundant in



the fetal heart. These difference probably reflect the fact that the sheep is a large precocial mammal and the rabbit is a small altricial. The sheep heart may mimic the rabbit heart during the first thirty days of gestation, but this has not been tested.

### Cloning Studies:

In this study I have reported the cloning and maturational expression pattern of the ovine cardiac NCX. It is interesting to note that although the gene is very well conserved across species, the maturational expression pattern is not. In the rabbit, the NCX gene is most highly expressed in the preterm heart (137). In contrast to this, the NCX gene has been shown to be more highly expressed in the adult human heart relative to a 17 week fetal heart (126). The data presented here show that the NCX gene in sheep is different than seen in other species. It is expressed at similar levels in the 80 day fetal compared to the adult heart.

The mechanisms which regulate the expression of the NCX gene have not been studied. It is likely that the different expression pattern of the NCX gene compared to rabbit reflects the fact that the rabbit is an altricial mammal whereas the sheep is precocial. However, until the large 3'untranslated region (UTR) is studied in detail with regard to regulatory elements and alternative splice sites we will not have a full understanding of why this highly conserved gene is expressed so differently across species.

I report, herein, the full 3' untranslated region including the poly (A) tail of the cardiac NCX, the first such report for any species. The 3' UTR is approximately 3.0 kb in length and is densely packed with "AT" residues. Although a detailed characterization has not been completed, similarities with other genes have been observed. Cytokines, lymphokines, and the

oncogenes *c-fos* and *c-myc* all contain 3' UTR which are rich in "AU" residues with two or more pentamer sequences "AUUUA". The mRNA for these genes is short lived ( $t_{1/2}$ =10-30 min), yet when stimulated the mRNA is rapidly stabilized (144). This "AUUUA" Shaw-Kamen element has been hypothesized to play a role in mRNA destabilization and perhaps under stimulatory conditions the domain is overridden resulting in mRNA stabilization. Recent studies by Cooper et al suggest that the cardiac NCX is rapidly induced in response to acute pressure loading of the right ventricle (145). Thus, one may hypothesize that under the influence of pressure load, the NCX mRNA is stabilized and accumulates within the cell.

Although more studies are required to substantiate this, I have detected 5 such Shaw-Kamen elements in the 3'UTR of the ovine cardiac NCX gene (fig. 33). From the size of the 3'UTR, the presence of the multiple Shaw-Kamen elements and the relative rapid induction of expression observed by Cooper et al, it is likely that future studies on the regulation of NCX in the fetal sheep heart will be exciting.

This model is of particular interest for studies of normal and abnormal heart growth. In the developing heart, growth is due to cell division (hyperplasia) and cell enlargement (hypertrophy). The former, however, only occurs prior to terminal differentiation. The precise signal which directs myocyte differentiation and prevents cell division is not known at this time.

Although modest hypertrophic growth accompanies hyperplastic growth during development, it is also a feature of pathological growth in the adult. For example, endurance athletes may experience a cardiac hypertrophic response to training. In this case, the "growth" is a normal compensatory response to intermittent increases in demand. On the other hand, individuals suffering severe aortic stenosis, will experience pathological left

ventricular hypertrophy. Unless corrected, compensatory growth leads to a decompensated myocardium and heart failure.

It has been clear for some time augmented myocardial loading in vivo initiates increased protein synthesis (146,147). Recent studies have begun to address the mechanisms by which hemodynamic load triggers protein synthesis which accompanies myocardial hypertrophy. Using stretch-induced protein synthesis as a marker of myocyte hypertrophy, Kent et al. suggest Na<sup>+</sup> influx as one possible transducer of the growth response (148). Stretch has been shown to increase Na<sup>+</sup> uptake by papillary muscles and is suggested to be mediated by stretch-activated ion channels in the sarcolemma. In addition, it has been shown that most if not all naturally occurring cellular growth factors also stimulate Na<sup>+</sup> influx (149).

Mitogen-induced Na<sup>+</sup> influx is a rapid and ubiquitous growth initiating event, with mitogen potency varying with the degree of Na<sup>+</sup> influx stimulation (6). These studies combined with the recent findings that NCX gene expression is enhanced within an hour of inducing a hemodynamic load on the heart, Kent et al. have suggested a possible role of the NCX in mediating the proposed Na<sup>+</sup>-mediated hypertrophic response. Future studies on the regulation of NCX gene expression during heart growth in health and disease will help to define the hypertrophic response.

In addition to the "AT" rich domains of the ovine 3' UTR I have identified two unique sequences adjacent to the poly(A) tail of this gene. This work is the first report of the native NCX poly(A) tail in any species to date. Previous investigators have been troubled by the absence of the apparent poly(A) tail (124). The first cloning studies reported functional expression of the canine cardiac NCX clone (TB11) in *Xenopus* oocytes (124). However, as mentioned previously, adequate expression was only observed upon splicing

the NCX clone with the 3'UTR and poly(A) tail from the glucose transporter. Thus it has been suggested that the poly(A) tail may stabilize mRNA. Although I have not attempted to express the full length ovine NCX clone it may be more readily expressed compared to canine NCX clone from the Nicoll lab if the poly(A) tail is indeed important for proper expression.

The unique 3' sequence adjacent to the poly(A) tail are interesting considering the recent reports of alternative splice sites in the 3'UTR (150). Clone pBSlex4 is missing a 105 bp portion compared to clone pBSlex3 (Fig 34). The sequence of the 105 bp segment does not contain the consensus sequence for RNA splicing (AG/gttc...cag/CTTT) in the junction where the homology is conserved between the two clones. Although this argues against alternative splicing, more studies are required to determine the precise nature of this sequence. This sequence may play a regulatory role in either the temporal or tissue specific expression of the NCX gene. As shown in fig. 34, at the junction site where homology is conserved between clones pBSlex3 and pBSlex4 a conserved Shaw-Kamen residue is observed. This may play a role in mRNA instability, thus this sequence in association with other cis or trans-elements may be involved in the processing of the NCX mRNA.

When I analyzed the positive clones from the fetal sheep heart library I detected this 105 bp sequence in all but clone pBSlex4. This suggests that it is either a cloning artifact or more likely it may be found in relatively low copy number. For the reasons stated in the results section, I believe this is not simply a cloning artifact.

### Summary:

In summary I have presented data on the development of the SR Ca<sup>2+</sup>-ATPase and the SL Na<sup>+</sup>-Ca<sup>2+</sup> exchanger proteins in the sheep heart. I have shown that the expression of the SERCA2a gene changes during the course of development based on northern and western blot data. The developmental pattern of the SERCA in sheep heart is similar to that observed in rabbit. The developmental pattern of the NCX in sheep heart is not similar to that of the rabbit. This supports the suggestion that results obtained in one species can not always be extrapolated to another species. Further study of these proteins is needed to elucidate the mechanisms by which the mammalian cardiac myocyte is able to enlarge rapidly and maintain calcium homeostasis during the cardiac cycle.

## Section VIII: References

## REFERENCES:

1. Friedman WF. The intrinsic physiologic properties of the developing heart. *Prog Cardiovascular Dis* 1972; 15:87-111.
2. Davies P, Dewar J, Tynan M, Ward R. Post-natal developmental changes in the length-tension relationship of cat papillary muscles. *J Physiology (Lond)* 1975; 253:95-102.
3. Urthaler F, Walker AA, Kawamura K, Hefner LL, James TN. Canine atrial and ventricular muscle mechanics studied as a function of age. *Circ Res* 1978; 42:703-713.
4. Park MK, Sheridan PH, Morgan WW, Beck N. Comparative inotropic response of newborn and adult rabbit papillary muscles to isoproterenol and calcium. *Dev Pharmacol Ther* 1980; 1:70-82.
5. Nakanishi T, Jarmakani JM. Developmental changes in myocardial mechanical function and subcellular organelles. *Am J Physiol* 1984; 246:H615-H625.
6. Nassar R, Reedy MC, Anderson PW. Developmental changes in the ultrastructure and sarcomere shortening of the isolated rabbit ventricular myocyte. *Circ Res* 1987; 61:465-483.
7. Anderson PW, Glick KL, Manring A, Crenshaw C, Jr. Developmental changes in cardiac contractility in fetal and postnatal sheep: in vitro and in vivo. *Am J Physiol* 1984; 16:H371-H379.
8. Teitel DF, Sidi D, Chin T, Brett C, Heymann MA, Rudolph AM. Developmental changes in myocardial contractile reserve in the lamb. *Ped Res* 1985; 19:948-955.
9. Thornburg KL, Morton MJ. Filling and arterial pressures as determinants of RV stroke volume in the sheep fetus. *Am J Physiol* 1983; 244:H656-H663.
10. Brutsaert DL, Sys SU. Relaxation and diastole of the heart. *Phys Rev* 1989; 69(4):1228-1315.
11. Smolich JJ, Walker AM, Campbell GR, Adamson TM. Left and right ventricular myocardial morphometry in fetal, neonatal, and adult sheep. *Am J Physiol* 1989; 257:H1-H9.

12. Ashley LM. A determination of the diameters of ventricular myocardial fiber in man and other mammals. *Am J Anat* 1945; 77:325-363.
13. Kenny JG, Plappert T, Coubiliet P, Satzman DH, Cartier M, Zollars L, Leatherman GF, St. John Sutton MG. Changes in intracardiac blood flow velocities and right and left ventricular stroke volumes with gestational age in the normal human fetus: a prospective Doppler echocardiographic study. *Circ* 1986; 74:1208-1216.
14. Brooks WH, Connell S, Cannata J, Maloney JE, Walker AM. Ultrastructure of the myocardium during development from early fetal life to adult life in sheep. *J Anat* 1983; 137 (4):729-741.
15. Carlsson E, Kjorell U, Thornell LE, Lambertsson A, Strehler E. Differentiation of the myofibrils and the intermediate filament system during postnatal development of the rat heart. *Eur J Cell Biol* 1982; 27:62-73.
16. Sheridan D, Cullen M, Tynan M. Postnatal ultrastructural changes in the cat myocardium: a morphometric study. *Cardiovasc Res* 1979; 11:536-540.
17. Legato M. Cellular mechanisms of normal growth in the mammalian heart. I. Qualitative and quantitative features of ventricular architecture in the dog from birth to five months of age. *Circ Res* 1975; 44:250-262.
18. Maylie JG. Excitation-contraction coupling in neonatal and adult myocardium of cat. *Am J Physiol* 1982; 242:H834-H843.
19. Forsgren S, Thornell LE. The development of Purkinje fibers and ordinary myocytes in the bovine fetal heart, an ultrastructural study. *Anat Embryol* 1981; 162:127-136.
20. Legato M. Cellular mechanisms of normal growth in the mammalian heart. II. Qualitative and quantitative comparison between the right and left ventricular myocytes in the dog from birth to five months of age. *Circ Res* 1979; 44:263-279.
21. Smith H, Page E. Ultrastructural changes in rabbit heart mitochondria during the perinatal period. Neonatal transition to aerobic metabolism. *Dev Biol* 1977; 57:109-117.



22. Page et al. Development of dyadic junctional complexes between SR and SL in rabbit left ventricular myocardial cells. *Circ Res* 1981; 48:519-522.
23. Nakanishi T, Okuda J, Kamata K, Abe K, Sekiguchi M, Takao A. Development of myocardial contractile system in the fetal rabbit. *Ped Res* 1987; 22:201-207.
24. Hoerter J, Mazet F, Vassort G. Perinatal growth of the rabbit cardiac cell: possible implications for the mechanism of relaxation. *J Mol Cell Cardiol* 1981; 13:725-40.
25. Page E, Early J, Power B. Normal growth of ultrastructures in rat left ventricular myocardial cells. *Circ Res* 1974; 34-35,(suppl II):12-16.
26. Sheridan D, Cullen M, Tynan M. Qualitative and quantitative observations on ultrastructural changes during postnatal development in the cat myocardium. *J Mol Cell Cardiol* 1979; 11:1173-1181.
27. Chen F, Mottino G, Klitzner TS, Philipson KD, Frank JS. Distribution of the Na<sup>+</sup>/Ca<sup>2+</sup> exchange protein in developing rabbit myocytes. *Am J Physiol* 1995; 268:C1126-C1132.
28. Litten RZ, Martin BJ, Buchthal RH, Nagai R, Low RB, Alpert NR. Heterogeneity of myosin isozyme content of rabbit heart. *Circ Res* 1985; 57: 406-414.
29. Lompre AM, Mercadier JJ, Wisnewsky C, Bouveret P, Pantaloni C, D'Albis A, Schwartz K. Species- and age-dependent changes in the relative amounts of cardiac myosin isoenzymes in mammals. *Dev Biol* 1981; 84:286-290.
30. Sweeney LJ, Nag AC, Eisenberg B, Manasek FJ. Developmental aspects of cardiac contractile protein. *Bas Res Cardiol* 1985; 80,(suppl 2):123-127.
31. Okuda H, Nakanishi T, Nakazawa M, Takao A. Effect of isoproterenol on myocardial mechanical function and cyclic AMP content in the fetal rabbit. *J Mol Cell Card* 1987; 19:151-157.
32. Hirsch DD, Morton MJ, Reller MD, Giraud GD, Jacobson S, Cobanoglu MA, Thornburg KL. Diastolic cardiac function in fetal sheep. Abstract, *AHA: Mol Cell Funct Aspects Card Dev*, New Orleans 1995; P70.
33. Guyton A. Textbook Medical Physiology, seventh edition. Dreibelbis D, ed. WB Saunders Co: Philadelphia, 1986.

34. Hodkin, Keynes. *J Physiol* 1957; 138:253-81.
35. Aidley DJ. The Physiology of Excitable Cells, third ed. Cambridge University Press: Cambridge, 1989.
36. Williamson JR, Williams RJ, Coll KE, Thomas AP. Cytosolic free Ca<sup>2+</sup> concentration and intracellular calcium distribution of Ca<sup>2+</sup>-tolerant isolated heart cells. *J Biol Chem* 1983; 258(22):13411-13414.
37. Carafoli E. Intracellular calcium homeostasis. *Ann Rev Biochem* 1987; 56:395-433.
38. Carafoli E. The signalling function of calcium and its regulation. *J Hypertension* 1994; 12,(suppl 10):S47-S56.
39. Ringer S. A further contribution regarding the influence of the different constituents of the blood on the contraction of the heart. *J Physiol (London)* 1883; 4:29-42.
40. Klee CB, Vanaman TC. Calmodulin [Review]. *Adv Protein Chem* 1983; 35:213-321.
41. Chapman R. Control of cardiac contractility at the cellular level. *Am J Physiol* 1983; 254(4):H535-H552.
42. Caroni P, Carafoli E. The Ca<sup>2+</sup>-pumping ATPase of heart sarcolemma. Characterization, calmodulin dependence, and partial purification. *J Biol Chem* 1981; 256:3263-70.
43. Reuter H. Ion channels in cardiac cell membranes. *Ann Rev Physiol* 1984; 46:473-84.
44. Bean BP. Classes of calcium channels in vertebrate cells. *Ann Rev Physiol* 1989; 51:367-84.
45. Brown AM, Camerer H, Kunze DL, Lux HD. Similarity of unitary Ca<sup>2+</sup> currents in three different species. *Nature* 1982; 299:156-58.

46. Mitra R, Morad M. Two types of calcium channels in guinea-pig ventricular myocytes. PNAS, USA 1986; 83:5340-44.
47. Hagiwara N, Irisawa H, Kameyama M. Contribution of two types of calcium currents to the pacemaker potentials of rabbit sino-atrial node cells. J Physiol 1988; 359:233-53.
48. Katz A. Physiology of the Heart, second edition. Raven Press: New York, 1992.
49. Reuter H. Ins and outs of Ca<sup>2+</sup> transport. Nature 1991; 349(14):567-568.
50. Yano K, Zarain-Herzberg A. Sarcoplasmic reticulum calsequestrins: structural and functional properties. Mol Cell Biochem 1994; 135(1):61-70.
51. Fabiato A. Calcium-induced release of calcium from cardiac sarcoplasmic reticulum. Am J Physiol 1983; 245:C1-C14.
52. Takeshima H, Nishimura S, Matsumoto T. Primary structure and expression from complementary DNA of skeletal muscle ryanodine receptor. Nature 1989; 339:439-445.
53. Sham J, Jones L, Morad M. Phospholamban mediates the  $\beta$ -adrenergic-enhanced Ca<sup>2+</sup> uptake in mammalian ventricular myocytes. Am J Physiol 1991; 261:H1344-H1349.
54. Tseng GN. Calcium current restitution in mammalian ventricular myocytes is modulated by intracellular calcium. Circ Res 1988; 63:468-482.
55. Tada M, Katz AM. Phosphorylation of the sarcoplasmic reticulum and sarcolemma. Ann Rev Physiol 1982; 44:401-423.

56. Solaro RJ, Briggs FN. Estimating the functional capabilities of sarcoplasmic reticulum in cardiac muscle. *Circ Res* 1974; 34:525-530.
57. Hasselbach W. Relaxation and the sarcotubular calcium pump. *Fed Proc* 1980; 23:909-912.
58. Shwartz AM. Calcium and the sarcoplasmic reticulum. In: Calcium and The Heart. Harris P, Opie LH, eds. Acaemic Press: New York, 66-92.
59. Kranias EG, Garvey JL, Srivastava RD, Solaro RJ. Phosphorylation and functional modifications of sarcoplasmic reticulum and myofibrils in isolated rabbit hearts stimulated with isoprenaline. *Biochem J* 1985; 26:113-121.
60. James P, Inue M, Tada M, Chiesi M, Carafoli E. Nature and site of phospholamban regulation of the Ca<sup>2+</sup> pump of sarcoplasmic reticulum. *Nature* 1989; 342(2):90-92.
61. Lindemann JP, Jones LR, Hathaway DR, Henry BG, Watanabe AM.  $\beta$ -adrenergic stimulation of phospholamban phosphorylation and Ca<sup>2+</sup>-ATPase activity in guinea pig ventricles. *J Biol Chem* 1983; 258:464-471.
62. Langer GA. Kinetic studies of Ca distribution in ventricular muscle of the dog. *Circ Res* 1964; 15:393-405.
63. Langer GA, Rich TL, Orner FB. Ca exchange under non-perfusion limited conditions in rat ventricular cells: identification of subcellular compartments. *Am J Physiol* 1990; 259:H592-H602.
64. Post JA, Langer GA. Cellular origin of the rapidly exchangeable Ca pool in the cultured neonatal rat heart cell. *Cell Calcium* 1992; 13:627-634.
65. Post JA, Langer GA. Sarcolemmal calcium binding sites in heart. I. Molecular origin in "gas-dissected" sarcolemma. *J Membr Biol* 1992; 129:49-57.

66. Langer GA, Rich TL. A discrete Na-Ca exchange-dependent Ca compartment in rat ventricular cells: exchange and localization. *Am J Physiol* 1992; 262:C1149-C1153.
67. Lehninger AL. Role of phosphate and other proton-donating anions in respiration-coupled transport of Ca<sup>2+</sup>-mitochondria. *PNAS, USA* 1974; 71:1520-1524.
68. Beuckelmann DJ, Wier WG. Mechanism of release of calcium from sarcoplasmic reticulum of guinea-pig cardiac cells. *J Physiol* 1988; 405:233-55.
69. Yue DT. Intracellular [Ca<sup>2+</sup>] related to rate of force development in twitch contraction of heart. *Am J Physiol* 1987; 252:H760-H770.
70. Sandow A. Excitation-contraction coupling in muscular response. *Yale J Biol Med* 1952; 25:176-201.
71. Schneider MF. Control of calcium release in functioning skeletal muscle fibers (Review). *Ann Rev Phys* 1994; 56:463-84.
72. Rios E, Brum G. Involvement of dihydropyridine receptors in excitation-contraction coupling in skeletal muscle. *Nature* 1987; 325:717-20.
73. Eisenberg RS, McCarthy RT, Milton RL. Paralysis of frog skeletal muscle fibers by the calcium antagonist D-600. *J Physiol* 1983; 341:495-505.
74. Tanabe T, Beam KG, Povel JA, Numa S. Restoration of excitation-contraction coupling and slow calcium current in dysgenic muscle by dihydropyridine receptor complementary DNA. *Pflugers Arch* 1987; 410: 75-82.
75. Miledi R, Parker I, Zhu PH. Extracellular ions and excitation-contraction coupling in frog twitch muscle fibers. *J Physiol* 1984; 351:687-710.
76. Sanchez JA, Stefani E. Kinetic properties of calcium channels of twitch muscle fibers of the frog. *J Physiol* 1983; 37:1-17.
77. Endo M. Calcium release from the sarcoplasmic reticulum. *Physiol Rev* 1977; 57:71-108.

78. Fabiato A. Rapid ionic modifications during the course of the aequorin-detected calcium transient in a skinned canine cardiac Purkinje cell. *J Gen Physiol* 1985; 85:189-246.
79. Fabiato A. Time and calcium dependence of activation and inactivation of calcium-induced release of calcium from the sarcoplasmic reticulum of a skinned canine cardiac Purkinje cell. *J Gen Physiol* 1985; 85:247-289.
80. Pederson PL, Carafoli E. Ion motive ATPases. I. Ubiquity, properties, and significance to cell function. *Trends In Bio Sci* 1987; 12:146-150.
81. Shull GE, Schwartz A, Lingrel JB. Amino acid sequence of the catalytic subunit of the (Na<sup>+</sup>+K<sup>+</sup>) ATPase deduced from a complementary DNA. *Nature* 1985; 316:691-695.
82. MacLennan CH, Brandl CJ, Korczak B, Green NM. Amino-acid sequence of a Ca<sup>2+</sup>+Mg<sup>2+</sup>-dependent ATPase from rabbit muscle sarcoplasmic reticulum, deduced from its complementary DNA sequence. *Nature* 1985; 316:696-700.
83. Dame JB, Scarborough GA. Identification of the phosphorylated intermediate of the *Neurospora* plasma membrane H<sup>+</sup>-ATPase as beta-aspartyl phosphate. *J Biol Chem* 1981; 249:10724-10730.
84. MacLennan DH. Purification and properties of an adenosine triphosphatase from sarcoplasmic reticulum. *J Biol Chem* 1970; 245:4508-4513.
85. Hasselbach W, Makinose M. *Biochem Biophys Res Comm* 1962; 7:132.
86. Ebashi S, Lipmann G. *J Cell Biol* 1969; 14:389.
87. Hasselbach W, Weber HH. *Biochim et Biophys Acta* 1953; 11:160.
88. Martonosi A, Feretos R. Sarcoplasmic reticulum. I. The uptake of Ca<sup>++</sup> by sarcoplasmic reticulum fragments. *J Biol Chem* 1964; 239(2):648-658.
89. Martonosi A. The role of phospho lipids in the ATPase activity of skeletal muscle microsomes. *Biochem Biophys Res Comm* 1967; 26:753-757.
90. Yamamoto T, Tonomura Y. Reaction mechanism of the Ca<sup>++</sup>-dependent ATPase of sarcoplasmic reticulum from skeletal muscle. I. Kinetic studies. *J Biochem (Tokyo)* 1967;62:558.

91. Martonosi A. Sarcoplasmic reticulum. VII. Properties of a phosphoprotein intermediate implicated in calcium transport. *J Biol Chem* 1969; 244(3):613-620.
92. Swynghedquw B. Changes in membrane proteins in chronic mechanical overload of the heart. *Am J Cardiol* 1990; 65:30G-33G.
93. Chiesi M, Boherr T, Schwaller R, Carafoli E. Cardiac phospholamban is related to the inhibitory domain of the plasma membrane Ca-pump. *Circulation* 1990; 82,(Suppl III):349.
94. Zubrzycka-Gaarn E, MacDonald G, Phillips L, Jorgensen AO, MacLennan DH. Monoclonal antibodies to the  $\text{Ca}^{2+}+\text{Mg}^{2+}$ -dependent ATPase of sarcoplasmic reticulum identify polymorphic forms of the enzyme and indicate the presence in the enzyme of a classical high-affinity  $\text{Ca}^{2+}$  binding site. *J Bioenerg Biomembr* 1984; 16:441-464.
95. Brandl CJ, Green NM, Korczak B, MacLennan DH. Two Ca ATPase genes: homologies and mechanistic implications of deduced amino acid sequences. *Cell* 1986; 44:597-606.
96. Tate CH, Bick R, Chu A, Van Winklem WB, and Entman ML. Nucleotide specificity of cardiac sarcoplasmic reticulum. GTP-induced calcium accumulation and GTPase activity. *J Biol Chem* 1985; 260:9618-9623.
97. Leberer E, Hartner KT, Brandl CJ, Fuji J, Tada M, MacLennan DH, Pette D. Slow/cardiac sarcoplasmic reticulum Ca-ATPase and phospholamban mRNAs are expressed in chronically stimulated rabbit fast-twitch muscle. *Eur J Biochem* 1989; 185:51-54.
98. Brody IA. Muscle contraction induced by exercise. A syndrome attributable to decreased relaxing factor. *N Eng J Med* 1969; 281:187-192.
99. Daly I, Clark AJ. The action of ions upon the frog's heart. *J Physiol (London)* 1921; 54:367-383.
100. Lüttgau HC, Niedegerke R. The antagonism between Ca and Na ions in the frog's heart. *J Physiol (London)* 1958; 143:486-505.
101. Niedegerke R. Movements of Ca in frog heart ventricle at rest and during contracture. *J Physiol (London)* 1963; 167:515-550.

102. Nidergerke R. Movements of Ca in beating ventricles of the frog heart. *J Physiol (London)* 1963; 167:551-580.
103. Langer GA. Kinetic studies of calcium distribution in ventricular muscle of the dog. *Circ Res* 1964; 15:393-405.
104. Reuter H, Seitz N. The dependence of calcium efflux from cardiac muscle on temperature and external ion composition. *J Physiol (London)* 1968; 195:451-470.
105. Kaback H R. Transport studies in bacterial membrane vesicles. *Science* 1974; 186:882-892.
106. Reeves JP, Sutko JL. Sodium-calcium ion exchange in cardiac membrane vesicle. *PNAS, USA* 1979; 76:590-594.
107. Reeves JP, Sutko JL. Sodium-calcium exchange activity generates a current in cardiac membrane vesicles. *Science* 1980; 208:1461-1464.
108. Pitts B, Jr. Stoichiometry of sodium-calcium exchange in cardiac sarcolemmal vesicles. *J Biol Chem* 1979; 254:6232-6235.
109. Wakabayashi S, Goshima K. Comparison of kinetic characteristics of Na-Ca exchange in sarcolemma vesicles and cultured cells from chick heart. *Biochim Biophys Acta* 1981; 645:311-317.
110. Bridge JHB, Bessinghwaighte HB. Uphill sodium transport driven by an inward calcium gradient in heart muscle. *Science* 1983; 19:178-180.
111. Cheon J, Reeves JP. Sodium-calcium exchange in membrane vesicles from *Artemia*. *Arch Biochim Biophys* 1988; 267:736-41.
112. Hale CC, Slaughter RS, Ahrens CC, Reeves JP. Identification and partial purification of the cardiac sodium-calcium exchange protein. *PNAS, USA*, 1984; 81:6569-6573.
113. Soldati L, Longoni S, Carafoli E. Solubilization and reconstitution of the Na<sup>+</sup>/Ca<sup>2+</sup> exchanger of cardiac sarcolemma. Properties of the reconstituted system and tentative identification of the protein(s) responsible for the exchanger activity. *J Biol Chem* 1985; 260:13321-13327.
114. Longoni S, Carafoli E. Identification of the Na<sup>+</sup>/Ca<sup>2+</sup> exchanger of calf heart sarcolemma with the help of specific antibodies. *Biochem Biophys Res Comm* 1987; 145:1059-1063.



115. Philipson KD, Longoni S, Ward R. Purification of the cardiac Na<sup>+</sup>-Ca<sup>2+</sup> exchange protein. *Biochim Biophys Acta* 1988; 945:298-306.
116. Philipson KD, Nishimoto AY. Stimulation of Na-Ca exchange in cardiac sarcolemmal vesicles by proteinase pretreatment. *Am J Phys* 1982; 243:C191-195.
117. Ledvora RF, Hegyvary C. Dependence of Na-Ca exchange and Ca-Ca exchange on monovalent cations. *Biochim Biophys Acta* 1983; 729:123-136.
118. Durkin JT, Ahrens DC, Aceto JF, Condresuc M, Reeves JP. Molecular and functional studies of the cardiac Sodium-Calcium exchanger. *Ann NY Acad Sci* 1991; 639:189-201.
119. Hilgemann DW, Nicoll DA, Philipson KD. Charge movements during Na<sup>+</sup> translocation by native and cloned cardiac Na/Ca exchanger. *Nature* 1991; 352:715-718.
120. Läuger PJ. Voltage dependence of sodium-calcium exchange: predictions from kinetic models. *J Memb Biol* 1987; 99:1-11.
121. Hilgemann DW. Numerical approximations of sodium-calcium exchange [Review]. *Prog Biophys Molec Biol* 1988; 51:1-45.
122. Collins A, Somlyo AV, Hilgemann DW. The giant cardiac membrane patch method: stimulation of outward Na<sup>+</sup>-Ca<sup>2+</sup> exchange current by MgATP. *J Physiol* 1992; 454:27-57.
123. Philipson KD, Ward R. Modulation of Na<sup>+</sup>-Ca<sup>2+</sup> exchange and Ca<sup>2+</sup> permeability in cardiac sarcolemmal vesicles by doxylstearic acids. *Biochem Biophys Acta* 1987; 897:152-158.
124. Nicoll DA, Longoni S, Philipson KD. Molecular cloning and functional expression of the cardiac sarcolemal Na<sup>+</sup>-Ca<sup>2+</sup> exchanger. *Science* 1990; 250:562-565.
125. Aceto JG, Condrescu M, Kroupis C, Nelson H, Nelson N, Nicoll D, Philipson KD, Reeves JP. *Arch Bioch Biophys* 1992; 298(2):553-560.
126. Komuro I, Wenninger KE, Philipson KS, Izumo S. Molecular cloning and characterization of the human cardiac Na<sup>+</sup>/Ca<sup>2+</sup> exchanger cDNA. *PNAS, USA* 1992; 89:4769-4773.

127. Low W, Kasir J, Rahamimoff H. Cloning of the rat heart Na<sup>+</sup>-Ca<sup>2+</sup> exchanger and its functional expression in HeLa cells. FEBS 1993; 316(1):63-67.
128. Li Z, Nicoll DA, Collins A, Hilgemann DW, Filoteo AG, Penniston JT, Weiss JN, Tomich JM, Philipson KD. Identification of a peptide inhibitor of the cardiac sarcolemmal Na<sup>+</sup>-Ca<sup>2+</sup> exchanger. J Biol Chem 1991; 266:1014-1020.
129. Matsuoka S, Nicoll DA, Reilly RF, Hilgemann DW. Initial localization of regulatory regions of the cardiac sarcolemmal Na<sup>+</sup>-Ca<sup>2+</sup> exchanger. PNAS, USA 1993; 90:3870-3874.
130. Nayler WG, Fassold E. Calcium accumulating and ATPase activity of cardiac sarcoplasmic reticulum before and after birth. Card Res 1977; 11:231-237.
131. Mahony L, Jones LR. Developmental changes in cardiac sarcoplasmic reticulum in sheep. J Biol Chem 1986; 261(32):15257-15265.
132. Machalak M. Sarcoplasmic reticulum membrane and heart development. Can J Card 1987; 3(5):251-260.
133. Pegg W, Michalak M. Differentiation of sarcoplasmic reticulum during cardiac myogenesis. Am J Physiol 1987; 252:H22-H31.
134. Arai M, Otsu K, MacLennan DH, Periasamy M. Regulation of sarcoplasmic reticulum gene expression during cardiac and skeletal muscle development. Am J Physiol 1992; 262:C614-C620.
135. Fisher DJ, Tate C, Philips S. Developmental regulation of the sarcoplasmic reticulum calcium pump in the rabbit heart. Ped Res 1992; 31(5):474-479.
136. Hanson GL, Schilling WP, Michael LH. Sodium-potassium pump and sodium-calcium exchange in adult and neonatal canine cardiac sarcolemma. Am J Physiol 1993; 264:H320-H326.
137. Artman M. Sarcolemmal Na<sup>+</sup>-Ca<sup>2+</sup> exchange activity and exchanger immunoreactivity in developing rabbit hearts. Am J Physiol 1992; 263:H1506-H1513.

138. Chen F, Mottino G, Klitzner TS, Philipson KD, Frank JS. Distribution of the Na<sup>+</sup>/Ca<sup>2+</sup> exchange protein in developing rabbit myocytes. *Am J Physiol* 1995; 268:C1126-C1132.
139. Langer GA, Frank JS, Nudd LM. Correlation of calcium exchange, structure, and function in myocardial tissue culture. *Am J Physiol* 1979; 237:H239-H246.
140. Grover AK, Khan I. Calcium pump isoforms: diversity, selectivity and plasticity. *Cell Calcium* 1992; 13:9-17.
141. Tsien RW. Calcium channels in excitable cell membranes. *Ann Rev Physiol* 1983; 45:341-358.
142. Mahony L. Maturation of calcium transport in cardiac sarcoplasmic reticulum. *Ped Res* 1988; 24:639-643.
143. Reller MD, Burson MA, Lohr JL, Morton MJ, Thornburg KL. Nitric oxide is an important determinant of coronary flow at rest and during hypoxemic stress in the fetal lamb. *Am J Physiol* 1995; 269:H2074-H2081.
144. Shaw G, Kamen R. A conserved AU sequence from the 3' untranslated region of GM-CSF mRNA mediates selective mRNA degradation. *Cell* 1986; 46:659-667.
145. Kent RL, Rozich JD, McCollam PL, McDermott DE, Thacker UF, Menick DR, McDermott PJ, Cooper G, IV. Rapid expression of the Na<sup>+</sup>-Ca<sup>2+</sup> exchanger in response to cardiac pressure overload. *Am J Physiol* 1993; 265:H1024-H1029.
146. Moroz LA. Protein synthetic activity in heart microsomes and ribosomes during left ventricular hypertrophy in rabbits. *Circ Res* 1967; 21:449-459.
147. Morgan HE, Gordon EE, Kira Y, Chua BHL, Russo LA, Peterson CJ, McDermott PJ, Watson PA. Biochemical mechanisms of cardiac hypertrophy. *Ann Rev Physiol* 1987; 49:501-518.
148. Kent R, Hooper K, and Cooper G, IV. Load responsiveness of protein synthesis in adult mammalian myocardium: role of cardiac deformation linked to sodium influx. *Circ Res* 1989; 64:74-85.
149. Leffert HL, Koch KS. Growth regulation by Na<sup>+</sup> ion influxes. In: Control of Animal Cell Proliferation, volume one. Boyton A, Leffert H, eds. Academic Press: New York, 1985:367-413.

150. Gabellini G, Iwata T, Carofoli E. An alternative splicing site modifies the carboxyl-terminal trans-membrane domains of the Na<sup>+</sup>/Ca<sup>2+</sup> exchanger. *J Biol Chem* 1995; 270(12):6917-6924.
151. Sambrook J, Fritsch EF, Maniatis T. Molecular Cloning: A Laboratory Manual, second edition, 1989.
152. Sanger FS, Nicklen, Coulson AR. DNA sequencing with chain-terminating inhibitors. *PNAS, USA* 1977; 74:5463-5467.
153. Philipson KD, Nicoll DA. Sodium-calcium exchange. *Curr Biol* 1992; 4:678-683.
154. Chomczynski P, Sacchi N. Single-step method of RNA isolation by acid guanidinium thiocyanate-phenol-chloroform extraction. *Analyt biochem* 1987; 162:156-159.
155. Brillantes A-M, Bezprozvannaya S, Marks AR. Developmental and tissue-specific regulation of rabbit skeletal and cardiac muscle calcium channels involved in excitation-contraction coupling. *Circ Res* 1994; 75:503-510.
156. Cable MB, Briggs FN. Labeling the adenine nucleotide binding domain of the sarcoplasmic reticulum Ca, Mg-ATPase with photoaffinity analogs of ATP. *J Biol Chem* 1984; 259:3612-15.
157. Maruyama K, Connectin an elastic filamentous protein of striated muscle. *Int Rev Cytol* 1986;104:81-114.
158. Labeit C, Kolmerer B, Titins: giant proteins in charge of muscle ultrastructure and elasticity. *Science* 1995; Oct 13, 270 (5234): 293-6.